

**HIGH-RESOLUTION ESTIMATION OF
GROUNDWATER RECHARGE FOR THE ENTIRE
STATE OF NEW MEXICO USING A SOIL-WATER-
BALANCE MODEL**

By

David Ketchum, Graduate Assistant

B. Talon Newton, Hydrogeologist

Fred Phillips, Emeritus Professor of Hydrology

FINAL REPORT

Subaward Q 1686

and

Subaward Q 01788

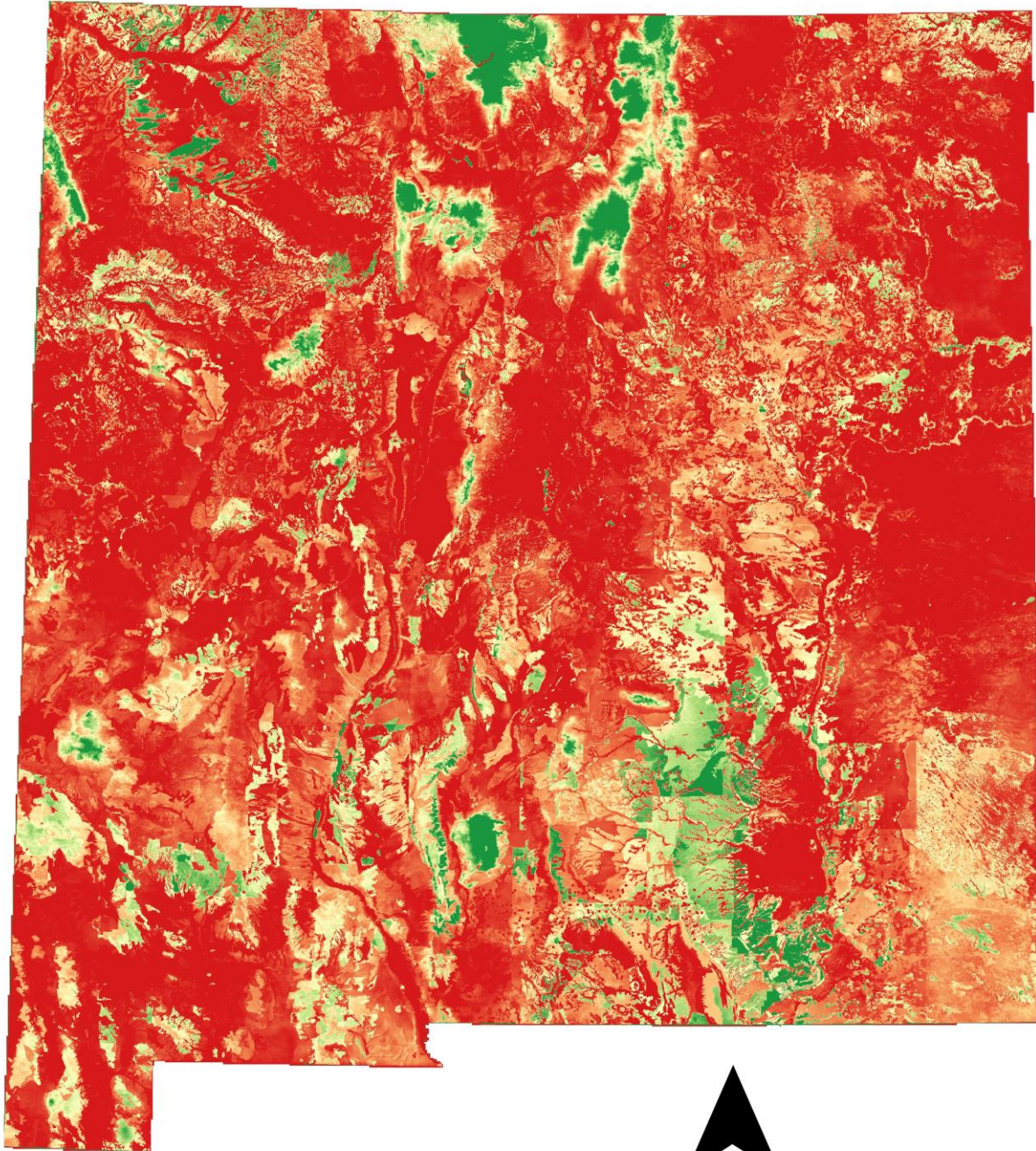
June 2016

Funded by:

New Mexico Water Resources Research Institute

New Mexico Bureau of Geology and Mineral Resources

New Mexico Institute of Mining and Technology



50 0 50 100 150 200 km

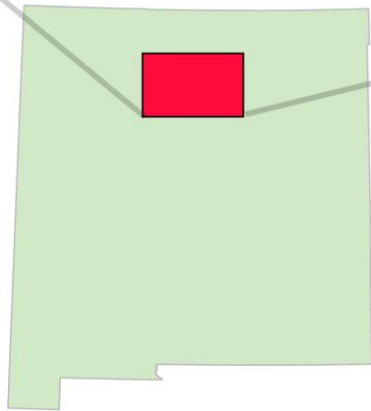
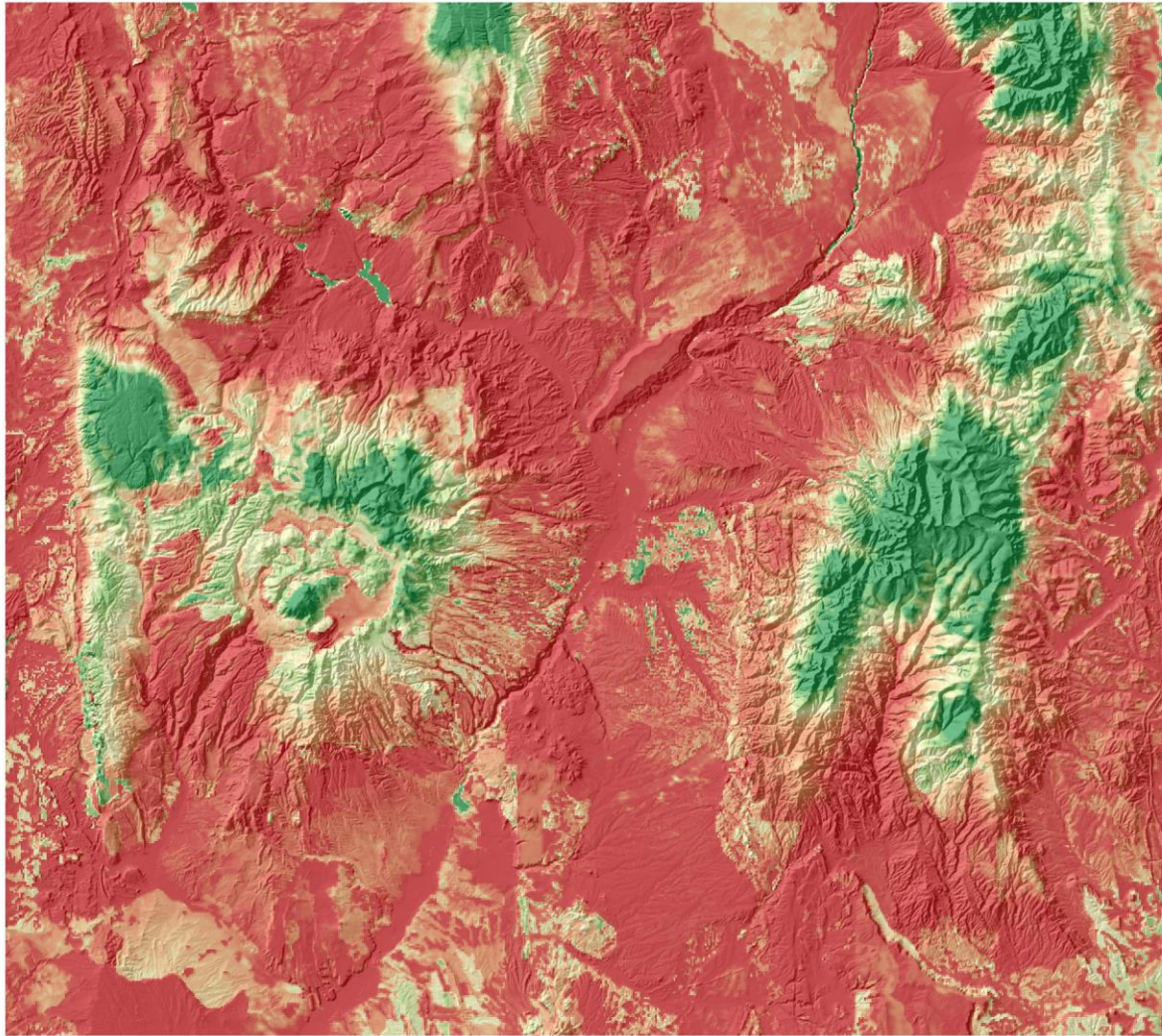


Legend

Recharge Index (%)

-  0.0
-  4.9
-  9.8
-  14.7
-  19.6
-  24.5
-  29.4

**Evapotranspiration and Recharge Model
Recharge as Percent of Precipitation**



Legend

Recharge Index (%)

- 0.0
- 4.9
- 9.8
- 14.7
- 19.6
- 24.5
- 29.4



ETRM Average Annual Recharge as Percent of Precipitation

DI

DISCLAIMER

The New Mexico Water Resource Research Institute and affiliated institutions make no warranties, express or implied, as to the use of the information obtained from this data product. All information included with this product is provided without warranty or any representation of accuracy and timeliness of completeness. Users should be aware that changes may have occurred since this data set was collected and that some parts of these data may no longer represent actual conditions. This information may be updated without notification. Users should not use these data for critical applications without a full awareness of its limitations. This product is for informational purposes only and may not be suitable for legal, engineering, or surveying purposes. The New Mexico Water Resource Research Institute and affiliated institutions shall not be liable for any activity involving these data, installation, fitness of the data for a particular purpose, its use, or analyses results.

ACKNOWLEDGMENTS

This research was supported by the New Mexico Statewide Water Balance Project, funded through the New Mexico Water Resources Research Institute by means of subawards Q 1686 and Q 01788.

ABSTRACT

The rate and distribution of groundwater recharge to New Mexico's aquifers is the least understood aspect of the state's water budget. Despite a history of precise and distributed measurements quantifying surface water flow, water table elevations, precipitation amounts, as well as current models that describe evapotranspiration, a statewide assessment of recharge has not previously been attempted. While recharge estimates and studies of recharge processes have been conducted, the effort to date has been on the basin scale, or by county and water-planning region. This study aims to quantify in-place recharge at the state scale. To map recharge areas, a GIS-based distributed-parameter soil-water-balance model, the Evapotranspiration and Recharge Model (ETRM) was developed to simulate recharge using gridded precipitation, reference evapotranspiration, geology, vegetation cover, and soils data as inputs. The model was run on a daily time step over the years 2000 through 2013. The model includes a snow module to simulate snowpack and a custom reference evapotranspiration product at a resolution of 250 x 250 m. Estimates of recharge were made in the mountains around the state using chloride mass balance in an attempt to test the results. Results show high recharge in the mountainous areas of the state, which typically have thinner soils, lower temperatures, and higher rates of precipitation than the lowlands. Future work should focus on improving the representation of New Mexico soil water storage capacity, the hydraulic conductivity of variably saturated soils, and refinement of the energy input for the ETRM.

Keywords: Recharge, groundwater, evapotranspiration, precipitation, soil water balance, distributed parameter model, reference evapotranspiration

TABLE OF CONTENTS

CHAPTER 1.	INTRODUCTION	1
1.1	Motivation	1
1.2	Scope	2
CHAPTER 2.	PREVIOUS RECHARGE ESTIMATES IN NEW MEXICO	4
2.1	Compilation of Previous Recharge Estimates	4
2.2	Examples Previous Recharge Estimate Techniques Used in New Mexico	6
2.2.1	Water Balance Method	6
2.2.2	Chloride Mass Balance	6
2.2.3	Numerical Simulations of Recharge	8
2.2.4	Maxey-Eakin Recharge Estimation Technique	9
2.2.5	Lumped Parameter Modeling	10
CHAPTER 3.	SOIL-WATER-BALANCE MODELING	11
3.1	Background	11
3.1.1	Basin Characterization Model	11
3.1.2	INFILv3 USGS Model	13
3.1.3	Model Estimates of ET	14
3.1.4	Dual Crop Coefficient Method	19
CHAPTER 4.	EVAPOTRANSPIRATION AND RECHARGE MODEL	24
4.1	Introduction	24
4.2	Materials and Methods	25
4.2.1	Modified FAO-56 Dual Crop Coefficient	26
4.2.2	Other Data Inputs	30
4.2.3	Snow Model	31
4.2.4	Model Simulations	32
4.3	Results	32
4.4	Discussion	37
4.5	Conclusion and Future Work	47
APPENDIX A:	CHLORIDE MASS BALANCE STUDY	i

A.1	Introduction	i
APPENDIX B:	ETRM SNOW MODEL	i
B.1	Background	i
B.2	Methods.....	iii
B.3	Calibration Results	v
B.4	Discussion	xi
APPENDIX C:	DERIVATION OF ETRM INPUTS	i
	NLDAS-Based Reference ET	ii
	High-Resolution Penman-Monteith Reference ET	ii
	Vegetation Index	iii
	Creating a Statewide SSURGO Soils Map	vi
	Total Available Water, Field Capacity, Wilting Point, Rooting Depth	vi
APPENDIX D:	References Cited.....	i

LIST OF FIGURES

Figure 1.1 The New Mexico recharge-area map integrates several existing spatial data sets, including elevation, precipitation, temperature, geology, and vegetation.	3
Figure 2.1 New Mexico and headwaters base map shows recharge estimate study points throughout the state. Selection of a point displays a window showing the recharge estimate (mostly in acre-feet per year, AFY), the sub-region the estimate pertains to, the estimation technique used, and a link to access the study.	5
Figure 4.1 The MODIS satellites collect images every 16 days over New Mexico. The ratio of near-infrared scatter to absorbed red light is normalized and used as a proxy for vegetation density. Green represents high vegetation density.	28
Figure 4.2 Gridded Atmospheric Data Downscaling Evapotranspiration Tools (GADGET) for High-Resolution Distributed Reference ET in Complex Terrain creates 250 m resolution gridded data representing tall-crop reference ET, the basis for energy-driven components of the ETRM. Red represents high reference ET.	29
Figure 4.3 Recharge (% of precipitation) calculated by the ETRM over the 14-year simulation period (2000-2013). The highest rates occur in the mountainous regions of the state. Possible problems mentioned in the discussion are numbered.	34
Figure 4.4 The ET Index (i.e., the fraction of precipitation lost to ET) shows ET is the dominant flux of water out of the soil layer. Over 85% of the state loses 70% of precipitation to evapotranspiration, by far the dominant flux of water from the soil layer.	36
Figure 4.5 Recharge estimates based on the ETRM were scattered when compared with CMB recharge estimates. No clear bias was identified.	37
Figure 4.6 Scatter plot of ETRM recharge estimates compared with previous estimates of recharge show that the ETRM generally makes much higher estimates.	38
Figure 4.7 Sensitivity analysis was conducted at 21 sites around the state.	39
Figure 4.8 Detail view of a transect along which sensitivity analysis was performed, the top image shows elevation, the middle lower image shows recharge rates in the area.	40
Figure 4.9 The Socorro site shows variations in recharge when input parameters are varied. The site has a clear threshold of precipitation necessary to cause recharge.	42
Figure 4.10 The La Jencia site is very sensitive to the input parameters, a small change in reference ET, soil water storage capacity, or precipitation causes large changes in Recharge.	43
Figure 4.11 The site at Water Canyon is well within the physical conditions conducive to recharge.	44
Figure 4.12 The South Baldy site, at 3190 m.a.s.l., is among the “sky islands” of New Mexico, where low available energy and high precipitation create conditions conducive to recharge.	45

Figure 4.13 Tornado plots from the three lower sites at Socorro, La Jencia, and Water Canyon show a high relative sensitivity to TAW, while humid sites such as South Baldy are less sensitive..... 46

CHAPTER 1. INTRODUCTION

1.1 Motivation

The goal of this study is to estimate in-place groundwater recharge (i.e., recharge due to vertical infiltration of soil moisture, not including recharge from precipitation that has moved laterally to flow or pond in stream channels or depressions) for the entire state as part of the Water Resources Research Institute (WRI) Statewide Water Assessment (SWA). The results of this study will ultimately be presented along with the other components of the state water balance as an interactive, web-based service. Groundwater recharge is the least understood component of the New Mexico state water budget. Despite a long history of systematic stream gauging, water-table elevation monitoring, and precipitation measurements, along with a burgeoning evapotranspiration (ET) estimation effort using remote sensing data, large-scale estimation of recharge in New Mexico has not previously been undertaken. Groundwater recharge defines a limit for the availability of water for humans and ecosystems, therefore estimating recharge for the State of New Mexico is critical for effective water resource management. New Mexico depends particularly on groundwater resources; 87 percent of the public supply of fresh water is from groundwater (USEPA). While efforts to conserve groundwater and utilize the state's surface water rights to a greater extent have made progress, the expected 15 percent increase in the population from 2000-2030 is likely to stress groundwater resources further. Water table levels in many New Mexico municipal groundwater production areas have declined significantly from pre-development levels; declines of 120 feet in Albuquerque, 300 feet in Santa Fe, and over 200 feet in the Las Cruces area have been observed (Bexfield and Anderholm, 2002; Bartolino and Cunningham, 2003; Leake et al., 2000). In some communities, precipitous water table declines have been observed; in Magdalena in 2013 the water level in the town's sole production well dropped over 16 feet in one year, causing the well, and the village water supply, to go dry (Albuquerque Journal, 2013). Other communities, including Las Vegas, Ruidoso, and Cloudcroft, have also had to bring water from elsewhere by truck and impose restrictions on pumping and municipal use. To effectively manage these resources, the fluxes of water into and out of New Mexico (i.e., the water balance) must be understood and quantified. A critical component of the water balance is groundwater recharge, the only process that replenishes groundwater aquifers.

Estimating recharge is difficult in New Mexico, where extremely heterogeneous topography and sporadic precipitation complicate recharge calculations. Efforts in New Mexico to date have typically employed methods of partitioning precipitation into a recharge fraction based on precipitation intensity, by stream base-flow estimates, or by completing water mass-balance calculations with recharge defined as the remainder of other measured components of the water budget. However, recent development of high-resolution data products offer insight to the spatial and temporal patterns of available energy, evaporation and transpiration, precipitation, temperature, and vegetative cover. This new data, combined with ever-increasing computational power has provided the opportunity to expand understanding of the water balance, and recharge in particular, to the state scale. In order to understand the water resources of New Mexico at this scale, accurate and large-scale estimation methods must be developed. The benefits of more extensive and accurate recharge estimates include enabling federal, state, and municipal

organizations to plan for sustainable use of groundwater resources as extraction increases and the groundwater system reacts to climate change.

1.2 Scope

Total recharge can be divided into two components: the part of recharge that infiltrates at the same location as where it encountered the surface as rain or snowmelt (i.e., diffuse, or in-place recharge), and the part which infiltrates in a focused manner after having moved across the surface as runoff (i.e., focused recharge). This study pertains to the former, diffuse recharge; future recharge studies will estimate the latter, focused recharge component. For the purposes of this study, recharge will henceforth be defined as the part of total precipitation that either infiltrates directly through the root zone within the soil layer, or the part that falls as snow and subsequently melts and infiltrates through the root zone within the soil layer. Other types of recharge (e.g. mountain-front, mountain-block) are geologic and geographic distinctions that are not differentiated in this study. The time period of interest for this study is limited to the years 2000-2013. This covers the period during which all of our high-resolution datasets are available. To test our simulations, we employ ‘chloride mass-balance’ recharge estimates based on groundwater chloride data. Objectives of This Study

Recharge estimates made in this study are expected to be refined in the future as the project continues and as new methods and data are employed. This report describes the results of the first two years of this study. The objectives were:

1. To compile existing recharge estimates that have been made in New Mexico and present them on a map, where the geographic position of each study site or area is shown, and where the data describing each study can be displayed.
2. To construct a New Mexico recharge-area map qualitatively distinguishing the areas of high to low recharge potential to help identify areas of likely recharge. The map was constructed using a Geographic Information Systems (GIS) framework, in which several individual data layers which represent precipitation, available energy, soils, vegetation, rooting depth, and geology were used to identify likely recharge areas (Figure 1.1).
3. To simulate the soil water balance over many years using statewide, gridded data sets in a computational model. This model simulates the water balance of the soil layer in each of millions of raster “pixels” that provide continuous coverage over the entire state. Simulations run each day for each of these cells, computing evapotranspiration (ET), runoff, soil-moisture-storage change, and recharge at every step.

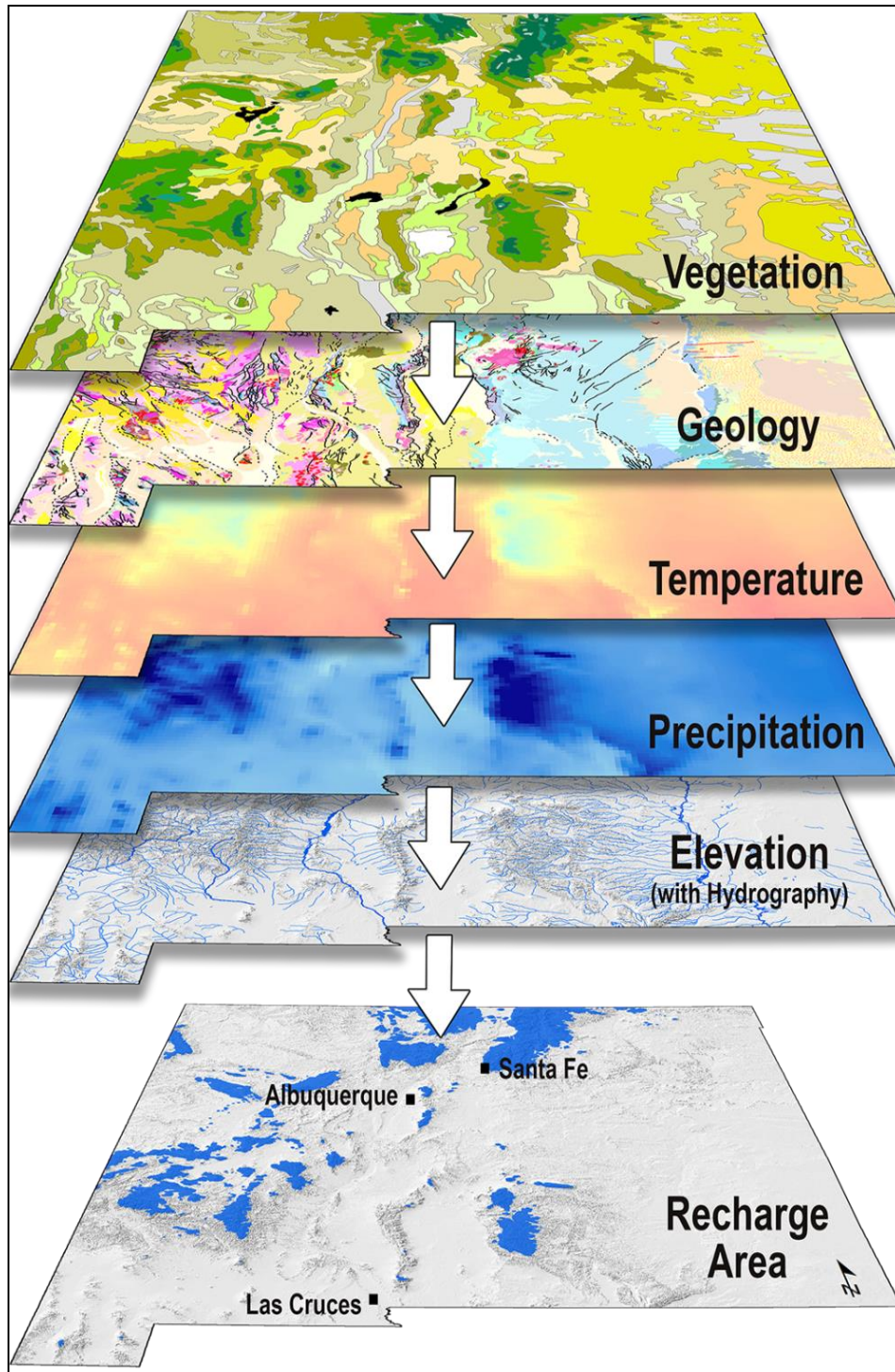


Figure 1.1 The New Mexico recharge-area map integrates several existing spatial data sets, including elevation, precipitation, temperature, geology, and vegetation.

CHAPTER 2. PREVIOUS RECHARGE ESTIMATES IN NEW MEXICO

2.1 Compilation of Previous Recharge Estimates

Previous recharge estimates made in New Mexico were compiled from a review of existing literature and consist of over 130 individual estimates. Estimates were made of recharge rates at both points and areas in the state. Geographic regions represent certain physical regions such as geologic formations, basins, or mountain ranges, and political regions such as counties or Water Resource Planning Regions (WRPRs). The principal source of recharge estimates are the Water-Resource Investigation Reports published by the United States Geological Survey (USGS), many of which are computational models of groundwater flow. The New Mexico Office of the State Engineer (OSE) has documents posted online describing the water resources of each of New Mexico's 16 WRPRs, many of which make estimates of regional recharge. These reports have typically been completed by private consultants.

The data pertaining to recharge was compiled in tabular form, associated with geographic points, and converted to a GIS "layer". Each layer represents a feature type that can be represented geographically by a point, line, or polygon. Each study in the compilation was included in the tabular data which was then converted to a point layer in a GIS. A base map of New Mexico and the outlying headwaters of inflowing rivers from other states was created. The purpose of the base map is to orient the viewer to where the points are located with familiar geographic features of New Mexico. The points layer on the map shows each study (Figure 2.1). This product will be made available to the public by means of ArcGIS software. The user will be able to simply select any point using the Identify Selection tool to view the information from the tabulated recharge data. This data includes the WRPR in which the study was conducted, the recharge estimate (in depth at a point or in acre-feet for an area), any specific geographic sub-region the study represents, the authors of the study, the estimation technique, and a link to the study online.

The compilation showed a great variation of recharge estimation techniques. The most commonly used are described below.

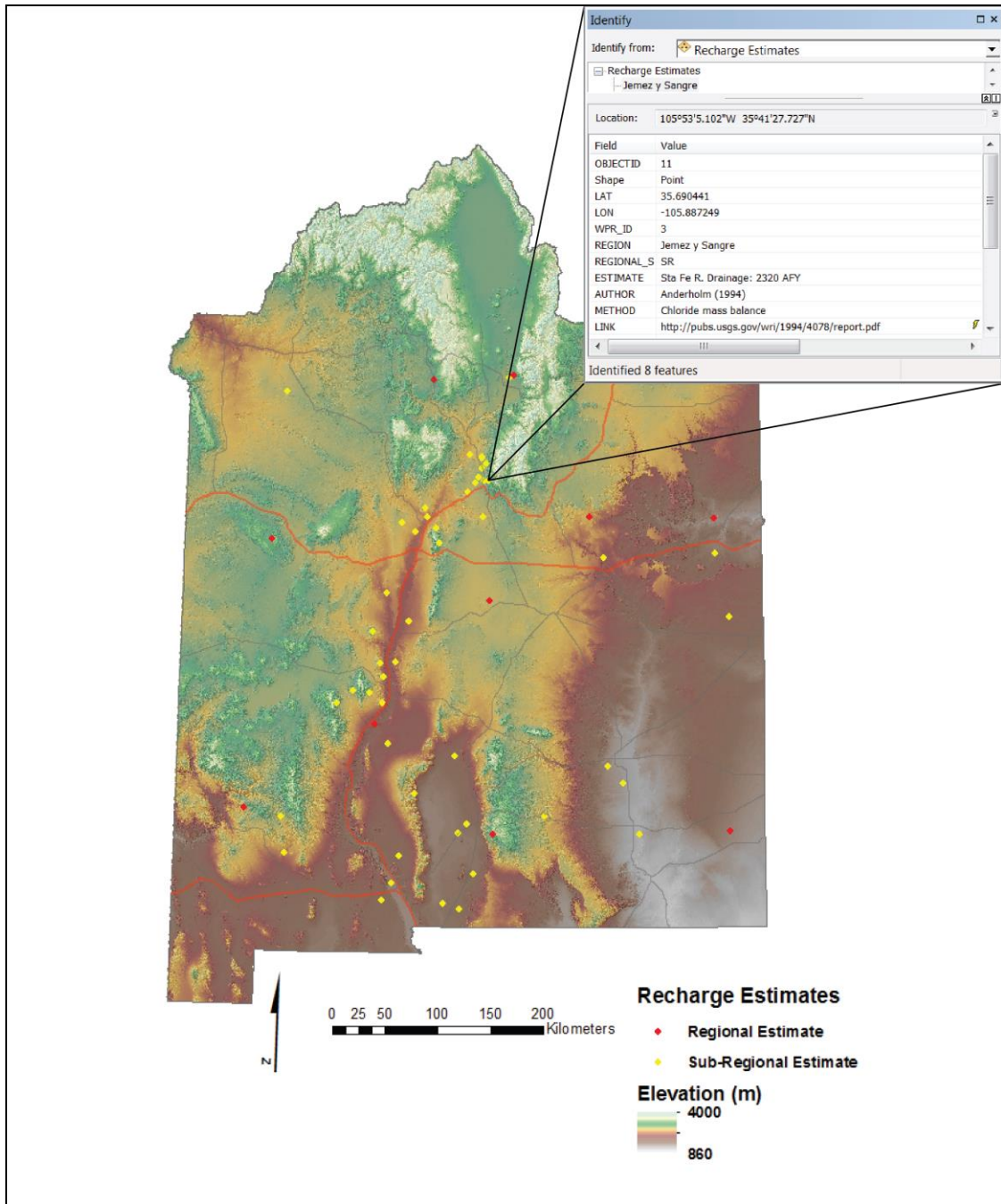


Figure 2.1 New Mexico and headwaters base map shows recharge estimate study points throughout the state. Selection of a point displays a window showing the recharge estimate (mostly in acre-feet per year, AFY), the sub-region the estimate pertains to, the estimation technique used, and a link to access the study.

2.2 Examples Previous Recharge Estimate Techniques Used in New Mexico

2.2.1 Water Balance Method

Perhaps the most common recharge estimate technique is the water balance/mass balance method, in which all outputs from a system are calculated (e.g., ET, stream flow, underflow) and subtracted from the inputs (e.g., rainfall, snowmelt, run-on). The difference is simply accounted for as recharge. This method has the advantage of being calculated remotely without necessitating field measurements of recharge through other means. A potentially serious problem with this method in the arid and semiarid Southwest is that the error associated with the estimation of stream flow and precipitation may be greater than the actual recharge. Thus this method must either be corroborated with other data or used as a first approximation.

Spiegel and Baldwin (1963) performed a thorough accounting of estimated streamflow, precipitation, snowmelt, groundwater exfiltration, stream loss, and recharge in the Santa Fe area. The geographic distribution of these water resources in relation to local physiographic features, measured water table elevations in wells, and the geohydrology of local formations was used to gain an understanding of the groundwater flow direction. Groundwater discharge to streams was assumed to be near steady-state and equated to recharge over each of two major geologic formations (i.e., Tesuque and La Cienega). Regional recharge rates were estimated at 14.5 mm yr^{-1} , or around 4% of annual precipitation.

McAda and Wasiolek (1988) used a water balance method equating groundwater recharge to the sum of precipitation minus ET and runoff. As distributed data for precipitation over this area was unavailable at the time, the authors used an altitude-precipitation relationship developed by Spiegel and Baldwin (1963) and by the U.S. Forest Service (USFS) for the study area above 9,600 ft. ET was estimated using pan-evaporation data in a seasonal rainfall-ET relation also developed by the USFS. The authors applied these recharge estimate techniques along the west slope of the Sangre de Cristo Mountains in the Santa Fe area, concentrating recharge to the model area near the mouths of the canyons draining the range. Recharge was estimated at $5390 \text{ acre-feet yr}^{-1}$ (AFY) in the Santa Fe River Basin, and 6080 in the Pojoaque Basin.

2.2.2 Chloride Mass Balance

Note: For a more detailed description of chloride mass balance theory, see Appendix A.

The chloride mass-balance (CMB) technique uses analyses of the chloride anion concentration to estimate recharge. Because chlorine dissolves readily in water, tends not to sorb to other molecules since it is a negatively charged ion, and is delivered to the surface in a fairly uniform distribution in dust and precipitation, it serves as a useful environmental tracer. To use CMB the following assumptions must be made: there is constant flux of Cl through the soil system; recirculation of Cl is at a steady state, there is no geologic contribution of Cl to groundwater, and Cl behaves conservatively. CMB can be applied to the vadose zone or to

groundwater, and can be calculated if the Cl concentration of infiltrating water and groundwater or soil water is known.

Anderholm (1994) conducted CMB recharge estimates in the foothills of the Sangre de Cristo Mountains and the Española Basin to estimate recharge rates to the Tesuque Aquifer. Vadose-zone Cl concentrations in soil were found to a depth of 50 ft., groundwater Cl concentrations were measured, and meteoric (bulk) Cl concentrations were taken by sampling any water found in a 5-gallon bucket checked bi-weekly for 1.5 years and corrected for evaporation. Precipitation was measured using a tipping-bucket rain gauge and a wedge rain gauge. While “arroyo-channel” (focused) recharge was not measured, low Cl concentrations in groundwater were interpreted as evidence that focused recharge from arroyos was not a significant contribution to total recharge. Chloride concentrations in mountain streams were found to be low during the spring runoff and highest in late winter and through early spring. Up-gradient increases in Cl concentration were suggest a transient Cl mass balance, possibly resulting from new Cl sources including septic tank effluent and infiltration of irrigation water. Recently created sources of Cl would violate the important assumption of zero net Cl storage change in the system.

Anderholm (2001) estimated mountain-front recharge (MFR) on the east side of the Middle Rio Grande using groundwater-based CMB and water-yield regression analysis. This study made the assumption that Cl concentrations near the mountain front were equal to those of the MFR and that bulk (wet and dry) Cl concentration of infiltrating water was 0.3 mg L^{-1} . MFR Cl concentration determination was not made using rigorous methods; intermediate Cl concentrations were determined based on the range of “most available data” from the USGS National Water Information System from samples taken, in some cases, at a considerable distance from the mountain-front. This was considered acceptable because chloride concentrations in the basin-fill alluvium adjacent to the mountain-front in areas of plentiful data were found to change little along the groundwater flow path. Recharge estimates ranged from a low of 0.66% of precipitation in the Abo Arroyo drainage to 5.0% in the North Sandia Mountains.

Stone and McGurk (1985) used vadose-zone Cl measurements to perform CMB recharge estimates in Curry and Southwest Quay Counties, New Mexico. A very high bulk precipitation Cl concentration value of 2.38 mg L^{-1} was based on measurements made at the Clovis Agricultural Experiment Station. An annual precipitation value of 385 mm was used. Estimates were made using soil chloride data from Stone (1984), with precipitation values adjusted downward from 444 mm yr^{-1} and Cl concentrations upward from the previous use of 0.59 mg L^{-1} as measured in Amarillo, Texas, which had excluded dry (dust) deposition of Cl. Results of this revised method showed strong dependence of recharge on the “landscape setting”; in Curry County, an estimated 54% of precipitation became recharge over sand, 37% became recharge in sand hills, and 9% became recharge in playa floors.

Naus and others (2006) used well and river water samples to perform CMB recharge estimates for debris-flow aquifers in the Red River Basin of Northern New Mexico. Wells in close proximity to the apex of debris flow were chosen for sampling. Red River water samples were taken upstream from the local sewage treatment plant during an August 2001 low-flow

tracer-injection study. Two snow-sample Cl concentrations taken during March 2002 (0.3 mg L^{-1} to 0.4 mg L^{-1}) were considered usable for recharge calculations because they were consistent with values found by bulk precipitation Cl analysis in Anderholm (2001). The average Cl concentration (0.35 mg L^{-1}) from the two samples was used. The study found that groundwater recharge represented 7-17% of mean annual precipitation from wells in Capulin Canyon and the Hansen, Hottentot, La Bobita, and Straight Creek Basins, and 21% of mean annual precipitation in the Red River Basin.

Rawling and Newton (2016) estimated recharge in the Sacramento Mountains of New Mexico using groundwater CMB and the water table fluctuation (WTF) method. The authors used mixing analysis to assume an effective concentration of 0.55 mg L^{-1} (~7x wet concentration) in the Sacramento Mountains. Chloride/bromide ratios were used to account for the admixing of geologic chloride. A range of recharge as percent of annual precipitation (relative recharge) of 4 to 42% was found, yielding an average of 22%. This was applied to the approximate average annual precipitation in the mountains (~ 26 in.), which was reduced by 30% to account for precipitation that was assumed to be intercepted by the forest canopy and lost to evaporation before reaching the soil surface. Making the assumption that the principal recharge areas were in the mountains at or above 8,200 ft., a volumetric recharge rate of 43,230 acre-feet/year (AFY) was estimated.

McCoy and Blanchard (2008) investigated the spatial and temporal distribution of recharge to aquifers along the eastern slopes of the Sandia Mountains using a variety of methods, including CMB. The authors sampled five springs several times between March 2005 and December 2007. Significant increases in Cl concentrations in all springs between March and July 2005 appeared to be caused by high precipitation events in the prior three months. Cl concentrations then steadily decreased over the next 12 months. An effective Cl concentration of 0.30 mg/L , estimated by Anderholm (2001) was used. Groundwater recharge estimates ranged from 0.7 – 23 percent of annual precipitation. Rice and Crilley (2014) updated these recharge estimates to between 5.5 and 23 percent of average annual precipitation, based on CMB calculations for eight springs in the East Mountain area.

2.2.3 Numerical Simulations of Recharge

Two-dimensional and three-dimensional groundwater flow models are simplified representations of real hydrologic systems used to solve the partial-differential equations that govern groundwater flow. The efficacy of any model depends on the ability of the model to mimic aquifer anisotropy and heterogeneity that exists in reality. Models always fall short of representing a real system, and must make approximations and assumptions. Typically, workers in possession of groundwater observations (e.g., water table (head) levels, geochemical data, estimates of the physical properties of materials of which a groundwater system is composed) attempt to solve the governing equations over a discrete grid of cellular elements (each with its own set of properties) while maintaining agreement with observed data. Success in this endeavor allows a worker to predict the changes in a groundwater system when one or more of the aquifer inputs or outputs changes. Recharge is one of the model parameters addressed in these studies. Examples of two important modeling studies in New Mexico follow.

Plummer and others (2004) estimated groundwater travel times, delineated boundaries of groundwater hydrochemical zones, and constructed a 156 x 80 x 9 cubic element grid to model historic groundwater flow in the Albuquerque Basin and estimate both modern recharge and paleorecharge. Aquifer properties were compiled from previous work, including aquifer porosity, hydraulic conductivity, discrete low-conductivity faults, and groundwater age data from carbon-14 analysis. Once the flow-path of discrete groundwater parcels was found, the water was traced back to its recharge location. The model was calibrated by adjusting the geometry of the element grid until the model agreed with observed data. Regional recharge was estimated at 61,000 AFY over the region, about 5% of precipitation.

McAda and Wasiolek (1988) used a three dimensional finite difference model which represented the Santa Fe-area mountain front as a constant head boundary. In this study, recharge was adjusted during initial calibration efforts within the estimates made using water-budget analysis to bring the model into agreement with locally measured well head elevations. This represents a common aspect of recharge estimation made for the purposes of modeling groundwater flow: rather than making an independent estimate, the estimate is made within a reasonable range that leads to model-observation agreement. If recharge is the only parameter being solved, this isn't particularly problematic; yet in this case hydraulic conductivity (itself a highly variable property) is also being adjusted. Thus, as is the case in this study recharge estimation is subordinate to other model parameters which are themselves quite uncertain.

2.2.4 Maxey-Eakin Recharge Estimation Technique

In sparsely populated areas lacking the infrastructure to monitor the fluxes of each component of the water balance, or in hydrologic systems not yet extensively studied, the need of an areal recharge estimate for use in water resource planning may necessitate cursory recharge estimates. The Maxey-Eakin (or modified Maxey-Eakin) technique is often used in such efforts as a first approximation. Maxey and Eakin (1949) postulated that precipitation was directly proportional to recharge in a semiarid region and that with increasing precipitation over an area, an increasing proportion of that water infiltrates to become groundwater (Maxey and Eakin, 1949). It should be noted that the specific correlations between precipitation and recharge used by Maxey and Eakin (1949) should not be used outside of the state of Nevada. For the best results, correlating average annual precipitation and recharge should be done independently for different areas. This technique has been shown to generally predict recharge within 50% of independent estimates in the arid and semiarid Southwest (Avon and Durbin, 1994) and has much precedent in the literature and use in the Southwest United States, so is often the method employed when a large area needs to be analyzed. The disadvantage is that this method assumes homogeneous conditions over a large surface area. Several of New Mexico's 16 WRPRs have not had large-scale studies performed; recharge estimates in the literature review for this study area were based solely on Maxey-Eakin type estimates.

Daniel B. Stephens and Associates (DBS&A), a private environmental consulting firm based in Albuquerque, NM used a modified Maxey-Eakin approach to estimate recharge in Colfax, Socorro-Sierra, Southwest New Mexico, Mora-San Miguel-Guadalupe, Northeast New Mexico, and Taos WRPRs (DBS&A, 2003, 2005a, 2005b, 2007). The area of each region was classified according to estimated precipitation amounts (i.e. 0 to 8 inches, 8 to 12 inches, 12 to

15 inches, 15 to 20 inches, >20 inches) and the total area falling within each range calculated. The area was then multiplied by an estimated percentage of precipitation that becomes recharge (i.e., 0%, 3%, 7%, 15%, 25%), according to the precipitation range in which it falls. The results were summed to find total recharge for the region. In all cases, the firm used published recharge estimates within the WRPR as a basis for the classification of percent of precipitation that infiltrates as recharge. Many of these estimates were themselves derived from Maxey-Eakin approaches.

2.2.5 Lumped Parameter Modeling

Lumped parameter models are those in which an entire hydrologic unit (e.g., basin) is represented by a single equation, or a few equations rather than using a spatially distributed grid of individual elements. In a lumped parameter model, spatially distributed parameters (e.g., precipitation, runoff, temperature) are replaced with a mean or aggregated value. Lumped parameter models have the advantage of reducing the need for large data inputs and the extensive model building necessary to sufficiently represent the physical reality of a hydrologic system. This simplification comes at the cost of detail; processes may be represented by a single term (e.g., runoff) that fails to quantify the importance of a particular sub-process operating at a smaller scale (e.g., saturated overland flow).

In New Mexico, where high mountain ranges with significantly higher precipitation than the surrounding basins drain through intermittent and perennial stream channels onto broad alluvial piedmont deposits, mountain-front recharge can be a significant portion of recharge. This mountain-front streamflow is often considered “potential” recharge. While the fraction of streamflow that is not lost to evaporation may be unknown, the streamflow itself is an important parameter in estimating focused recharge. Waltemeyer (1993, 2001) used two streamflow regression methods to estimate streamflow at or near mountain-fronts in the Tularosa Basin in southern New Mexico. In the Basin-Climatic Characteristics Method, 13 stream gauging sites were chosen, the basins above the gauges were delineated to find total area using GIS, and mean precipitation for the basin was found using U.S. Weather Bureau maps. A regression equation with standard error of 46 percent was then used to calculate the expected flow of 46 ungauged channels. Using the Channel-Geometry Characteristics Method, the active-channel width of 12 channels was used as the sole independent variable to derive a regression equation for stream flow. This equation was found to have a standard error of 26%.

CHAPTER 3. SOIL-WATER-BALANCE MODELING

3.1 Background

Despite long-term and systematic measurement of other components of the water budget such as precipitation and stream flow, accurate estimation of recharge is hindered by difficulty in closing the water budget by finding a reasonable method to estimate distributed evapotranspiration (ET) over large areas. The variation of evapotranspiration and thus recharge by infiltration varies to a great degree over space depending on topography, elevation, vegetation, soil characteristics, bedrock geology, rainfall intensity, and radiation, among other factors. With the advent of powerful Geographic Information Systems (GIS), integrating components of the water budget over large areas has become possible, but finding accurate estimates of water budget components remains a challenge.

One effective physically based approach to modeling the water budget in order to find recharge over large areas is by soil water balance (SWB). Soil-water-balance models have been utilized to find recharge in the arid and semiarid southwest United States. Efforts by Flint and Flint (2007) and Hevesi (2003) have attempted to constrain the water balance by using some combination of radiation, soil and bedrock characteristics, vegetative cover, and distributed climatic data to estimate runoff, recharge, and evapotranspiration.

A SWB model is a physical model of the pedosphere (i.e., soil layer) in which the soil acts as a reservoir for water. A control volume of soil, typically a discretized grid cell representing a definite area of the surface of the earth is the basis for the model. Inputs can include rainfall, on-flow of running surface water from adjacent cells, irrigation water, and snowfall. SWB accounts for and adds the inputs to the control volume. The model serves to partition the input between storage in the soil reservoir, loss to evaporation and transpiration, loss to deep percolation (recharge), and surface runoff. Typical assumptions of the soil-water-balance model are that the water in the control volume does not flow laterally to adjoining control volumes, and that the vadose (unsaturated) zone is only as thick as the soil layer, i.e. any water that percolates beyond the depth of the soil becomes recharge. Studies of the vadose zone in the southwest show that the unsaturated zone can be up to hundreds of meters in thickness (Flint et al., 2002). Lateral flow of groundwater is an important source of discharge to surface-water bodies by excess saturation flow, and can provide significant water for transpiration and evaporation at topographical depressions (Guentner et al. 1999). Assumptions are thus unrealistic physically in some cases, but are necessary to maintain a simple model and probably have a small effect over large areas in arid climates.

3.1.1 Basin Characterization Model

Flint and Flint used the Basin Characterization Model (BCM) to quantify potential recharge first in the Basin and Range Carbonate Aquifer System of White Pine Counties, Nevada and adjacent areas (2004) and then at a larger, regional scale (2008) for a large part of the southwest US. The BCM uses spatially distributed parameters discretized to a 270 m grid.

Inputs include a 30 m resolution DEM resampled to 270 m. The National Resources Conservation Service's STATSGO soils database was used for distributed soil thickness and to derive necessary soil physical parameters. Soil-water-storage capacity is calculated as the product of soil thickness and porosity, after Topp and Ferre (2002). Soil water content at field capacity (i.e., amount of water retained after drainage per volume soil at -0.1 MPa) and wilting point (water content at which most plants can no longer transpire, -6.0 MPa) were calculated after Campbell (1995).

Vegetation was cited as an input in Flint and Flint (2007b) but no precise description of how it was incorporated into the model was found.

Geology was integrated into the model through the use of GIS to incorporate geological data from state geological maps: California: Jennings, 1977; Idaho: Johnson and Raines, 1996; Nevada: Stewart and others, 2003; Utah: Hintze and others, 2000. These map resources were low resolution (1:500,000 to 1:750,000). Using data estimating saturated bedrock (and unconsolidated alluvial material) hydraulic conductivities (K) from the literature, a table was compiled which classified hydraulic conductivity according to rock type. Of the Quaternary alluvial deposits, the highest K was assigned to eolian (windblown sand) and gravel deposits, while clayey lacustrine, fine grain silt, and playa surface deposits were assigned the lowest K values of the basin-fill sediments (Flint et al., 2011). Carbonates and sandstone have among the highest K values for bedrock (Bedinger and others, 1989). Where carbonate bedrock is fractured and/or weathered to a high degree, the conductivity can approach that of unconsolidated basin sediments (Winograd and Thordarson, 1975; Dettinger and others, 2000). Intrusive and metamorphosed rocks have among the lowest conductivities (Davis and DeWiest, 1966; Freeze and Cherry, 1979). Many volcanic flows are rough and have high vesicular density, allowing for high conductivity, yet not as high as unconsolidated basin fill sediments (Glancy, 1986; Winograd and Thordarson, 1975).

Soil water accounting in the BCM is performed on a monthly basis. PRISM precipitation data are used to find rainfall and snow amounts. Precipitation falling as snow (temperatures under 0°C) remains in storage, losing water to sublimation at 5 mm per month. Snowmelt is treated as precipitation and is calculated by the NOAA SNOW-17 model (Anderson, 1976) as a function of air temperature and an empirical melt factor. Precipitation falling as rain (precipitation during temperatures in excess of 0°C) is allowed to enter the soil control volume. Since the purpose of this model is to simulate recharge in natural settings and the BCM calculates in-place recharge, surface run-on and irrigation are ignored (Flint et al., 2004). The total water storage capacity is calculated as the product of porosity and soil thickness. Available storage is water storage capacity minus antecedent soil moisture from the previous month. Total incident precipitation is thus limited by the infiltration rate (saturated soil hydraulic conductivity); any precipitation in excess of this amount is deemed runoff. Water meeting the evaporative demand as calculated by potential evapotranspiration (next section) is subtracted from the available water. The remaining water is available to infiltrate as groundwater recharge. The water draining as recharge is constrained by the saturated hydraulic conductivity of the bedrock. An excess of the evaporative demand and monthly infiltration to bedrock and soil storage is also deemed runoff. Runoff is not routed over the surface to other cells or a "channel" but is simply added to the total runoff of the area of interest.

Calibration of the BCM is complex, as there is considerable uncertainty associated with each of the data inputs (Flint and Flint, 2011). Snow accumulation was compared with data from the Moderate Resolution Imaging Spectroradiometer (MODIS), elevations of snow were observed and the temperature at which snow melts was adjusted to maintain fidelity to the observed snowpack density and duration (Lundquist and Flint, 2006). Temperature of melting was adjusted to 1.5°C. Calibration of recharge estimates was performed by modifying the saturated hydraulic values of the bedrock, considered a particular source of uncertainty. Some 67 hydrographs from 44 streams were used to find actual runoff minus calculated base flow and results were compared to modeled runoff. Complexity in the calibration was encountered due to the heterogeneous nature of watershed geology, as each watershed contained mixed geology. As the saturated hydraulic conductivity of each geological unit was held constant across the study area, calibration in one watershed led to error in others (Flint et al., 2011).

Uncertainties in the BCM result from the great spatial variability encountered in the physical attributes of the variables used (soil, geology, etc.) and low spatial resolution of those attributes in the input data sets. In sensitivity analysis, temperature was adjusted over the whole domain by an increase and a decrease of 3°C, increase and decrease in soil thickness of 10 cm, precipitation increase and decrease of 5%, and testing of the sublimation rate set at 10% and 50% of potential evapotranspiration. Many of these small changes (within the uncertainty of some data sets) caused predicted recharge to change by over 100%. The scale of the geological maps decreases the spatial variability inevitably found in nature; small outcrops, faults, fractures and other important geological features are ignored at the model scale.

3.1.2 INFILv3 USGS Model

Hevesi and others (2003) used the United States Geological Survey distributed parameter watershed model INFILv3 to estimate infiltration rates on a daily time step at Yucca Mountain and the surrounding Death Valley region in southern Nevada and eastern California. The purpose of the model was to find modern infiltration rates as well as infiltration rates based on hypothetical future climates. Recharge is an important factor in quantifying the exposure to moisture of a deep nuclear waste repository proposed in the tuff of Yucca Mountain. The efficacy of the INFIL model was questioned after adherence to the quality assurance methods was put in doubt (NWTRB, 2007). This model was succeeded by another similar model, MASSIF (Mass Accounting System for Soil Infiltration and Flow; (Sandia National Laboratories, 2007) by Sandia National Labs that was created in order to check the results from INFIL, but was deemed less effective at estimating infiltration by the U.S. Nuclear Waste Technical Review Board due to the insufficient use of available data (NWTRB, 2007). This model has since been emulated and improved upon in private industry, specifically by Daniel B. Stephens & Associates (Distributed Parameter Watershed Modeling System; DPWM). The DPWM allows for variable grid size, the use of model precipitation inputs (e.g., PRISM), and has options for snowmelt and sublimation (Hendrickx et al., 2016).

The INFIL model used daily climate records from 132 weather stations spread through the region, with a high concentration of instruments around Yucca Mountain in the Nevada Test Site. Monthly atmospheric properties were derived from NOAA data. The digital map files (DEM) were used to find topographic characteristics for each of the grid cells that included

dozens of metrics including aspect, hillslope, shading, ridge shading, etc. Soils data were derived from the STATSGO database. Vegetative cover was used to distribute a root density over the five soil layers, such that the evaporative and transpirative demand increased toward the surface, and the lower layers behaved as a more conservative moisture reservoir. Vegetation and bare soils data were collected from the National Gap Analysis (Jennings, 2000).

The INFIL model utilizes five core subroutines that deal with the important physical quantities and other subroutines that allow for user defined discretization, constants, output selection, statistical analysis, etc. The five subroutines are: DAYDIST, to interpolate daily precipitation and temperature for each cell; POTEVAP, potential evapotranspiration calculation; SNOW, snowfall, melting, and sublimation calculations; ETINFIL, root-zone infiltration and actual evapotranspiration calculations; and SWINFIL, soil water runoff and infiltration calculations (Hevesi, 2003). The control volume for the model makes the same assumptions as that of the BCM about the infiltration of water to the groundwater system as recharge upon drainage out of the lower soil layer. Incident precipitation is partitioned on the basis of a maximum infiltration rate to the soil surface based on the soil characteristics, from which wilting point, field capacity saturation, and porosity have been derived. A function to calculate storm intensity takes advantage of finer discretization of a daily time step. Thus the intensity of precipitation is modeled more realistically, as each day another calculation of change in storage can be made. Precipitation in excess of the rate allowed by the soil saturated hydraulic conductivity is routed as runoff. In contrast to the BCM, runoff is routed to adjacent cells and eventually an exit, much as surface water runoff moves in nature. Each of six soil layers in the control volume is allowed a portion of the drainage of the overlying soil layer or the surface, as controlled by its conductivity. The water is moved downwards, and output of the water from the system is a function of the drainage through the final layer into the bedrock or underlying unconsolidated material at the rate of the corresponding bedrock saturated hydraulic conductivity, and evapotranspiration (see next section).

Calibration of the INFIL model was conducted using trial-and-error to fit the simulated streamflow to measured streamflow as recorded in Death Valley. Evaluation of the INFIL model was completed by comparing model estimates of net infiltration with previous estimates of groundwater recharge (Hevesi et al., 2003). The process of running the model, comparing streamflow estimates, and comparing basin-wide recharge estimates was iterated until the closest fit to known data from the Death Valley Regional Flow System was found.

3.1.3 Model Estimates of ET

Evapotranspiration (ET) is the process whereby liquid water vaporizes and re-enters the atmosphere, either by evaporation from the surface of an open water body, the wet surface of a solid or soil matrix, through sublimation of ice or snow, or by transpiration through the stomata of a leaf during plant respiration. In many places in the US southwest, most precipitation is returned to the atmosphere as ET. ET is notoriously difficult to measure; unlike precipitation, where the quantity to be measured can be made to accumulate in some control volume and can easily be recorded, ET must be measured by proxy (Allan, 1998). Several methods are available for point measurements of ET: sap flow in trees (Wilson et al., 2001), weighing lysimeters (Burman et al., 19875), eddy covariance (Williams et al., 2004), and scintillometers

(Hemakumara et al., 2003) are all relatively common methods used in forest, agricultural, and mixed vegetation settings, respectively.

ET measurement, while well established at a point scale, exhibits such extreme variability over small spatial scales that interpolating ET from point measurements is inadvisable. However, energy-related climatic parameters such as temperature and radiation are more easily interpolated or measured by satellite. ET depends on both available water and available energy, and workers have exploited the widespread use of distributed temperature and radiation data to solve the energy balance and estimate ET. Independent, energy-based estimates of ET can then be used in water balance calculations. In terms of energy:

$$R_n - G - \lambda ET - H = 0 \quad (1)$$

where R_n is net radiation, G is soil heat flux, H is sensible heat, and λET latent heat flux (Allen, 1998). Using instrumentation that records the net radiation, soil heat flux, and sensible heat, the radiation balance can be completed and the energy used in vaporization can be calculated. Using the ratio of energy to evaporated water (latent heat of evaporation), the latent heat flux can be converted to the equivalent depth or volume of water lost to the atmosphere through ET. In terms of the soil water budget in natural settings:

$$P - ET - R_{runoff} - R_{recharge} = \Delta S \quad (2)$$

where P is precipitation, ET is evapotranspiration, and ΔS is change in soil water storage. As ET appears in both of these equations, estimates can be made from an energy balance or from the water balance. The BCM and INFILv3 attempt to accurately estimate ET using the energy balance, then use this estimate to quantify available water for runoff and recharge.

3.1.3.1 Basin Characterization Model ET (PET) Estimate

Taking advantage of well-established methods to model incoming solar radiation using known constants, easily obtained data, and topographic parameters described by Flint and Childs (1987), the BCM uses a simple model for finding potential evapotranspiration. Potential evapotranspiration is defined as the equivalent depth of water that would evaporate from a “uniform saturated surface (Priestly and Taylor, 1972).” The BCM model uses the method described by Priestly and Taylor to employ net radiation to find the potential evaporation (PET):

$$PET = \alpha \cdot s / (s + \gamma) \cdot (R_n - G) / \lambda \quad (3)$$

where α is the Priestly-Taylor coefficient (1.26), s is the slope of the vapor-deficit curve, γ is the psychrometric constant, λ is the latent heat of vaporization, R_n is net radiation, and G is soil heat flux. To find net radiation, the BCM uses the radiation-balance equation from Shuttleworth (1993, Eq. 4.2.17):

$$R_n = K * (1 - a) + L_{in} + L_{out} \quad (4)$$

where K is incoming solar radiation, a is surface albedo (reflectance), and L is incoming and outgoing long wave radiation. As solar radiation is attenuated by ozone, water vapor, atmospheric pollutants, and is blocked by topographic features, methods described in detail in Flint and Childs (1987) are employed along with the integration of averaged data from the National Radiation Energy Laboratory (http://rredc.nrel.gov/solar/old_data/nsrdb/1961-1990) and detailed site geometry derived from the DEM product. Albedo is found by monthly-varying inverse square methods as described in Iqbal (1983). Outgoing long-wave radiation is found by use of the Stephan-Boltzmann radiative emission equation:

$$L_{in} \text{ or } L_{out} = \varepsilon \sigma T^4 \quad (5)$$

where L is long-wave radiation, ε is atmospheric emissivity for a clear sky, σ is the Stephan-Boltzmann constant, and T is air temperature for incoming long wave radiation or surface temperature for outgoing long wave radiation. Emissivity is also dependent on temperature according to the relation described by Swinbank (1963):

$$\varepsilon = 9.2 * 10^{-6} * T^2 \quad (6)$$

Potential evapotranspiration is a problematic metric to use as a component in the water balance of this model. As evapotranspiration is assumed to proceed at the potential rate for the entire month of each time step, evaporation reductions due to the distribution of soil water through a column of soil as the near-surface moisture evaporates are ignored. In desert environments, precipitation events are often short and intense. In this model, the entire monthly PET demand of a given soil control volume must be satisfied for any water to infiltrate. As the time step spans a month, it is likely that very few locations receive enough precipitation to overcome this demand and allow water to infiltrate past the soil layer thickness. An intense storm could temporarily satisfy the maximum saturated soil water capacity of a control volume, causing infiltration to the groundwater system at the rate of soil hydraulic conductivity despite the PET calculation predicting a greater potential evaporation that month than total precipitation. In this case, the temporal restrictions of the model cause possible infiltration events to be ignored in the monthly calculation. This assumption is however valid for some situations in the arid Southwest. Sandvig and Philips (2004) found that in areas of thick soils of semiarid central New Mexico, recharge rates were negligible. In the high mountain ranges of Nevada where the BCM

was applied, low temperatures and deep winter snowpack can lead to large amounts of available water during spring, potentially overcoming the PET of the spring months.

3.1.3.2 INFILv3 ET Estimate

The INFILv3 model takes a more complex approach to the calculation of ET by first using a modified Priestley-Taylor equation to find PET, then partitioning energy and water among the five layers of the soil profile in the model control volume with an empirical function of PET and soil water content to find actual evapotranspiration (Hevesi et al., 2003). As in the BCM, INFIL uses SOLRAD from Flint and Childs (1987), with monthly atmospheric data from the National Weather Service and DEM-derived site geometry to calculate incoming solar radiation on an hourly time step. The critical component in the INFIL model is the subroutine ETINFIL, in which the PET is used in an empirical but physically justified set of functions. ETINFIL makes a daily calculation using precipitation as input and runs through a four step routine to partition the water:

1. Initial runoff is calculated according to a constraint by the soil saturated hydraulic conductivity. A storm duration and intensity parameter is used to discretize the incidence of the precipitation, in order to constrain infiltration of water to the control volume.
2. Downward drainage according to the soil saturated conductivity and storage change for the five layers of the root zone is calculated.
3. ET from the root zone layers is calculated based on available energy and water.
4. Excess water in the lowest root-zone soil layer is released downward as infiltration according to the saturated hydraulic conductivity of the bedrock or underlying unconsolidated sediment. Excess water in the soil column at the end of the partitioning is calculated as saturated excess flow. Total runoff, net infiltration, and soil water storage are recalculated:

$$\Delta W_j^i = RI_j^i + I_j^i - DR_j^i - ET_j^i - RO_j^i \quad (7)$$

where ΔW_j^i is change in layer j water content, at grid element i , RI_j^i is infiltrated surface water run-on from the previous day, I_j^i is infiltration into layer j from above, DR_j^i is drainage through layer into the next layer, ET_j^i is ET from layer based on water content, root zone parameters and weighting function applied to PET, and RO_j^i is the contribution to layer j from run-on of surface water from adjacent cells. This equation is applied from the top soil layer to the bottom. Temporary storage terms allow excess water in the upper soil layers to be sequestered as lower

the lower layers' soil storage is calculated. If this water exceeds the remaining soil water storage capacity as well as the maximum daily recharge, it is routed as runoff.

Evapotranspiration is estimated for each soil layer successively through the soil thickness. The modified Priestly-Taylor coefficient, α , is adjusted based on the following function (eqn. 20, Hevesi et al., 2003):

$$\alpha' = \alpha(1 - e^{\beta\theta}) \quad (8)$$

where α' is allowed to vary from 1 to 1.5; and α is 1.26 (Priestly and Taylor, 1972). β is a user-defined empirical coefficient, usually set to -10.0. θ is relative saturation (eqn. 21, Hevesi et al., 2003):

$$\theta = \frac{\theta - \theta_r}{\theta_s - \theta_r} \quad (9)$$

where θ is volumetric soil water content, θ_r is residual soil water content at wilting point, and θ_s is saturated soil water content (porosity). In ETINFIL the modified form of the Priestly-Taylor equation is used (with α') for both bare soil evaporation (BSE) and transpiration. The bare-soil evaporation coefficient is calculated for the top two layers of soil (Hevesi et al., 2003; Eq. 22):

$$BSE_j^i = \left\{ BSEA * \left[1 - e^{BSEB * \theta_j^i} \right] \right\} (1 - VEGCOV^i) (PETE_j^i) \quad (10)$$

where BSE_j^i is daily bare soil evaporation, $BSEA$ is 1.04, the “standard” value used for bare soil surfaces, expressed as α above, $VEGCOV^i$ is estimated vegetation cover, and $PETE_j^i$ is potential evapotranspiration rate; this is set to PET on the top layer, and $PET - BSE$ for the second layer. BSE from the first and second layers is subtracted from the available energy for transpiration (Hevesi et al., 2003; Eq. 23):

$$PETT_o^i = (VEGCOV^i * PET^i) - (BSE_1^i + BSE_2^i) \quad (11)$$

where $PETT_0^i$ is the available energy for transpiration and PET is from the modified Priestly-Taylor equation. This step accounts for the energy already expended in the evaporation from bare soils and applies remaining available energy to potential transpiration, according to the fraction of vegetated land surface.

Simulation of transpiration uses a root-density weighting factor for each layer and distribution of water in each layer. The ET simulation is applied successively from the top layer downwards (Hevesi et al. 2003, Eq. 24):

$$ET_j^i = WGT_j^i \left(ETA \left[1 - e^{ETB * \theta_j^i} \right] \right) * PETT_j^i \quad (12)$$

where ET is actual transpiration from each root layer, WGT is the weighted product of root zone density and relative soil saturation, ETA is a user-defined empirical coefficient, ETB is β from above (-10.0), and $PETT$ is potential transpiration. Each successive layer is limited in available energy for transpiration by what was available as potential transpiration in the previous layer minus what was actually transpired (Hevesi et al., 2003, Eq 26):

$$PETT_j^i = PETT_{j-1}^i - ET_{j-1}^i \quad (13)$$

thus the top layers expend available energy on transpiration first, and the residual available energy for transpiration is passed onto the lower root zones.

This formulation of ET is physically based yet relies on many user-defined empirical coefficients in order for the soil water and available energy to be constrained. The physical reality of bare soil evaporation playing a large part in the partitioning of available energy after a rainfall is realistic, as is the assumption that the soil surface will dry sooner than the deep soil layers. This model makes the assumption that root zone density is highest near the surface, and that the density of rooting decreases with depth. This assumption is valid in many cases, but may be unreliable in the case of certain desert plants that derive a larger percentage of transpired water from the deep soil layers. Certain aspects of soil physics, such as later flow, vapor flow, varied hydraulic gradients, capillary forces and variation in the density of water as a function of temperature were not included in the model.

3.1.4 Dual Crop Coefficient Method

The well-established FAO Penman-Monteith method finds a reference evapotranspiration value with which actual transpiration can be derived by calculating a stress factor coefficient (K_s), a basal vegetation transpiration coefficient (K_{bc}), and a bare surface evaporation coefficient (K_e). This method is known as the dual-crop-coefficient method (Allan et al., 1998). Jensen and others (1990) found that of 20 ET estimation methods, results varied considerably in varying

climates and showed the need for rigorous and expensive calibration methods when a method developed in one climate was then applied to another. The FAO Penman-Monteith was devised in the 1990s as a method that needed less rigorous local calibration than other, more empirical and local methods such as the BCM and INFIL. The operational goal of the method is to find a constrained and reasonable estimate of ET with a minimum of climate data inputs. The method contains many possible variations to allow for the continuation of the ET calculation despite missing or incomplete data. Jabloun and Sahli (2008) found that use of FAO-56 recommended methods of calculating ET with missing data produced results close to those found using complete data.

The Penman-Monteith equation was used to find evapotranspiration from crop or bare surfaces using climate records that included wind speed, humidity, temperature, and radiation terms. The equation has since been modified to include resistance factors allowing application of the equation to crops. Eventually a combination equation was formulated that included most of the variables that affect the rate of energy exchange and latent heat transfer. This formulation is known as the Penman-Monteith Equation (Allen et al., 1998; Eq. 3):

$$\lambda ET = \frac{\Delta(R_n - G) + \rho_a c_p \left(\frac{e_s - e_a}{r_a}\right)}{\Delta + \gamma\left(1 + \frac{r_s}{r_a}\right)} \quad (14)$$

where Δ is the slope of saturation vapor pressure vs. temperature [kPa °C⁻¹] at the ambient temperature, ρ_a is mean air density at constant pressure [kg m⁻³], c_p is the specific heat of water at constant pressure [MJ kg⁻¹ °C⁻¹], $(e_s - e_a)$ is the difference between saturated and actual vapor pressure [kPa] at 1.5 to 2.5 m height, r_a and r_s are the bulk aerodynamic and surface resistances [s m⁻¹], R_n is net radiation [MJ m⁻² day⁻¹], G is the ground heat flux [MJ m⁻² day⁻¹], and γ is the psychrometric constant [kPa °C⁻¹].

In FAO-56, Allen and others used natural relationships, approximations, and mathematical simplifications to reduce the form of the original Penman-Monteith equation to the modified, FAO Penman-Monteith equation, which calculates reference ET (ET_{ref}) for both standard short (ET_o) and long crops (ET_r). ET_r is defined as the rate of ET in conditions "...when the alfalfa crop was well watered, actively growing, and at least 30 cm tall; so that measured ET was essentially at the maximum expected level for the existing climatic conditions" (Wright, 1982). Allen and others (1998) assume a fixed crop height of 0.5 m; Chapter 2, Eq. 6:

$$ET_r = \frac{0.408\Delta(R_n - G) + \gamma \frac{900}{T + 273} u_2 (e_s - e_a)}{\Delta + \gamma(1 + 0.34u_2)} \quad (15)$$

where ET_r is reference ET [mm day^{-1}] for a long crop with fixed resistance and albedo, and u_2 is the wind speed at 2 m above the surface [m s^{-1}]. The FAO Penman-Monteith equation requires radiation, air temperature, wind speed, and humidity for daily calculations.

Actual evapotranspiration is calculated using the dual-crop coefficient method (Allen et al., 1998):

$$ET_a = [K_s K_{cb} + K_e] ET_r \quad (16)$$

where ET_a is actual evapotranspiration [mm day^{-1}], K_s is the crop stress factor, K_{cb} is the basal crop coefficient, and K_e is evaporation crop coefficient. This equation is designed to reduce the reference ET from a maximum value, and decrease ET_a according to the stress a crop is experiencing, the evaporative skin effect of the surface, and reduced basal transpiration due to non-reference conditions.

The psychrometric constant is calculated according to the following formulation (Allen et al., 1998):

$$\gamma = \frac{c_p P}{\varepsilon \lambda} \quad (17)$$

where γ is the psychrometric constant [$\text{kPa } ^\circ\text{C}^{-1}$], c_p is the specific heat of water at constant pressure [$1.013 \times 10^{-3} \text{ MJ kg}^{-1} \text{ } ^\circ\text{C}^{-1}$], P is atmospheric pressure [kPa], ε is the ratio of molecular weight of water vapor to dry air (0.622), and λ is the latent heat of vaporization of water [2.45 MJ kg^{-1}].

Average saturation vapor pressure is calculated as a function of air temperature (Allen et al., 1998; Eq. 11):

$$e_a = 0.6108 \exp \left[\frac{17.27T}{T + 273.3} \right] \quad (18)$$

where e_0 is saturation vapor pressure [kPa] at temperature T [$^\circ\text{C}$]. Using e_0 , actual vapor pressure can be calculated with relative humidity data (Allen et al., 1998; Eq. 17):

$$e_a = \frac{e_0[T_{min}] \frac{RH_{max}}{100} + e_0[T_{max}] \frac{RH_{min}}{100}}{2} \quad (19)$$

where RH_{max} is maximum relative humidity and RH_{min} is minimum relative humidity. If only a maximum relative humidity is available, e_a can be calculated (Allen et al., 1998, Eq. 36):

$$e_a = e_0[T_{min}] \frac{RH_{max}}{100} \quad (20)$$

The basal crop coefficient (K_{cb}) is the fraction of potential transpiration from a reference surface of a reference crop. K_{cb} can be adjusted for plant height, daily wind speed, and relative humidity. (Allen et al., 1998, Eq. 62 and 100):

$$adj = [0.04(u_2 - 2) - 0.004(RH_{min} - 45)] \left(\frac{h_{plant}}{3} \right)^{\frac{1}{3}} \quad (21)$$

where h_{plant} is the mean maximum height of the vegetation, with value allowed up to 2 m, which should be estimated from general field observations (Allan et al., 1998, p.124).

The leaf area index is a method by which the ratio of surface area of leaves to ground surface is estimated. Using the Leaf Area Index (LAI) function, the LAI is used to find mid-season K_{cb} (Allen et al., 1998, Eq. 97):

$$K_{cb\ mid} = K_{cb\ min} + [K_{cb\ full} - K_{cb\ min}] [1 - \exp[-0.7LAI]] \quad (22)$$

where $K_{cb\ mid}$ is mid-season basal crop coefficient in condition less than full coverage, $K_{cb\ full}$ is mid-season, full coverage basal coefficient, $K_{cb\ min}$ is minimum crop coefficient for bare soil (0.15-0.20). For an LAI of greater than 3.0 this equation gives results close to $K_{cb\ full}$ (Ritchie, 1983).

K_{cb} is then reduced according to the stomatal control factor (Allen et al., 1998, Eq. 102):

$$F_1 = \frac{\Delta + \gamma(1 + 0.34u_2)}{\Delta + \gamma(1 + 0.34u_2 \frac{r_1}{100})} \quad (23)$$

where r_1 is the mean leaf resistance for the vegetation in question [$s m^{-1}$]. Values for various vegetation types are found in Körner and others (1978) and Allen (1996). If the calculated value is greater than maximum K_{cb} according to reference conditions (Allen et al., 1998, Eq. 72), then the maximum basal crop coefficient is constrained by local climatic conditions:

$$K_{c \max} = \max\left(\left\{1.2 + [0.04(u_2 - 2) - 0.004(RH_{\min} - 45)] \left(\frac{h}{3}\right)^{0.3}\right\}, \{K_{cb} + 0.05\}\right) \quad (24)$$

where h is average maximum plant height during the part of the growing season in question, and \max indicates the selection and use of the higher of the two terms in the brackets, separated by a comma.

If the vegetative ground cover is not constant over the area in question, it is computed (Allen et al., 1998, Eq. 76):

$$f_c = \left[\frac{K_{cb} - K_{c \min}}{K_{c \max} - K_{c \min}} \right]^{1+0.5h} \quad (25)$$

where f_c is the fraction of the ground with vegetative cover, and $K_{c \max}$ is the maximum K_{cb} following wetting.

Once K_{cb} has been adjusted, a check is performed; if the $K_{c \max}$ is lower than K_{cb} , $K_{c \max}$ is returned for use.

To find the evaporation crop coefficient, a function is used to estimate the reduction in evaporation as the soil dries after having been wetted. As the soil surface behaves as a barrier to diffusive evaporation, rapid, reference-like evaporation is short lived. Once the soil surface has dried, evaporation from the bare soil slows rapidly (Allen et al., 1998, Eq. 71):

$$K_e = \min(K_r [K_{c \max} - K_{cb}], f_{ew} K_{c \max}) \quad (26)$$

where K_e is the soil evaporation coefficient, K_r is the evaporation reduction coefficient, $K_{c \max}$ is the maximum value of K_c after wetting, and f_{ew} is the fraction of wetted soil.

$$K_r = \min\left(\frac{TEW - De}{TEW - REW}, 1.0\right) \quad (27)$$

where TEW is the total evaporable water, De is the depth of evaporation in the evaporable layer, and REW is the readily evaporable water within the top 100 mm of soil, the difference of field capacity water content and one-half wilting point soil water content. The TEW and REW represent water storage capacity that can contribute to stage-one and stage-two evaporation.

A transpiration reduction coefficient is included to calculate relative saturation of the soil in the root zone and reduce the transpiration rate as soil saturation decreases:

$$K_s = \min\left(\frac{TAW - Dr}{TAW - RAW}, 1.0\right) \quad (28)$$

where TAW is the maximum total available water for transpiration, Dr is root-zone moisture depletion, and RAW is readily available water for transpiration.

CHAPTER 4. EVAPOTRANSPIRATION AND RECHARGE MODEL

4.1 Introduction

In New Mexico, adequate understanding of current groundwater recharge fluxes has been hindered by the application of disparate estimation methodologies and the lack of coherent large-scale efforts that represent the entire hydrologic system at the surface. Recharge is often used as an adjustment for closing regional water budgets or is used as a variable for calibrating groundwater flow models, but is less often the focus of thorough studies. In the past, recharge has been difficult to study due to lack of relevant physical data: precipitation, energy, topography, and vegetation vary to an extreme degree over the state, making large-scale spatial generalizations of recharge processes impossible. In the absence of high quality data inputs and the computational power needed to analyze them, most efforts at recharge estimation have been limited in scope. As most of the area of the state has an arid or semiarid climate regime, recharge may be temporally sporadic and spatially highly variable and in many places there is none. Furthermore, recharge is generally a small-to-very-small component of the total water budget; any errors in calculation of the major fluxes (i.e., precipitation and evapotranspiration) may result in unreasonable recharge estimates. Only recently have most important physical parameters been constrained by robust models that interpolate climatic data between observations or which use high-resolution and frequent remote sensing products to estimate surface physical parameters. As the surface conditions that control recharge processes are spatially and temporally heterogeneous, a model that accounts for recharge via a spatially distributed approach at a short time step is desirable. Soil water balance is an obvious modeling approach for the problem of estimating recharge, as soil represents the interface between the atmosphere and the groundwater system. The soil layer is the critical zone at which all processes

affecting recharge interact and thus provides a physical domain where these processes can be simulated and recharge estimates made.

Previous estimates of recharge using distributed soil water balance have either used large amounts of expensively gleaned local data to parameterize and calibrate relatively complex models (e.g., Yucca Mountain, Hevesi; 2003); or have used overly simplified methods for finding actual evapotranspiration (e.g. Basin Characterization Model). In this study, the Evapotranspiration and Recharge Model (ETRM) was created with the aim of maintaining a representation of the soil layer over the entire state that is sufficiently simple to be computationally reasonable, while retaining the capability of incorporating the latest gridded datasets from interpolated and remotely sensed sources. This model uses daily inputs of precipitation, reference ET, temperature, vegetation density, and derived soil physical parameters to perform a daily soil water balance using a modified FAO-56 dual-crop-coefficient method of estimating ET. Most importantly, this model is constrained by energy and water at all time steps and over the entire model domain.

4.2 Materials and Methods

The ETRM is designed to solve the soil water balance in three layers of soil on a daily time step. The three layers of soil represent three possible processes by which the soil can lose water to vaporization: stage-one evaporation from the “skin layer”: the surficial layer of soil that has relatively direct communication with the atmosphere, stage-two evaporation via slow diffusion from deeper in the soil profile, and transpiration through plant respiration. The maximum stored water available within each of these layers when at field capacity (0.33 bars matric pressure) is termed readily evaporable water (REW) for stage-one evaporation, total evaporable water (TEW) for stage-two evaporation, and total available water (TAW) for the transpirative layer, or root zone. A daily calculation of the depletion of these layers is performed by the ETRM, modified after Allen (2005, 2011):

$$Drew_i = Drew_{i-1} + RO + E - P - MLT \quad (29)$$

$$De_i = De_{i-1} + E - P_{res} - MLT_{res} \quad (30)$$

$$Dr_i = Dr_{i-1} + R + T - P_{res} - MLT_{res} \quad (31)$$

where the subscripts i and $i-1$ denote the current and previous day, $Drew$, De , Dr are soil water depletions of the REW , TEW , and TAW soil layers, respectively. RO is runoff, E is evapotranspiration, R is recharge, P is precipitation, and MLT is snowmelt. P_{res} and MLT_{res} are residual water in excess of the overlying layer water capacity that have been transferred to the underlying soil layer. All terms are reported as depth of water in millimeters. Soil-water depletion is a convenient parameter with which to account for the water transfers from day to day. At any cell in the model extent, maximum soil-water capacity is estimated based on a combination of the National Resource Conservation Service soil surveys (see below); the

depletion term represents the depth of water that could be added by precipitation and melt to the soil layers before runoff and recharge begin. If depletion is zero, the soil is at field capacity. When the soil water balance is calculated, depletion from the previous day plus water loss from runoff, ET, and recharge defines a new soil depletion at each cell. Only when the soil depletion is negative (during prolonged or intense precipitation events) does recharge occur.

4.2.1 Modified FAO-56 Dual Crop Coefficient

In New Mexico, evapotranspiration consumes nearly all of the available water in most of the low-lying areas of the state; according to chloride mass balance results, it may consume over 85% of precipitation even in the relatively cool and humid mountains. The calculation of ET, therefore, is critical to estimate the water that is left for other processes. Furthermore, as the ETRM is designed to estimate ET in arid and semiarid natural environments, the reduction in ET due to water stress must be represented. The FAO-56, mentioned in the previous chapter, has been shown to constrain evaporation rates and correlate them to available energy and vegetative density.

The ETRM uses the dual crop coefficient in a modified form, excluding terms specifically applied to crops (e.g., irrigation inputs), and incorporating developments described in Allen (2011), namely the skin surface evaporation term (equation 29, 30). The formulation for finding reference ET (Chapter 3; Eq. 15 – 23) has been replaced by a modified reference ET (ET_{rs} ; see below). In order to reduce mass balance error, K_{cmax} has been set to $K_{cmax} = K_{cb} + 0.001$. The stage-one evaporation stress coefficient has been modified by approximating the fraction of the day during which evaporation proceeds at stage-one rates after a wetting event (Allen, 2011; Eq. 12):

$$F_t = \min\left(\frac{REW - D_{rew_{i-1}}}{ET_{rs}}, 1.0\right) \quad (32)$$

where F_t is the fraction of the day experiencing stage-one evaporation. K_e (Eq. 26) has been replaced with a stress coefficient combining residual water in the stage-one evaporation layer with water evaporated at the stage-two rate (Allen, 2011; Eq. 13a):

$$K_e = \min\left([F_t + (1 - F_f)Kr](K_{cmax} - K_s K_{cb}), f_{ew} * K_{cmax}\right) \quad (33)$$

where f_{ew} is the fraction of the soil surface exposed to direct sunlight.

TEW is found using the soil volumetric saturation at field capacity and wilting point, modified after Allen (2011; Eq. 8):

$$TEW = (\theta_{fc} - 0.5 * \theta_{wp}) * z_e \quad (34)$$

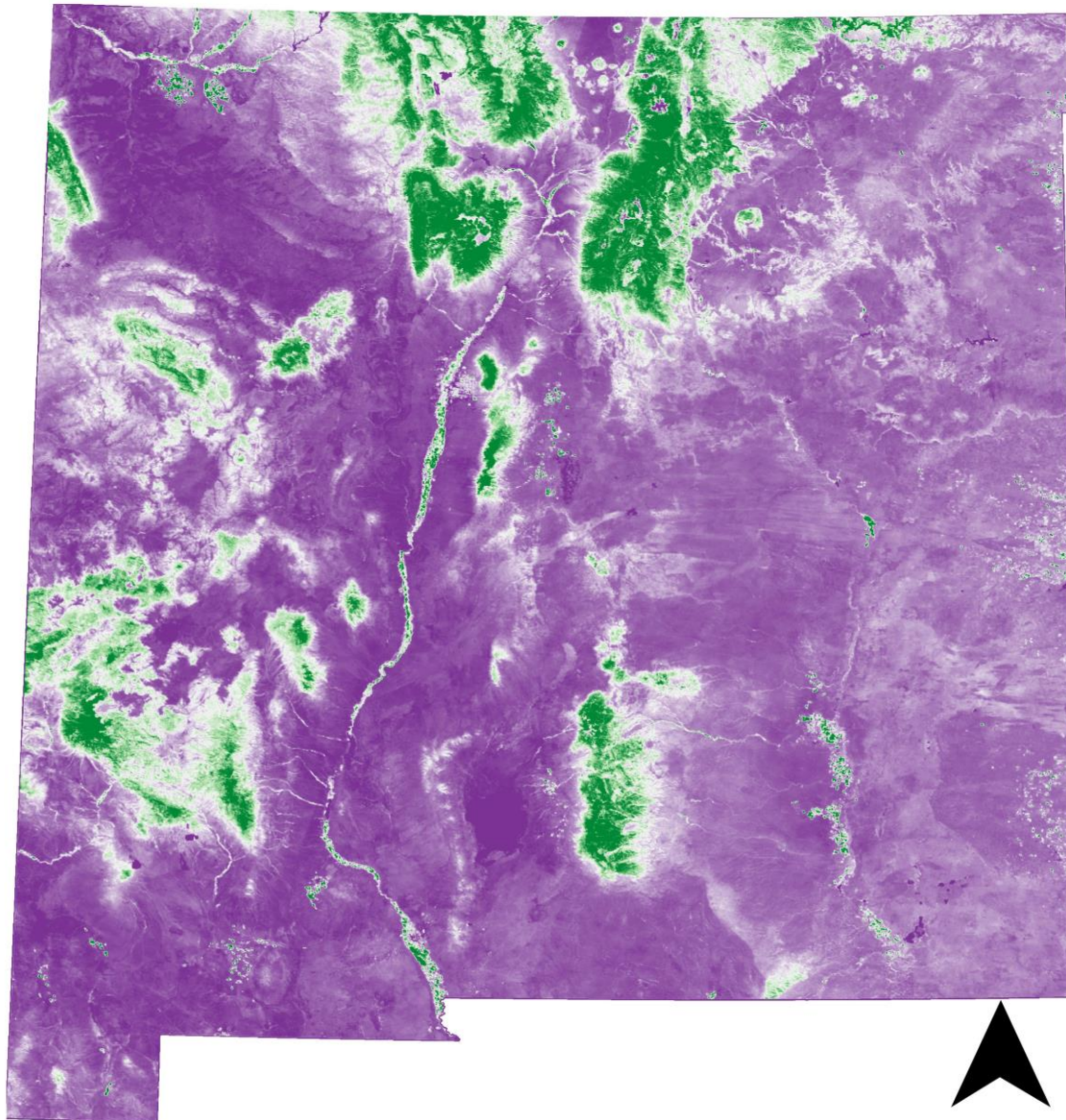
where θ_{fc} and θ_{wp} are volumetric water content at field capacity and wilting point, respectively, and z_e is the depth of the evaporation layer, set at 100 mm. REW depends on TEW , After Allen (2011; Eq. 10):

$$REW = \min\left(2 + \frac{TEW}{3}, 0.8 * TEW\right) \quad (35)$$

The ETRM uses remotely sensed Normalized Difference Vegetation Index (NDVI) from the Moderate Resolution Imaging Spectroradiometer (MODIS), a remote-sensing product that is increasingly used in agricultural areas (González-Dugo et al., 2009; Mateo et al., 2013; González-Dugo et al., 2013). The NDVI is computed using data acquired from MODIS satellites every 16 days. The ETRM uses a linearly interpolated data set weighted between the previous and subsequent available “images” (Figure 4.1). Agricultural areas are typically well watered and vaporize water at near or slightly above the reference ET rate. In areas of natural vegetation, the effect of soil-water stress on the stomatal control of transpiration by plants that have evolved to survive arid conditions reduces the ET rate, a response not fully accounted for in NDVI data (Glenn et al., 2011), but that the stress coefficients of the FAO-56 in the ETRM are designed to incorporate. The relationship used in this study is an approximation of that given by Hassan-Esfahani and others (2015):

$$K_{cb} = 1.25 * NDVI \quad (36)$$

This approximation of the relationship between K_{cb} and NDVI is an approximation, and thus a potential source of uncertainty, and is discussed below.



50 0 50 100 150 200 km

MODIS Normalized Difference Vegetation Index

Legend

NDVI 24 May 2011

- 0.11
- 0.23
- 0.35
- 0.46
- 0.58

Figure 4.1 The MODIS satellites collect images every 16 days over New Mexico. The ratio of near-infrared scatter to absorbed red light is normalized and used as a proxy for vegetation density. Green represents high vegetation density.

The reference ET found via the FAO-56 modified Penman-Monteith equation calls for seven environmental variables, each of which is easily obtained with instrumentation at experimental agricultural sites, agricultural water use being the principal focus of FAO-56 development. Over the large scale of the ETRM domain, however, the lack of instrumentation and the extreme topographic heterogeneity pose a serious challenge. Concurrent with this study a gridded, daily, topographically corrected, modified long-crop Penman-Monteith product (ETrs) was under development (ReVelle et al., in press; Figure 4.2).

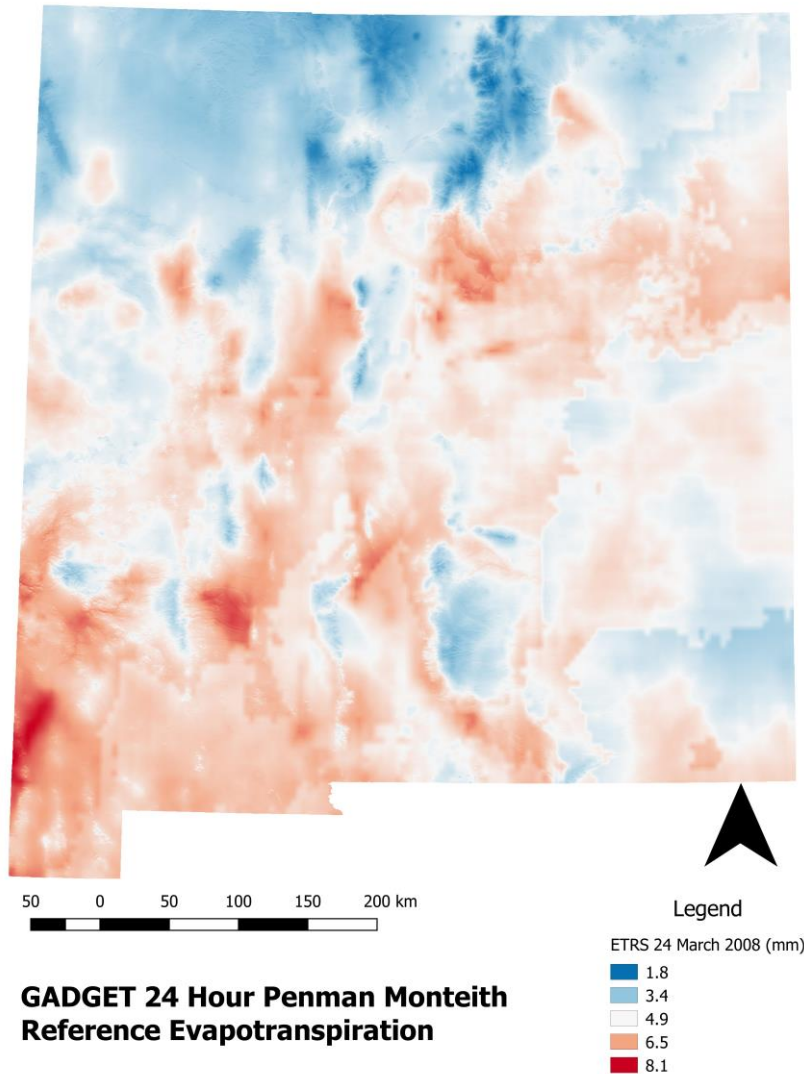


Figure 4.2 Gridded Atmospheric Data Downscaling Evapotranspiration Tools (GADGET) for High-Resolution Distributed Reference ET in Complex Terrain creates 250 m resolution gridded data representing tall-crop reference ET, the basis for energy-driven components of the ETRM. Red represents high reference ET.

In mountainous topography, variations in slope, aspect, and topographic shading over short distances cause corresponding variations in net solar radiation (Aguilar, 2010). It is critical that the energy component of the ETRM reflects this spatial variability by taking topography into account in the calculation of reference ET. This was achieved by a partner study under the WRRISWA that created the Gridded Atmospheric Data Downscaling Evapotranspiration Tools for High-Resolution Distributed Reference ET in Complex Terrain (GADGET) model. This model uses three operational gridded products: NLDAS, METDATA (see below), and a 30-m resolution DEM resampled to 250 m. PRISM and NLDAS were merged in METDATA to create a daily, 1/24° (~4 km) meteorological dataset (Abatzoglou, 2013). After Cosgrove and others (2003) and Abatzoglou (2013), this dataset was downscaled to 250 m using a lapse rate (6.5 K km⁻¹) and terrain-height adjustment for air temperature and barometric pressure. Specific humidity and downward longwave radiation were then used adjusted using the lapsed air temperature and barometric pressure by holding relative humidity constant (after Mitchell et al., 2004). GADGET provides a 250 m, daily ET_{rs} gridded dataset for use as the energy input for the ETRM. For further details, see Hendrickx and ReVelle (2016) and Appendix C.

4.2.2 Other Data Inputs

Note: for detailed explanation of the derivation of ETRM model inputs, see Appendix C.

Additional data inputs used by the ETRM include the 800 m gridded Parameter-elevation on independent Slopes Model (PRISM; Daly et al., 1997, 2008). PRISM is a sophisticated interpolation method that creates local regression equations that interpolate meteorological data using terrain information. This model has been shown to effectively account for precipitation and temperature over varying elevations, topographic aspects, cold air drainages, and coastal proximity, among other factors. The ETRM uses PRISM for model daily input temperature (used in the ETRM snow model only) and for model precipitation. Soil parameters, including field capacity volumetric saturation, wilting point saturation, and available water storage were obtained from the State Soils Geographic (STATSGO) Database (USDA, 1994) and Soil Survey Geographic (SSURGO) Database (USDA, 1995). This data is provided as polygons and were converted for use in the ETRM to a raster grid based on the predominant soil type over area of the grid cell. These data sets are extracted from the Soil Data Viewer in ESRI© ArcMap. The available SSURGO databases currently cover approximately 80% of the state of New Mexico. Where SSURGO data was lacking, STATSGO data was used in its place. This increased the scale of the soils layer used in the ETRM from 1:250,000 to between 1:12,000 and 1:63,000 with the larger scale SSURGO data. Using higher resolution soil maps has been shown to increase hydrological model accuracy (Mednick, 2010; Moriasi and Starks, 2010). This soils map was subsequently examined using SSURGO data where possible and replacing gaps in the data with STATSGO. The New Mexico Bureau of Geology 1:500,000 Geologic Map of New Mexico was used to classify areas where soils data indicated thin or absent soils, and where the geologic map represented Quaternary playa and alluvial deposits (NMBGMR, 2003). These areas are unlikely to transfer soil water frequently through the thick, unconsolidated material in these areas, and were given TAW values of 300 mm. Plant height and rooting depth were derived from the National Land Cover Dataset (NLCD; Homer et al., 2015). The NLCD classifies the US surface into 16 land use/land cover categories including natural and human-impacted land surface types.

The 30 m dataset was reclassified into rooting depth and plant height classifications after Zhou et al. (2006).

4.2.3 Snow Model

Note: For a detailed background and explanation of the ETRM snow model, see Appendix B.

In New Mexico, up to 23% of the state receives 10% or more of its precipitation in the form of snowfall, according to initial PRISM precipitation and temperature analyses. The occurrence of snow poses a special problem for soil water balance: the sequestering of a significant part of the total precipitation in a frozen reservoir over months and the release of that water in the spring have considerable implications for recharge. During the spring, the timing and rate of snow melt may have a great effect on recharge, because it is a time of year when the available energy is relatively low and the input of liquid water to the soil rapid.

Modeling snow melt is a difficult task and has been attempted on many scales using a variety of physical and empirical methods (Martinec, 1975; Anderson, 1976; Cazorzi and Dall Fontana, 1996; USACE, 1998; Hock, 1999; Hevesi, 2003). See Essery et al. (2013) for a description of many recent snow models and comparison of their performance and parameterization. Generally, snow modeling has fallen into two categories: models which solve the energy balance in the snow pack (Anderson, 1976; Koivusalo and Kokkonen, 2002); and models which use a temperature index (e.g., degree day factor) to estimate snow melt (Hevesi, 2003; Flint and Flint, 2008). Solving the energy fluxes in a snow physics model requires many physical input parameters and intensive computation, while temperature index models use readily available meteorological data and can be applied to large areas operationally. The ETRM uses a degree day factor (DDF) approach in combination with a shortwave radiation term in an attempt to approximate melting and to account for the varying energy availability over complex terrain.

Snow accumulation is simply computed adding any precipitation that falls when the mean daily temperature is below freezing to a snow reservoir using PRISM data. The snow layer is represented by snow water equivalent (SWE; [mm]). No attempt is made to simulate the evolution the snowpack in terms of density, depth, or texture. An albedo decay function continually reduces the albedo (i.e., reflectance) of the snow layer from 0.9 at the time of snow fall to a minimum of 0.45, according to the following function (after Rohrer, 1991):

$$a = a_{min} + (a_{prev} - a_{min}) * e^{-k} \quad (37)$$

where a is albedo, a_{min} is the minimum albedo of 0.45 (after Wiscombe and Warren; 1980), a_{prev} is the previous day's albedo, and k is the decay constant. The decay constant varies depending on recent snowfall; on days with subfreezing mean temperature k is set to 0.12, on days of above freezing temperature, k is set to 0.05, after Rohrer (1991). Any new snowfall of greater than 3 mm SWE resets the albedo to a maximum. During days of above-freezing temperatures, the snow melts according to the following formulation:

$$melt = (1 - a) * rg * \alpha + (T - 1.5) * \beta \quad (38)$$

where *melt* is snow melt in SWE, *a* is albedo, *rg* is incoming shortwave radiation [W m^{-2}], α is the radiation term calibration coefficient [-], *T* is temperature [$^{\circ}\text{C}$], and β is the temperature correlation coefficient. The snow model was calibrated using 23 of New Mexico's 27 Snow telemetry (SNOTEL) sites. For a detailed description of calibration methods, see Appendix C.4.

4.2.4 Model Simulations

The ETRM was coded in the Python computer language and set to run from 1 January 2000 through 31 December 2013, the dates through which both PRISM and NDVI data are available. Currently, the model is coded to perform simulations using publicly available and open source computational tools. The most important of these is the Geographic Data Abstraction Library (GDAL) by Open Source Geo, and the Numerical Python (“Numpy”) packages. The model also has versions written with the ArcPy proprietary python package created by ESRI©, which is slow and has rather opaque computational methods, but is more user friendly and is better documented than the open-source options. Runs included distributed-parameter simulations, in which all data inputs were standardized and resampled to a 250 m resolution. The resulting gridded data sets measure 2272 x 2525 cells, totaling 5,736,800 individual cells covering the 315,000 km^2 area of New Mexico. For calibration of the snow model, comparison with chloride mass balance sites, sensitivity analysis, and comparison with eddy covariance stations, a point scale ETRM was constructed. This serves the purpose of quickly running simulations with data that has been extracted from the gridded inputs and transferred to tabulated files. The ETRM was run from an initially dry soil condition for two years (2000-2001). The results from this “spin up” were used as the initial conditions for the 14-year simulation.

4.3 Results

Results of the ETRM simulation include recharge, ET, soil-moisture-storage change, total precipitation, and runoff for each month of each simulated year, each year of the simulation, and the 14-year simulation (2000-2013). Results are presented in the same standard grid the model uses as well as tabulated totals for each month, year, and 14-year simulation period. Results tables present totals for various geographical divisions in New Mexico: NM Office of the State Engineer declared groundwater basins, NM Interstate Stream Commission River Basins, NM Water Resources Planning Regions, NM counties, and the state as a whole.

Recharge rates are presented here as a percentage of precipitation that becomes recharge (“recharge index”). Recharge index varied from an annual mean of 0% to a high of around 83% on the summits of the highest peaks in the Sangre de Cristo Mountains near Santa Fe, with a statewide mean of 6.1%. There is zero modeled recharge over about 43% of the state; in 29.5% of the state, recharge index is between 1 and 10%; 10% of the state has a recharge index of 10 to 20%; about 3.5% of the state has a recharge index over 20% (Figure 4.3). In absolute terms, the statewide mean annual recharge from 2000-2013 was about 17 mm, with a range from a low of 0 mm to a high of over 850mm yr^{-1} around Truchas Peak, in the Sangre de Cristo Mountains, a

location that also received the statewide high of 1140 mm yr^{-1} of precipitation, according to PRISM data.

The fate of the vast majority of the precipitation in New Mexico is to be evapotranspired (Figure 4.4). Nearly 70% of the state loses more than 90% of precipitation to ET. Of the mean statewide annual precipitation of around $200 \text{ billion m}^3 \text{ yr}^{-1}$ (162 million acre-feet per year (MAFY)), 92.5% is lost to ET, 6.1% becomes recharge, and 0.5% becomes runoff (Table 4-1). Over the course of the simulation, approximately 3.3 billion m^3 (2.7 MAFY), or a mean of 0.2% of annual precipitation was added to soil layer storage. At the end of the simulation on 31 December 2013, $5.1 \text{ billion m}^3 \text{ yr}^{-1}$ (4.1 MAFY), or 4.5% of the final model year precipitation was stored in the snow layer. Mass balance error was positive; 0.19% more water was accounted for in non-precipitation fluxes than that which fell as precipitation, amounting to 14.2 m^3 (11.5 MAF) out of a total precipitation of 1494 billion m^3 (1212 MAF).

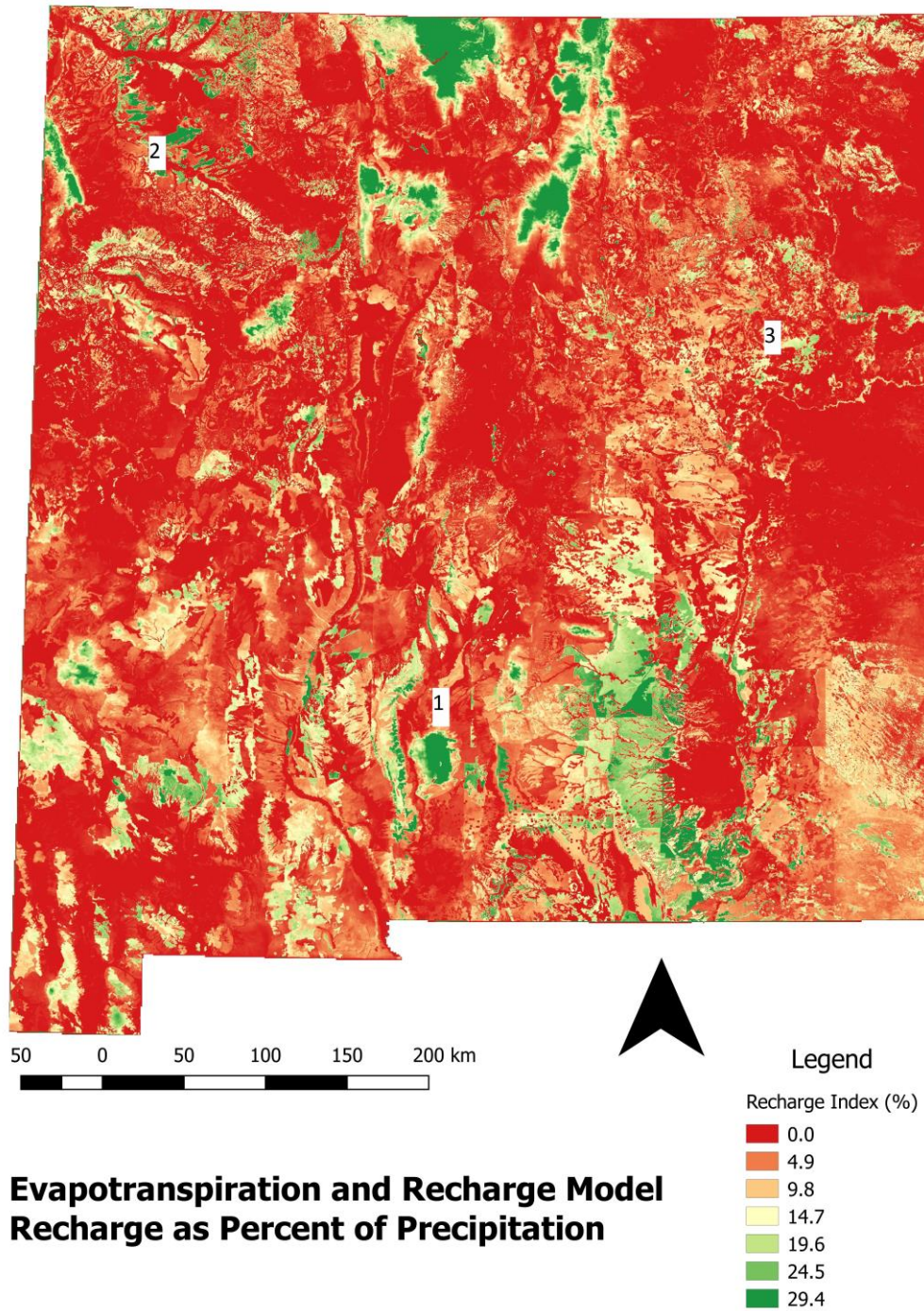
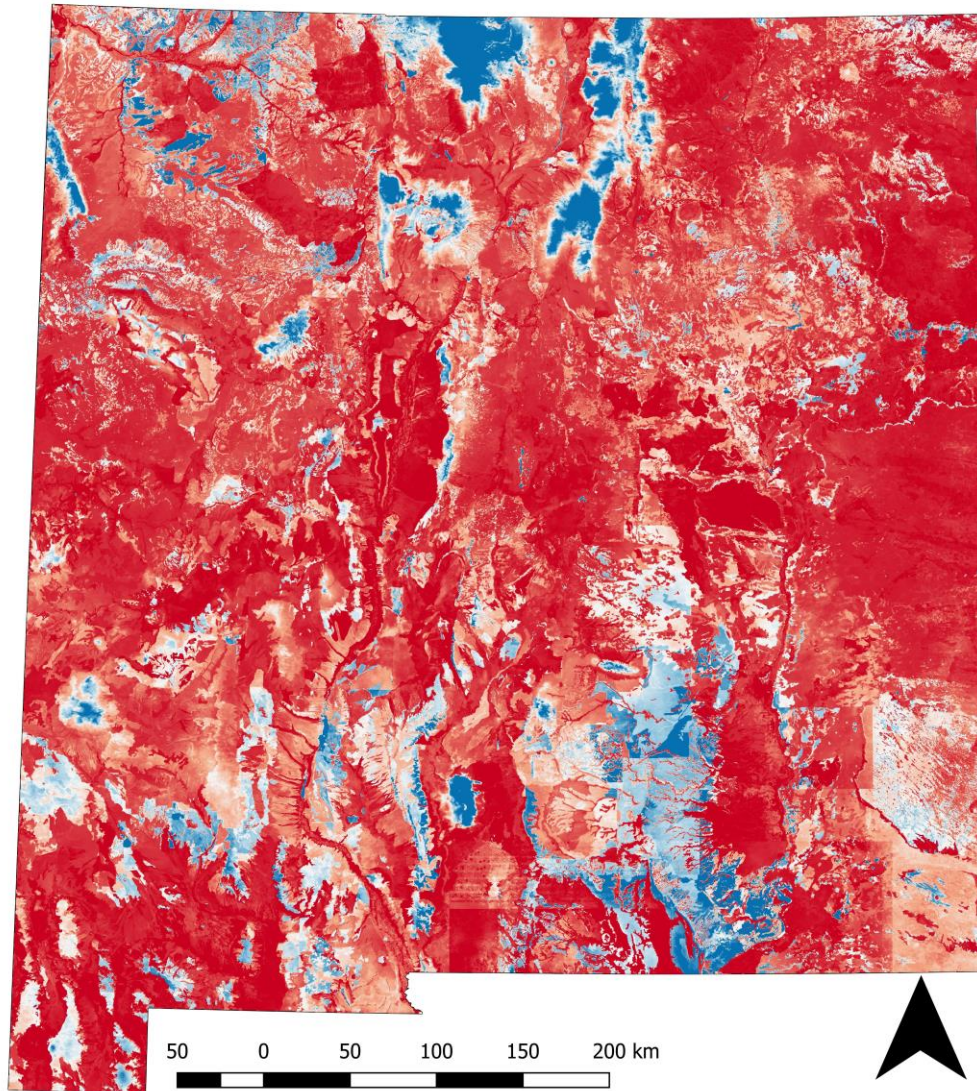


Figure 4.3 Recharge (% of precipitation) calculated by the ETRM over the 14-year simulation period (2000-2013). The highest rates occur in the mountainous regions of the state. Possible problems mentioned in the discussion are numbered.

Table 4-1. Statewide totals for precipitation, evapotranspiration, and recharge over each of the ETRM model years.

Year	Precipitation [AF]	Snow Water Equivalent [AF]	Evapotranspiration [AF]	Diffuse Recharge [AF]	Soil Water Storage Change [AF]	Total Storage Change	Runoff
2000	8.60E+07	3.91E+06	7.00E+07	4.29E+06	9.52E+06		
2001	7.36E+07	9.35E+06	8.10E+07	4.20E+06	-1.14E+07		
2002	8.23E+07	3.76E+06	7.70E+07	2.32E+06	9.98E+06		
2003	6.36E+07	2.99E+06	7.07E+07	2.10E+06	-9.44E+06		
2004	1.18E+08	3.49E+06	9.50E+07	8.96E+06	1.30E+07		
2005	9.65E+07	4.36E+06	1.02E+08	8.65E+06	-1.53E+07		
2006	1.08E+08	5.01E+06	8.34E+07	1.08E+07	8.36E+06		
2007	9.97E+07	6.86E+06	9.84E+07	4.39E+06	-2.96E+06		
2008	9.43E+07	8.37E+06	8.41E+07	7.46E+06	1.14E+05		
2009	8.14E+07	4.83E+06	7.54E+07	2.75E+06	2.24E+06		
2010	1.01E+08	1.32E+07	9.88E+07	6.92E+06	-6.38E+06		
2011	6.69E+07	2.78E+06	5.28E+07	2.06E+06	1.17E+07		
2012	5.44E+07	3.98E+06	6.51E+07	1.46E+06	-1.42E+07		
2013	9.21E+07	4.17E+06	7.28E+07	7.85E+06	1.06E+07		
Total	1.22E+09	7.71E+07	1.13E+09	7.42E+07	5.83E+06	2.68E+06	6.25E+06
Mean	8.70E+07	5.50E+06	8.05E+07	5.30E+06	4.17E+05	1.92E+05	4.46E+05
Percent of Precipitation	100.0%	0.3%	92.5%	6.1%	0.5%	0.2%	0.5%
Mass Error	0.2%						



**Evapotranspiration as Fraction of Total
Precipitation
2000-2013**



Figure 4.4 The ET Index (i.e., the fraction of precipitation lost to ET) shows ET is the dominant flux of water out of the soil layer. Over 85% of the state loses 70% of precipitation to evapotranspiration, by far the dominant flux of water from the soil layer.

4.4 Discussion

The results of this study are reasonable in most places. New Mexico, as an arid to semiarid state, would be expected to lose most precipitation to ET eventually. Recharge has been shown to be very low or negligible in the many parts of the state by several workers (Mattick et. al., 1987; Havens, 1966; Falquist, 2003; Walvoord and Phillips, 2004; Sandvig and Phillips, 2006). A serious obstacle to the quantification of model error is the lack of observed data. This was addressed in this study by conducting chloride mass balance studies around the state and by compiling a database of previous recharge estimates made using several approaches. These estimates are themselves quite uncertain, and few address solely diffuse recharge as in this study.

It was originally planned to use the results of a chloride mass balance (CMB) study to make point estimates of recharge and calibrate the model to the results (see Appendix A). However, the CMB study did not identify a uniform bias of the ETRM, rather it showed that the ETRM makes low estimates compared with the CMB in some places, and high estimates in others. This data may become useful in future versions of the ETRM.

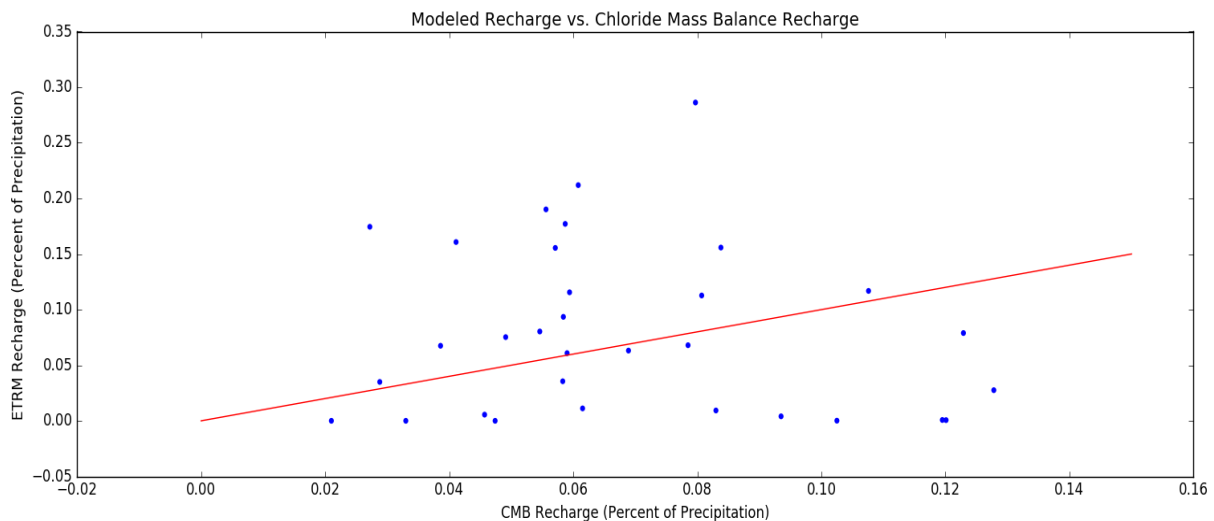


Figure 4.5 Recharge estimates based on the ETRM were scattered when compared with CMB recharge estimates. No clear bias was identified.

ETRM recharge estimates are generally much higher than regional estimates made for NM Water Resource Planning Regions (Figure 4.6). This is likely a bias in the ETRM that is not yet understood, combined with systematic problems related to the input soils data, from which soil water storage capacity is derived. The lack of reliable soils data in certain geographic areas in New Mexico is an obvious problem with the ETRM. As the reservoir in the ETRM is the soil, a lack of soils data or inaccurate soils data causes over and underestimates of recharge.

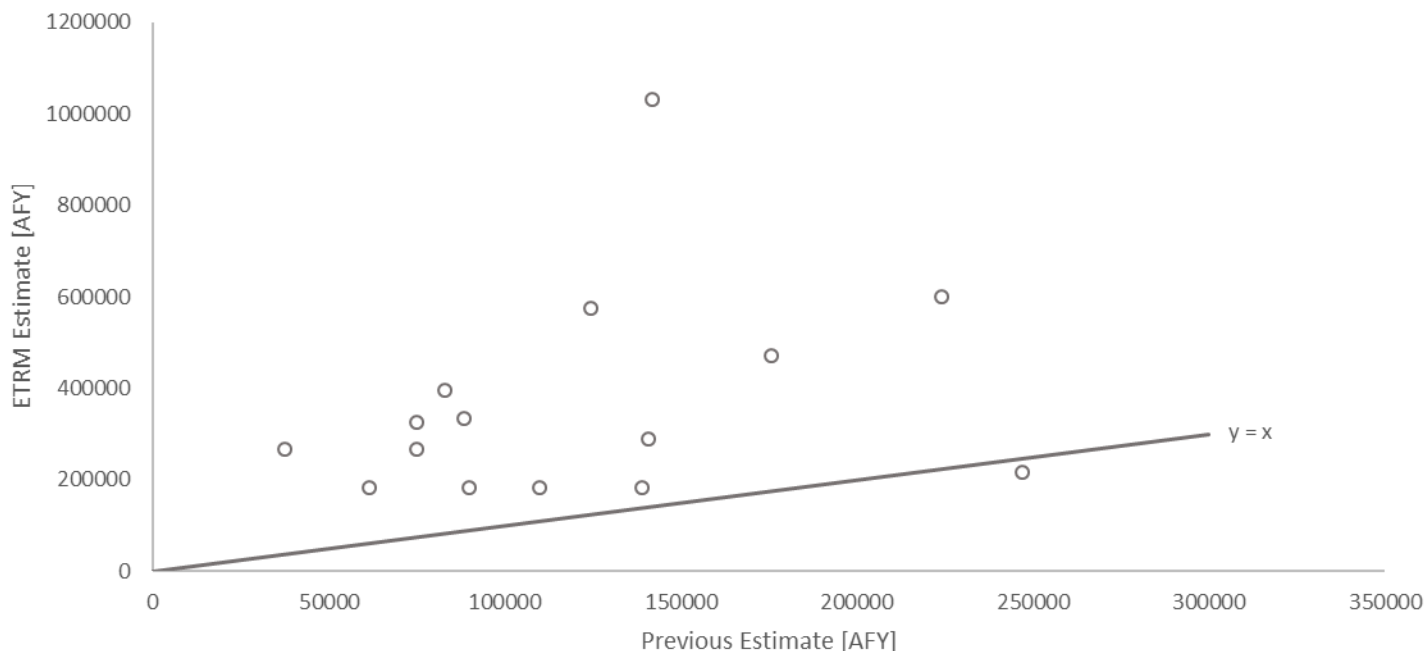


Figure 4.6 Scatter plot of ETRM recharge estimates compared with previous estimates of recharge show that the ETRM generally makes much higher estimates.

Soils data that describe a thin soil in places where there is a significant layer of unconsolidated material near the surface would cause an overestimate of recharge. This is because the soil water storage would be very low; a small rainstorm could exceed the storage capacity and recharge would occur. Upon examination of the recharge map (Figure 4.3), areas with this problem are numerous. The sink of the Tularosa Basin (1), the arroyos of the San Juan Basin (2), and the mesas along the Canadian River (3) are examples where there are likely overestimates of recharge. A possible solution to this problem is the identification of Quaternary alluvial and playa deposits. By identifying these deposits and assigning a much higher TAW (the principal soil water storage capacity term), these areas would receive no recharge.

During the period simulated in this study, 8 of 14 years were drier than average. During this period average precipitation in New Mexico was approximately 4-5 cm less than the statewide average of 14 cm per year (NOAA, 2016). These low precipitation values during most of the simulated period probably reduce recharge by a considerable amount (see sensitivity analysis below).

Through a simple analysis of the sensitivity of the ETRM to various data inputs, the effect that problems in the input data will have can be compared. Sensitivity analysis was performed at 21 sites in New Mexico at a range of elevations from the low point of the state at the Pecos River on the border with Texas (“LP”), at the high point of the state at Wheeler Peak (“HP”), and over four transects crossing from lowlands to local high points on various mountain ranges (Figure 4.7). General trends are well represented at the Socorro County transect (Figure 4.8).

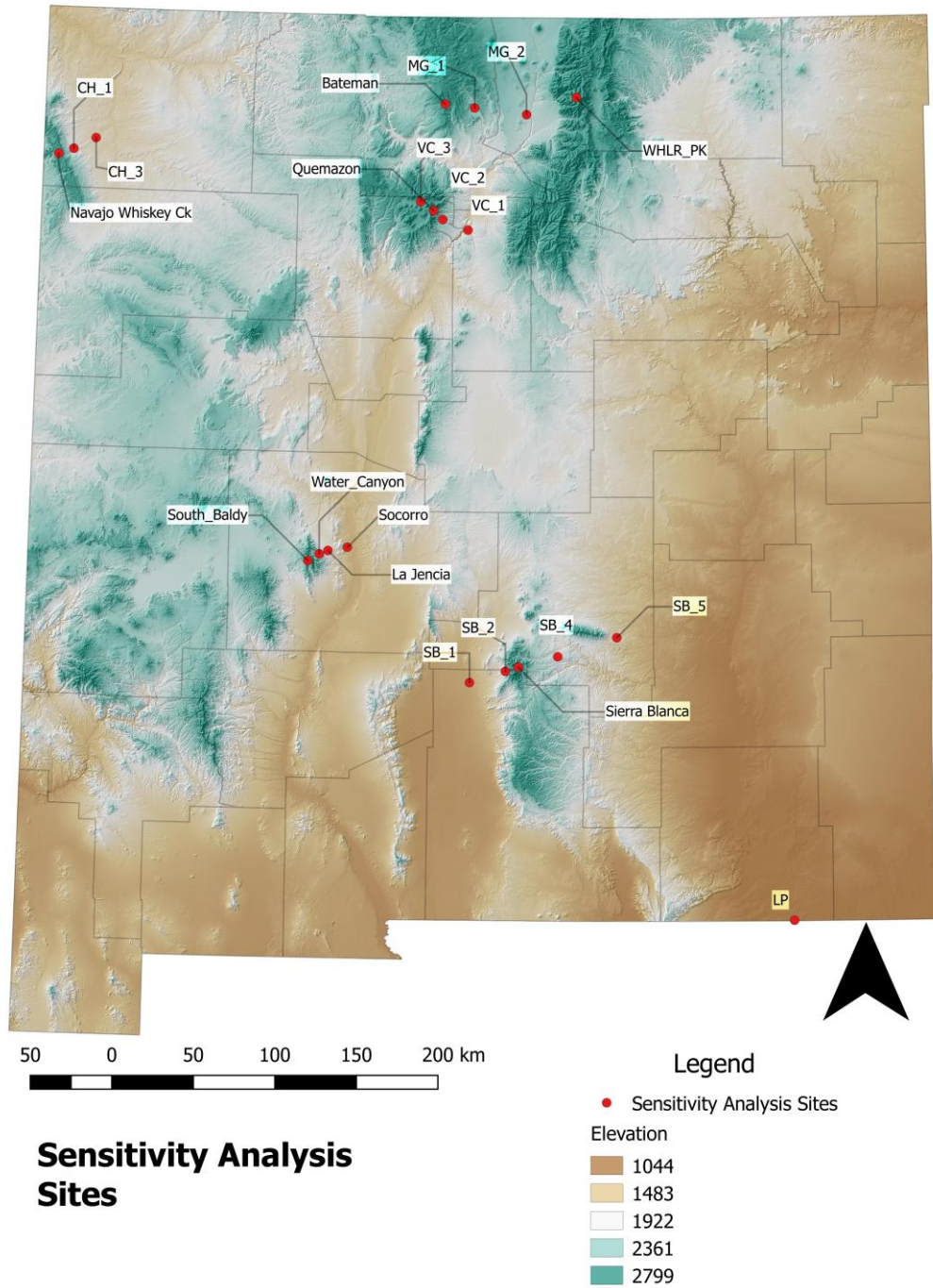


Figure 4.7 Sensitivity analysis was conducted at 21 sites around the state.

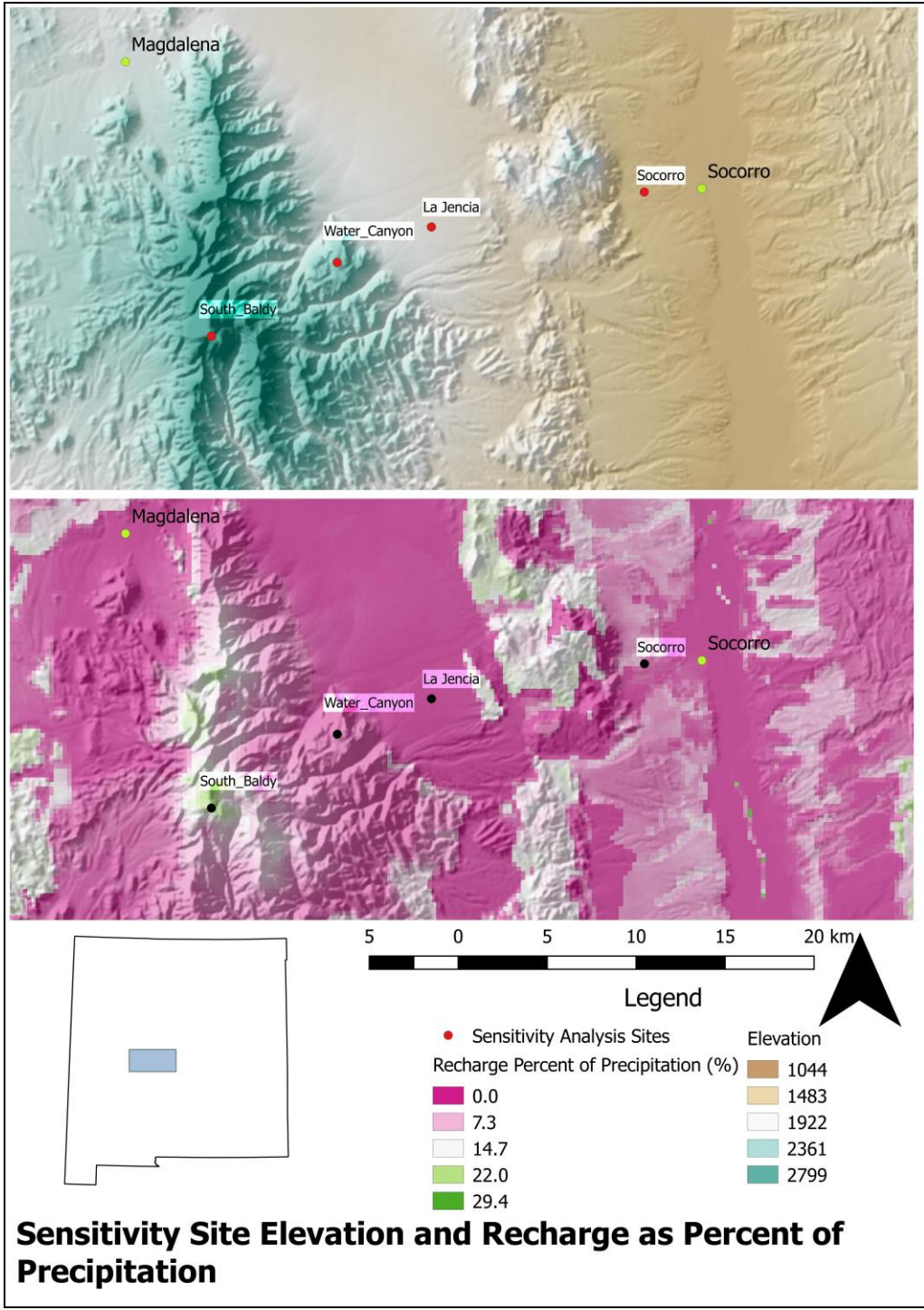


Figure 4.8 Detail view of a transect along which sensitivity analysis was performed, the top image shows elevation, the middle lower image shows recharge rates in the area.

In the sensitivity analysis the ETRM input parameters that have the largest effect on model performance were varied over a range of values. These parameters are temperature, precipitation, reference ET, available water storage (a proxy for soil water storage capacity, or TAW), NDVI, and the depth of soil available for evaporation. Precipitation, reference ET, and soil evaporation layer thickness were set at ten points ranging from -50% to +50% of the extant data. The NDVI conversion factor ($K_{cb} = 1.25 \text{ NDVI}$) was varied from 0.9 to 1.8. The temperature was varied from the assigned temperature minus 5° C to plus 5° C in 0.5° C increments. The ETRM was then run at each of the 21 sites over each of the ten variations for each of the chosen parameters, a total of 1470 model runs. The variation of each parameter was independent; one parameter was varied while all other parameters were held at the normal input value. Spider plots were created, showing the magnitude of recharge over the ten simulations for each parameter that was varied (Figure 4.9 - 4.12). At Socorro, a site situated on the alluvial piedmont of a steep mountain, the ETRM recharge estimate is 5 mm yr⁻¹. The ETRM at this site shows threshold effects from precipitation; there is zero recharge until precipitation reaches 90% of the PRISM value of 230 mm yr⁻¹ and increases at an increasing rate with precipitation. At La Jencia, the ETRM shows non-linear sensitivity to input parameters. With a small decrease of soil water storage or reference ET, or with a small increase in precipitation, recharge occurs. The change in recharge relative to a change in these inputs is nonlinear, the change accelerates with linearly increasing changes in the parameters. This site is also clearly at the threshold of conditions conducive to recharge. Sites such as La Jencia are typical of New Mexico: the site is within about 11% of the statewide mean elevation, precipitation, and soil water storage capacity. This site illustrates the sensitivity of large areas of New Mexico to small changes in reference ET, soil water storage capacity (TAW), and precipitation, and the need to constrain these inputs. The much higher sites at Water Canyon (1870 m.a.s.l.) and South Baldy (3190 m.a.s.l.) are less sensitive to changes in input parameters; they are cold and humid enough that changes in reference ET, precipitation, temperature, NDVI, or soil water storage are unlikely to prevent recharge. The site at South Baldy also shows linear changes in recharge with changing input parameters.

Using an estimate of the accuracy of model inputs, tornado plots were created to illustrate model sensitivity relative to input uncertainty (Figure 4.13). The PRISM and NDVI data sets have been widely scrutinized and have been under continuous development and validation for years and systematic bias and error are generally understood (Daly et al., 1997; Johnson et al., 2000; Daly et al., 2002; Pan et al., 2013; Miura et al., 2008; Sesnie et al., 2012; Lyapustin et al., 2012; Ponce-Campos et al., 2013). Verification of reference ET by comparison with other data sets have found the data is generally within 20% of observed data (Revelle, 2016). The least certain data input used by the ETRM is the soil-derived parameters, especially TAW; the effect its low resolution (compared to natural spatial heterogeneity of soils) on soil hydrologic behavior is not well understood (Basu, 2010; see Appendix B.5). The tornado plots indicate that at arid sites, water storage capacity introduces a considerable uncertainty to which the model is very sensitive, while at cool, humid sites, climatic inputs are the main source of uncertainty in recharge estimates by the ETRM.

Variation of ETRM Physical Parameters at Socorro

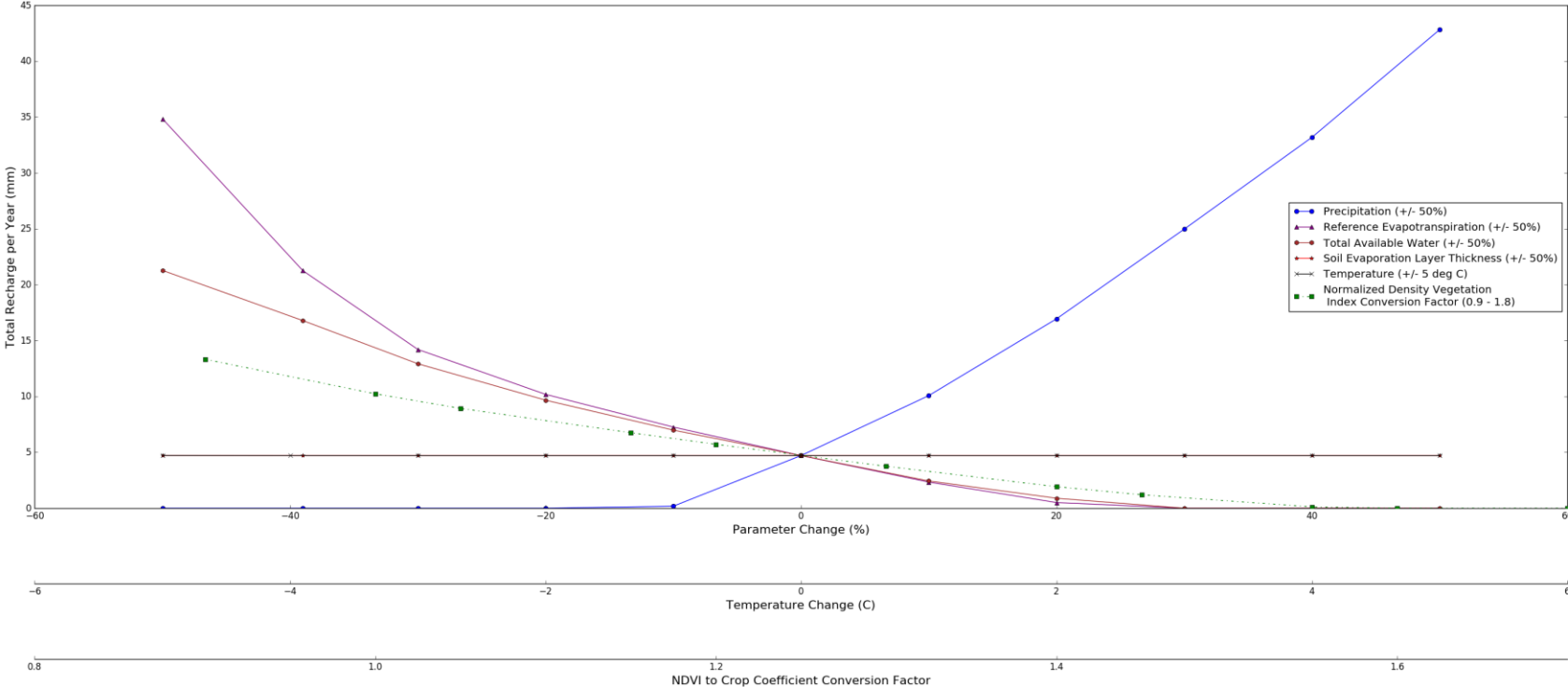


Figure 4.9 The Socorro site shows variations in recharge when input parameters are varied. The site has a clear threshold of precipitation necessary to cause recharge.

Variation of ETRM Physical Parameters at La Jencia

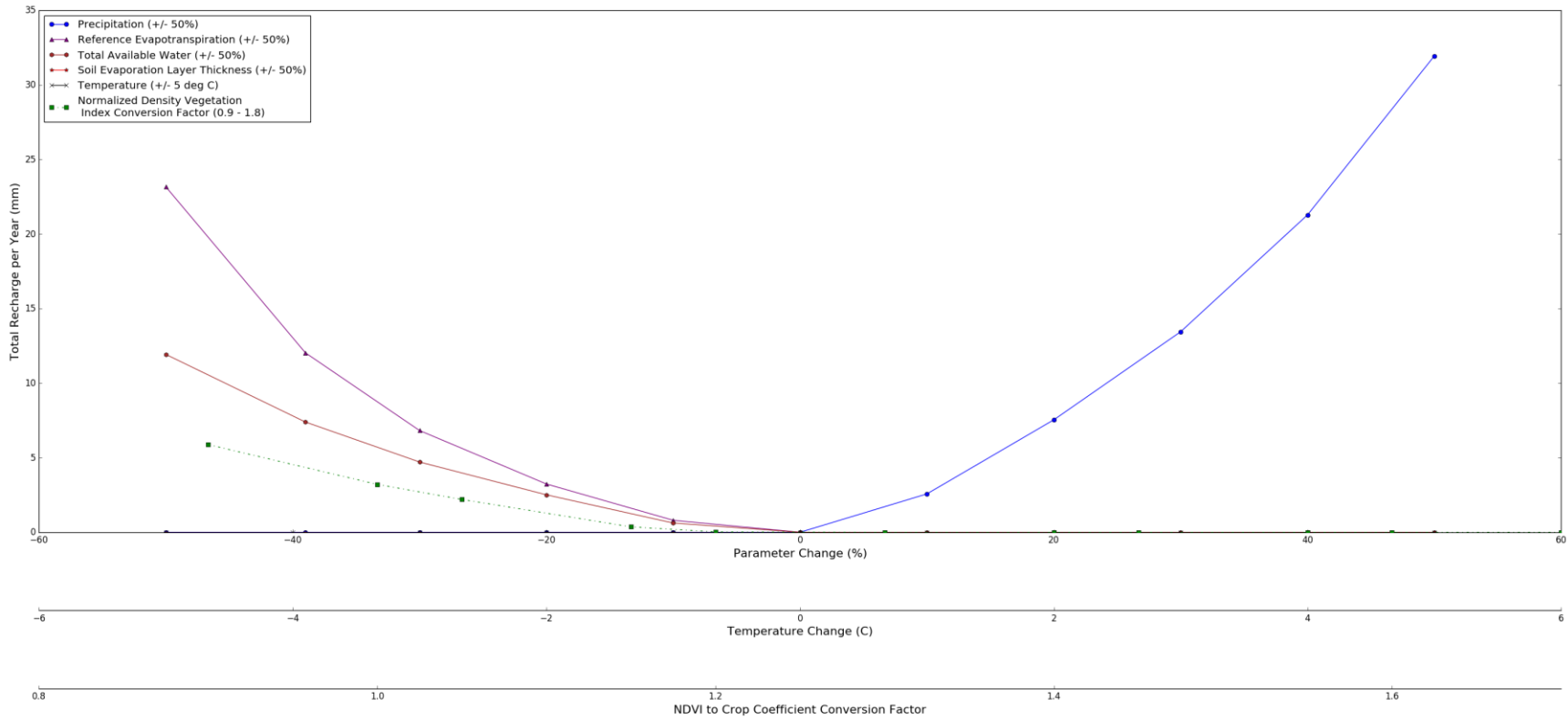


Figure 4.10 The La Jencia site is very sensitive to the input parameters, a small change in reference ET, soil water storage capacity, or precipitation causes large changes in Recharge.

Variation of ETRM Physical Parameters at Water Canyon

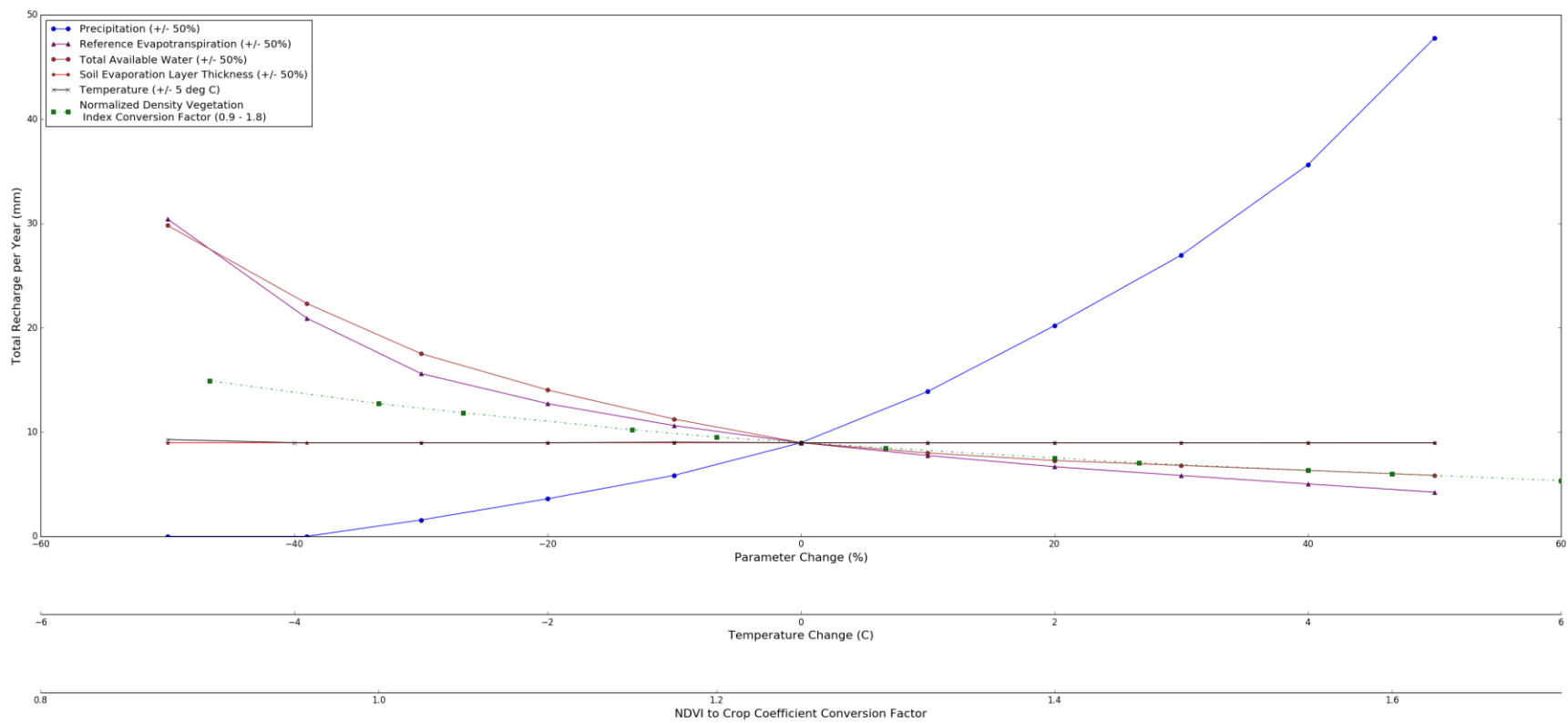


Figure 4.11 The site at Water Canyon is well within the physical conditions conducive to recharge.

Variation of ETRM Physical Parameters at South Baldy

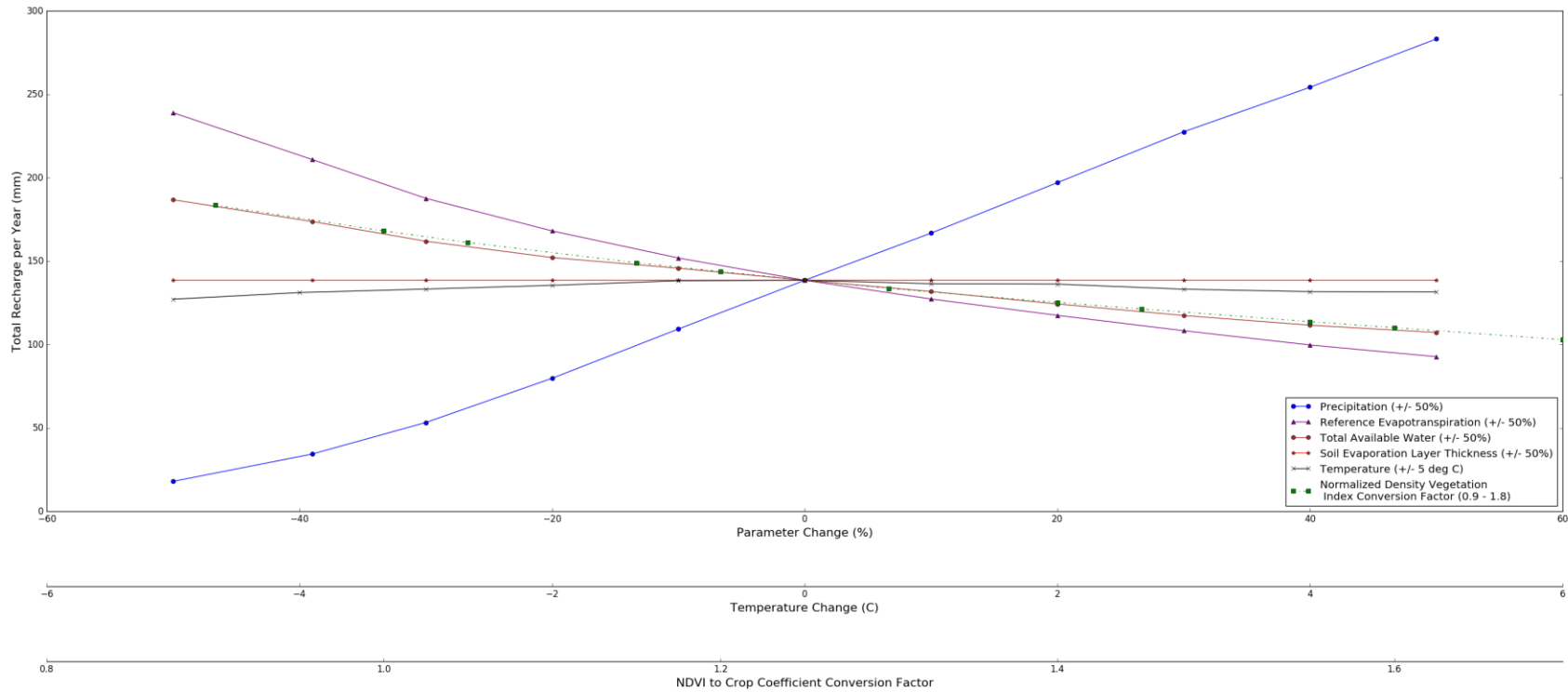


Figure 4.12 The South Baldy site, at 3190 m.a.s.l., is among the “sky islands” of New Mexico, where low available energy and high precipitation create conditions conducive to recharge.

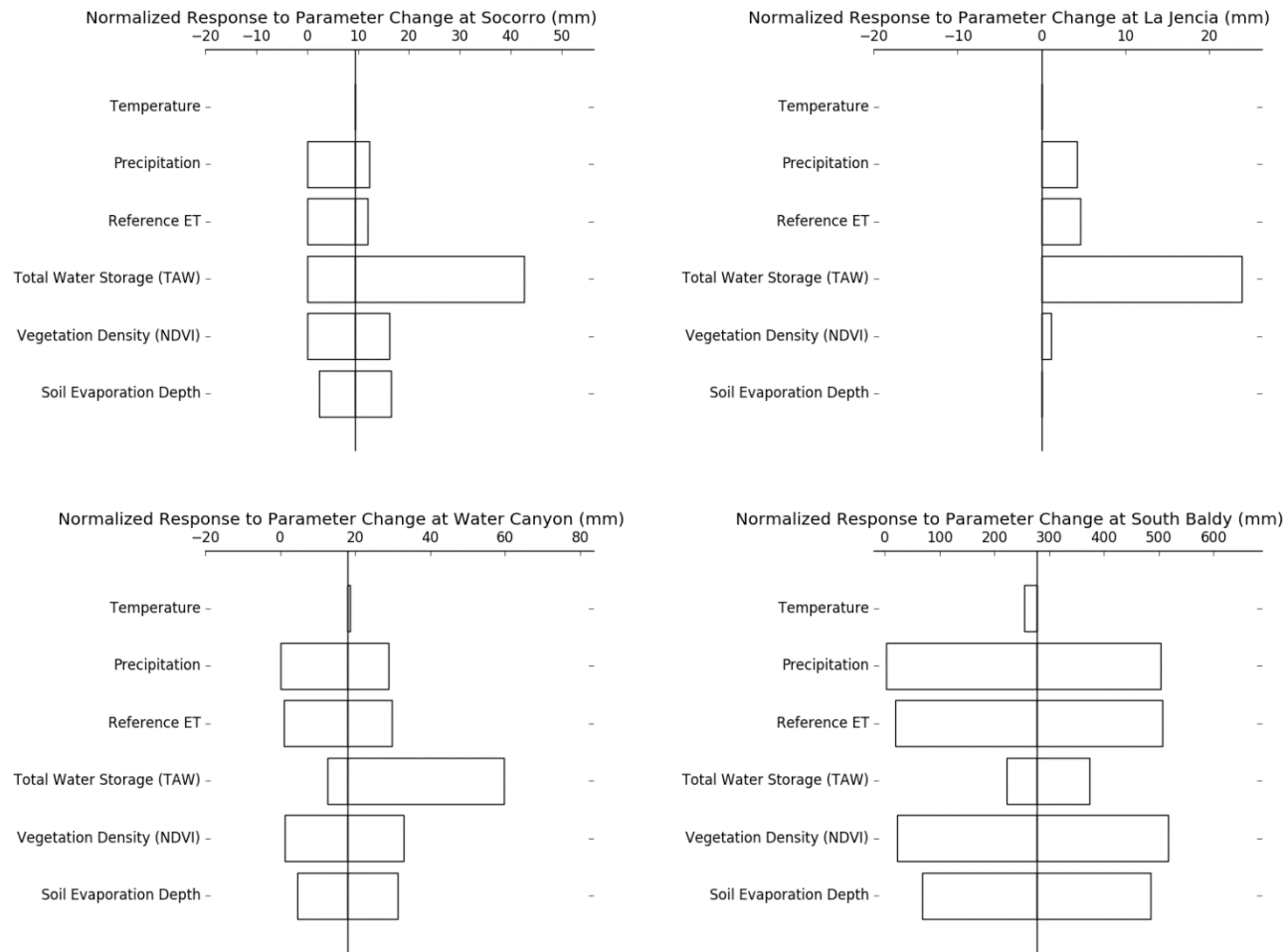


Figure 4.13 Tornado plots from the three lower sites at Socorro, La Jencia, and Water Canyon show a high relative sensitivity to TAW, while humid sites such as South Baldy are less sensitive. TAW is a function of soil texture, vegetation type, and thickness of the root zone.

The model appears to be insensitive to PRISM air temperature. However, this is misleading because the energy component of the ETRM (i.e., ET_{rs}) incorporates, and depends on air temperature. The only aspect of the ETRM which is controlled by PRISM air temperature itself, however, is the snow model. Thus variations in PRISM air temperature in this analysis only affect whether snow is accumulated and how fast snow melts. Work on GADGET ET_{rs} is ongoing and discussions of its sensitivity will be made available when development is complete.

The model sensitivity to TAW in arid to semiarid climate regimes underscores the importance of this uncertain input. While soil water balance is an appropriate method for modeling processes that control in-place recharge in New Mexico, results should be considered preliminary until a methodology is developed to better parameterize water storage capacity across the state.

4.5 Conclusion and Future Work

Diffuse recharge was estimated over the entire State of New Mexico using a high resolution soil water balance model running on a daily time step. Inputs to the ETRM include gridded precipitation, reference ET, vegetation, temperature, and soils data. ET was calculated using a modified FAO-56 dual crop coefficient method. This method divides the ETRM soil layer into three sections in which stage-one evaporation, stage-two evaporation, and transpiration occur. The depletion of water from each layer is computed daily and incorporated into stress coefficients designed to simulate the reduced ET rate from vegetation and soil due to soil moisture stress. Results show that about 92.5% of precipitation in New Mexico is lost to ET, while around 6.1% becomes recharge, and 0.5% becomes runoff. ET estimates do not include sublimation. Comparison with previous recharge estimates indicate that this estimate is probably high. The high recharge bias of the ETRM is not well understood, but probably stems in part from incomplete or inaccurate soils data. The ETRM is highly sensitive to inputs derived from soils data, which have obvious deficiencies in certain areas in New Mexico.

The ETRM appears to overestimate recharge in certain areas due to inaccuracies in its ET estimates, causing excessive water availability and thus recharge. In other areas, the converse may be true; the soils layer may be excessively thick, allowing the storage and eventual loss to ET of all water. The ETRM could benefit greatly from the incorporation of independent ET measurements that could be used to constrain these soil-derived model parameters. Landsat satellite imagery may provide an avenue to accomplish this. The Mapping EvapoTranspiration at High Resolution and Internalized Calibration (METRIC) model is designed to solve the land surface energy balance using Landsat thermal and shortwave image bands (Allen, 2007). By constraining ET, METRIC could be used to replace the soil water storage terms (i.e., TAW, TEW, REW) with a storage parameter tailored specifically to the ETRM.

To date, the ETRM only estimates in-place recharge, and makes no attempt to quantify recharge that is a result of runoff. The ETRM should be coupled to another model that can effectively predict and quantify runoff that becomes recharge. This could include empirical models derived from observed data or runoff routing algorithms derived from topographic and hydrographic data.

APPENDIX A: CHLORIDE MASS BALANCE STUDY

This study was funded by the FY16 New Mexico Water Resources Research Grant Subaward Q 01788.

A.1 Introduction

A significant problem in modeling SWB to estimate in-place recharge with the ETRM is the lack of field data for use in model calibration and corroboration. In order to present recharge estimates that can be considered reasonable, a quantitative assessment of model accuracy must be made. This is extremely difficult with recharge; direct measurements of recharge can only be made with weighing lysimeters. Furthermore, both lysimeters and other indirect methods such as soil moisture probes may not represent the spatial heterogeneity of recharge over large areas. Installation of this type of equipment for this study was not possible. In an effort to corroborate results from this study, chloride mass balance was chosen as the least expensive and most direct method of increasing confidence in modeling results.

A.2 Conceptual Model Background

Recharge estimates using environmental tracers can be made at many points using inexpensive methods. These methods provide independent constraints on modeled or physically based recharge estimation techniques (Wood and Sanford, 1995). In arid regions where precipitation may measure less than $\sim 700 \text{ mm yr}^{-1}$, recharge is often highly variable in time and space, and the total recharge flux is very small compared to other components in the water budget (Allison et al., 1994; Peck et al., 1981). Chloride mass balance (CMB) takes advantage of a ubiquitous environmental tracer (Cl^-), the concentration of which is easily analyzed with standard laboratory equipment. CMB is an estimation technique using Cl^- concentrations measured from both atmospheric deposition and Cl^- present in the vadose (unsaturated) zone or in groundwater. Atmospheric Cl^- originating from sea spray or dust blown from the land surface is deposited on the surface of soils as dry deposition or dissolved in precipitation. Cl^- deposited on the surface as dry deposition is easily dissolved by precipitated water and remains in solution as water is lost to evaporation into the atmosphere, increasing concentration. As water infiltrates through the surface and descends into the soil column, Cl^- is excluded from root uptake of water for transpiration, further increasing concentration. Cl^- is anionic and thus unlikely to participate in mineral ion-exchange processes, or in geochemical reactions and thus behaves conservatively while in the subsurface (Feth, 1981; Scanlon, 1991).

Vadose Zone CMB

In the vadose zone, the concentration of chloride increases with depth to the point where it is no longer concentrated by ET, typically at the lower extent of the root zone. At this depth, the concentration of chloride is at a maximum, and the drainage (potential recharge) past this point can be calculated. Assuming steady state conditions and one-dimensional piston-flow, the mass of Cl^- reaching the water table is equated to Cl^- deposited on the surface with precipitation and as dry fallout, after Phillips (1994):

$$J_R = \frac{D_{Cl}}{C_{Cl}} \quad (39)$$

where J_R is the flux of deep drainage (potential recharge) [$L T^{-1}$], D_{Cl} is the rate of combined wet and dry Cl deposition [$M L^{-2} T^{-1}$], and C_{Cl} is the Cl concentration in the soil water [$M L^{-3}$]. Chloride soil residence time can also be calculated, assuming piston-flow and a constant chloride deposition rate, after Phillips (1994):

$$t_z = \frac{\int_0^z \theta C_m dz}{D_{Cl}} \quad (40)$$

where t_z [T] is the time in transport of Cl to depth z [L], θ is the soil volumetric water content [$L^3 L^{-3}$], and D_{Cl} is the Cl deposition rate [$M L^{-2} T^{-1}$]. Studies in semiarid lowlands in New Mexico of vadose-zone Cl concentrations (Walvoord and Phillips, 2004; Sandvig and Phillips, 2006) have shown Cl residence times of thousands of years and no recharge during recent geological history (~ 12 kyr) over large areas of New Mexican grassland, creosote, and desert-scrub vegetation regimes. Long-term average recharge through soils in wooded vegetation regimes have also been quantified. Chloride concentration vs. depth profiles showing decreasing concentrations with depth beyond the local maximum concentration can indicate changing climatic conditions, diffusion of chloride to the water table, evaporative enrichment near the surface, or preferential flow paths (Stone, 1984; Mattick et al., 1987).

The assumption of one-dimensional piston flow in the vadose zone can be problematic in soils where preferential flow paths exist. Preferential flow routes water quickly through the vadose zone without interacting with Cl sequestered in the soil matrix. CMB performed on such a soil matrix would underestimate recharge if the preferential flow is not considered (Wood, 1999). The advantage of using vadose zone CMB is that the integrated soil column can be used to find long-term recharge on the order of thousands of years in arid areas.

Groundwater CMB

Groundwater is used in a technique similar to that of the vadose zone recharge estimate: instead of using pore water Cl⁻ concentration, the Cl⁻ concentration of groundwater is used. Eriksson and Khunakasem (1969) calculated recharge to the aquifers of arid coastal Israel using the following equation:

$$\bar{P}C_m = \bar{R}C_{gw} \quad (41)$$

where \bar{P} is average precipitation [L] and \bar{R} is average recharge in depth of water [L], and C_m and C_{gw} are the concentrations [$M L^{-3}$] of meteoric (wet and dry deposited) Cl and groundwater Cl⁻, respectively. By measuring precipitation rates, meteoric Cl deposition, and groundwater Cl concentration, recharge can be calculated. This method requires that several assumptions be made: (1) no chloride in the groundwater originates from a geological source; (2) chloride is conserved in the system; (3) the chloride mass-flux is constant (i.e., net change in storage is zero); and (4) there is no recirculation of chloride within the system (Wood, 1999).

Using both vadose zone and groundwater CMB can reveal spatial heterogeneity in the recharge process. Sharma and Hughes (1985) found that while groundwater Cl⁻ concentrations were relatively constant spatially in deep sand soils of SW Australia, vadose zone concentrations were spatially heterogeneous. The relatively high Cl concentration in the soil matrix and low Cl concentration along preferential flow path indicated that possibly 50% of recharge occurred through preferential flow paths.

The advantage of using groundwater CMB for this study is that the chloride concentration in well-mixed groundwater is an average of infiltrating waters over the area; the effects of preferential flow paths and spatial and temporal heterogeneities in infiltration due to soil, vegetation, and energy availability are integrated.

Methods of Validation of Assumptions

Chloride mass balance studies in small mountain watersheds have shown that constraints on the source (area above the sample site) increase the reliability of recharge estimates by reducing possible non-meteoric sources of chloride (Aishlin et al., 2011). In order to validate the first assumption of the CMB method (i.e., no Cl flux of geological origin), the ratio of chloride to bromide is measured; any deviation from established groundwater ranges indicates a non-meteoric source (Davis, 1998). The chloride/bromide ratios resulting from known geochemical processes have been described in detail (Rittenhouse, 1967; Mazor and Mero, 1969; Carpenter, 1978). Chloride/bromide ratios were used in studies of the Yucca Mountain site to identify possible mechanisms of recharge (e.g. fracture infiltration) and results suggested that atmospheric halides are fractionated as water infiltrates through the subsurface (Fabryka-Martin et al., 1998). Davis and others (1998) found in a survey of chloride/bromide analysis that chloride should not be used as a tracer alone, but should be used with accurate bromide data to validate assumptions of water provenance.

General chemistry also aids in validating assumptions. High levels of total dissolved solids and sodium generally indicate greater residence time and geochemical evolution of groundwater (Bartos and Ogle, 2002). Thus, high TDS or sodium concentrations could cast doubt on the validity of the above mentioned assumptions.

Effective Chloride Concentration

As explained previously, recharge determination using the CMB method depends on groundwater or vadose zone chloride concentration, precipitation depth, and the concentration of

infiltrating waters. As chloride is highly soluble, and precipitation has low (~ 0.05 to ~ 0.13 mg L⁻¹ in New Mexico) concentrations, chloride from dry deposition readily dissolves and adds its mass to any water that is infiltrating through the surface during or after a precipitation event. It is critical then that efforts be made to determine likely effective (dry plus wet) Cl concentration in infiltrating waters, as they vary spatially and temporally over New Mexico.

Wet Deposition

Wet deposition of chloride has been measured extensively around the US for over 35 years since the National Atmospheric Deposition Program (NADP) network began collecting and analyzing precipitation chemistry. Through rapid expansion in the 1980s, the network has grown to 250 sites, 5 of which are in New Mexico (Figure A.1). Of these 5 sites, 3 have discontinued collection after 25 - 30 years of service, and 2 continue service after 30+ years, sampling precipitation weekly. The NADP has made spatial interpolations of annual concentration and wet deposition in order to display gridded, continuous-coverage data over the conterminous US. Interpolations are made using an Inverse Distance Weighted (IDW) surface and a PRISM precipitation surface. Rather than directly interpolating deposition surfaces, the combination of the corresponding modeled concentration and actual precipitation measurement at NADP stations along with an adapted annual PRISM precipitation surface are used. The PRISM dataset (see Appendix B) is the product of sophisticated regressions that account for precipitation variation depending on aspect, slope, topographic sheltering, and elevation, among other things. Original PRISM datasets are modified by using NADP precipitation measurements that affect a radius of 30 km around the NADP station. Thus the gridded precipitation values approach the original PRISM data values as distance from the NADP station approaches 30 km, and values between these NADP-influenced coverages are populated with original PRISM data.

National Atmospheric Deposition Program Precipitation Collection Sites in New Mexico

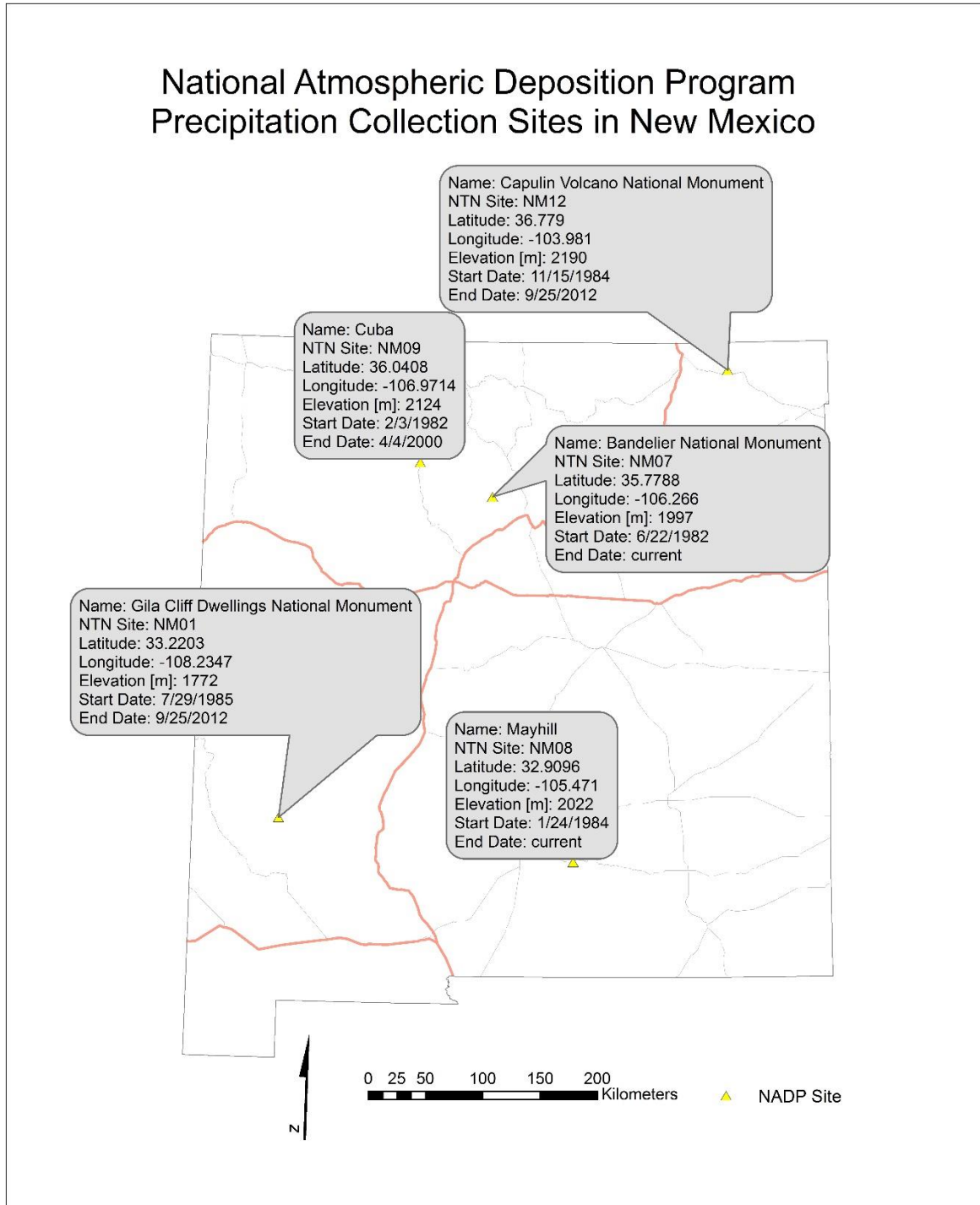


Figure A.1 New Mexico locations of National Atmospheric Deposition Network collection stations.

Dry Deposition

Of the four parameters needed to estimate recharge (i.e. wet deposition, dry deposition, precipitation, groundwater Cl concentration), dry deposition is the least certain. In New Mexico, dry deposition has been measured at very few locations, sampling methods are not standardized, and dry deposition appears to vary spatially and temporally to a great degree.

Many estimates of dry deposition have been made simply by assuming that dry deposition is some percentage of wet deposition, avoiding the difficult task of measurement. Work by Bentley and others (1986) and Moysey (1999) assumed dry deposition to be 1.3 times the measured concentration of wet deposition. Healy and others (2004), Scanlon (2006), and Scanlon and Goldsmith (1997) assumed that dry deposition accounted for half of total deposition, and thus doubled measured wet deposition concentrations. In New Mexico, Rawling and Newton (2016) used end-member analysis to estimate an effective concentration of 0.55 mg L^{-1} ($\sim 7\times$ wet concentration) in the Sacramento Mountains. Anderholm (1994) used a bulk precipitation Cl concentration of 0.29 mg L^{-1} near Santa Fe. Stone and McGurk (1985) used an effective Cl concentration of 2.38 mg L^{-1} . Lewis and others (1984) found an average bulk precipitation Cl concentration of 0.58 mg/L .

Sterling (2000) found regression slopes between deposition and precipitation and used an inverse-distance weighting algorithm in a GIS to interpolate NADP wet deposition rates spatially. Dry deposition data available at the time were scant, as the NADP sites were required to collect dry deposition chemistry only from 1978 to 1984, with fewer stations reporting dry deposition data in subsequent years. This data was culled to remove incomplete, unreliable, or suspect data. A continuous data set covering the conterminous US was then created using inverse distance weighting (Figure 4.15). The results were found to vary spatially, and were in general agreement with dry deposition rates as a percent of total found by Eriksson (1960; 20%), Hainsworth (1994; 25%), Bentley and others (1986; 30%), Li (1992; 50%), Whitehead and Feth (1964; 50%), and the Sevilleta National Wildlife Refuge (40%).

A.3 Methods

Sampling

During the spring, summer, and fall of 2015 a total of 34 springs and seeps were sampled (Figure A.2). Six samples were taken from seeps during the early spring (April and May) that were probably temporary flows caused by the spring snowmelt. Twenty-seven of the sample sites were permanent or semi-permanent springs and were sampled repeatedly. As only groundwater samples were desired, possible sampling sites were scrutinized accordingly. Sites were selected for sampling only if the flow was from a discrete point; sites with diffuse discharge or sites where the water may have been evaporating for some time from a saturated surface were rejected. The area topographically above the discharge site was examined to ensure that the sampled water did not infiltrate from surface flow only to reemerge at the surface. Sample sites were chosen at the highest point where groundwater discharge to the surface could be located to minimize the area of the contributing watershed. The site was photographed, the geographic coordinates and elevation noted, wildlife or fire disturbance recorded, and infrastructure (tank, trough) described. Field parameters (i.e., specific conductance [$\mu\text{S cm}^{-1}$], pH, and discharge temperature [$^{\circ}\text{C}$]) were measured as closely as possible to the discharge point using the YSI 556 Multiparameter System handheld device. The device has an accuracy rated to a temperature of

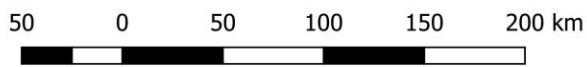
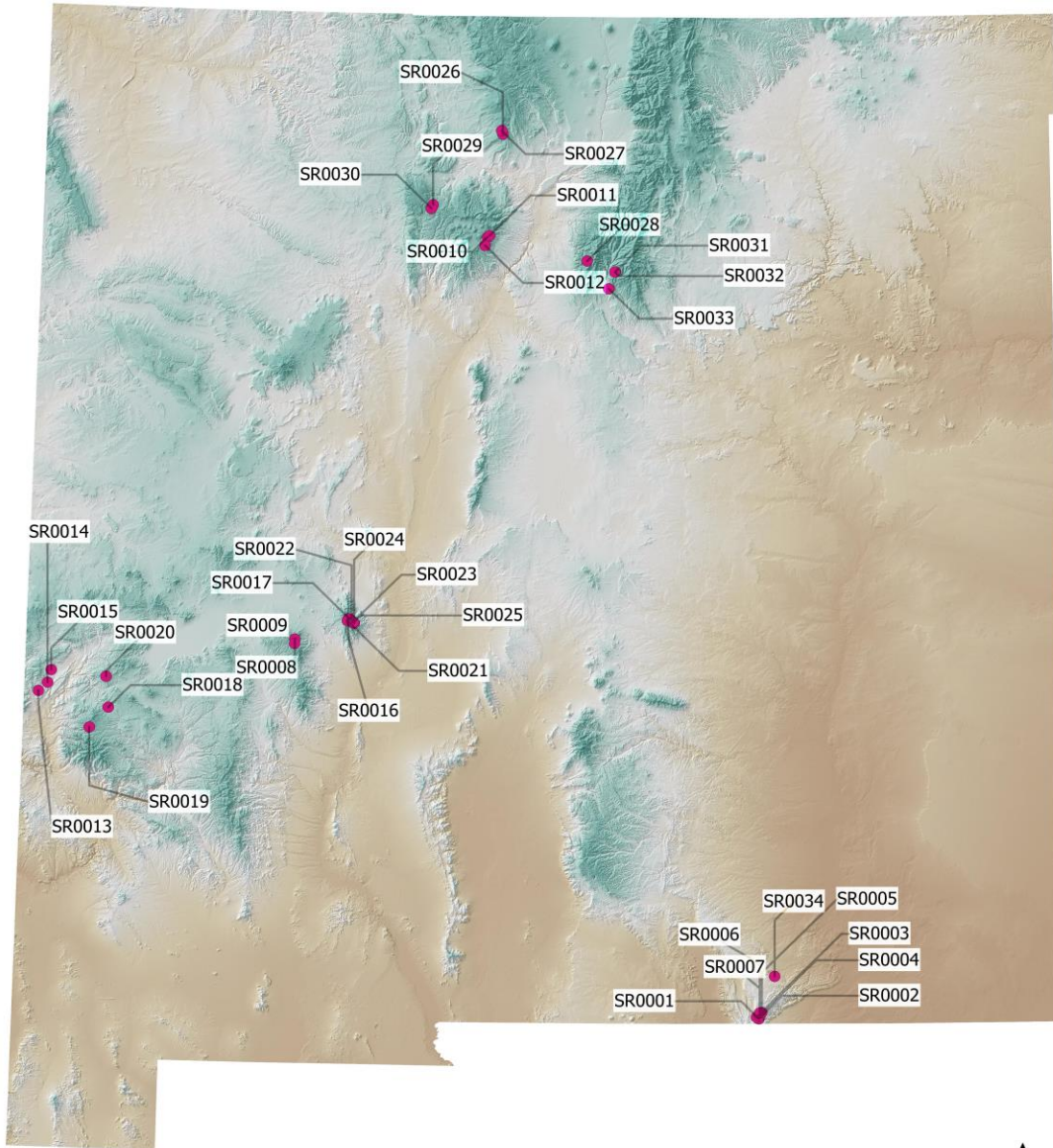
0.15 °C, to 0.5 percent specific conductance, and 0.2 pH. Samples were taken using 500 ml HDPE or 1 L LDPE water sampling bottles after rinsing three times with water from the sampling site. The rinse water was discarded downstream. Sample bottles were filled to leave minimal air space in the closed sample bottle. With the exception of the first round of six samples taken from the Guadalupe Mountains, which were at room temperature for a week, the samples were refrigerated until analysis was performed. The first round of samples was analyzed for general chemistry, chloride and bromide anionic concentration, and stable isotopes of oxygen and hydrogen.

In the first analysis of bromide concentrations, the detection limit was not reached. The samples were then concentrated by evaporation. In this procedure, a beaker was weighed, about 160 mL of sample water was added and the beaker was weighed again. The sample was then placed on a heated surface with a watch glass covering the top with an opening left through the spout of the beaker. The sample was then set at a simmer for one to two hours. Each sample was concentrated by a factor of 2.2 to 18 times by mass. These samples were then re-submitted for analysis.

Analysis

Laboratory analysis of the samples was completed using an Orion 420A meter to measure pH, and a YSI 3200 meter to measure specific conductance. Groundwater concentrations of calcium (Ca), sodium (Na), magnesium (Mg), potassium (K), bicarbonate (HCO_3), sulfate (SO_4), chloride (Cl) and bromide (Br) were analyzed. Anions Cl and SO_4 were measured using the Dionex DX-600 ion chromatograph. Cations Ca, Mg, Na, and K were measured with a Perkin Elmer OPTIMA 5300 DV inductively coupled plasma optical emission spectrometer. Stable isotopes of oxygen and hydrogen (i.e., oxygen-18 or $\delta^{18}\text{O}$ and deuterium, δD) were analyzed using the Picarro L1102-I Isotopic Water Analyzer. Only Cl and stable isotope concentrations were made for the second and third round of samples.

In order to make point estimates of recharge using sample water concentrations, the effective Cl concentration of precipitation needed to be estimated. As this project required a distributed model of effective Cl concentration in infiltrating waters, the dry deposition model developed by Sterling (2000) was used to find dry deposition. Wet deposition was found using NADP data. The values from Sterling were interpreted visually from a contoured map (Figure A.3). The NADP values were extracted to the sample point automatically using GIS. The average NADP wet deposition Cl concentration from the years 2000-2013 was divided by the wet fraction of total deposition (i.e., one minus dry deposition fraction) after Sterling (2000). Average chloride concentrations from sampled groundwater and PRISM 800 m 1981-2010 average precipitation were then used in equation 41 to find recharge rates at each sample point [mm yr^{-1}].



Legend

- Sample Sites

**Chloride Mass Balance
Sample Sites**

Figure A.2 The map of New Mexico shows the locations of the 34 sampling sites where spring water samples were collected.

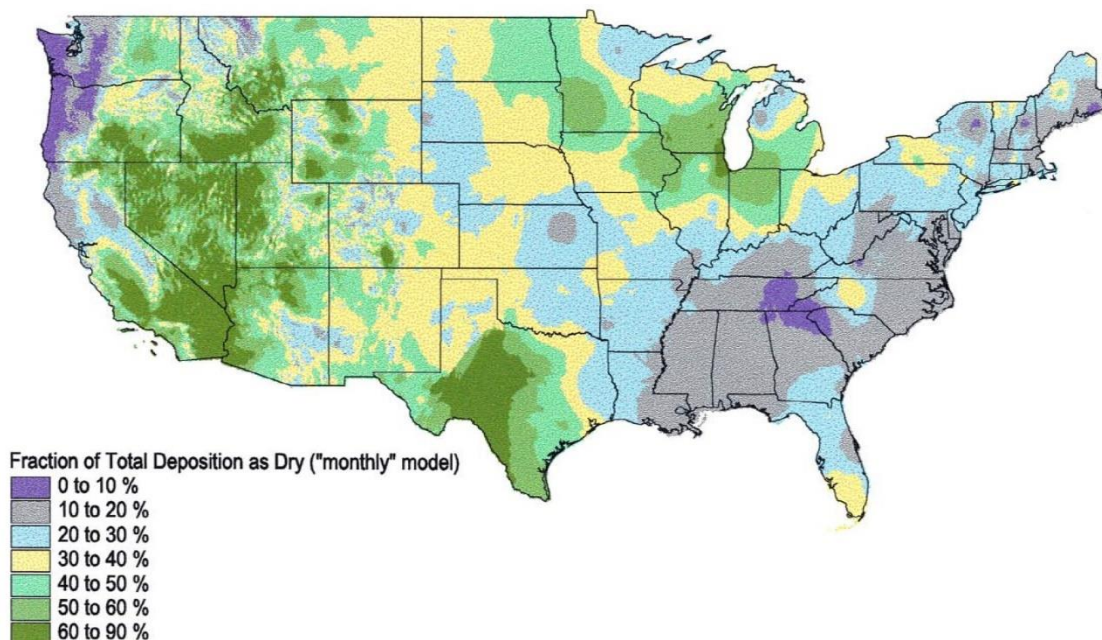


Figure A.3 Map of the conterminous United States showing the percent of total Cl deposition deposited as dryfall (Sterling, 2000).

A.4 Results

General chemistry analysis was performed on 21 of 34 sample sites to provide information on the sampled water's mingling with subsurface geology and evolution toward higher total dissolved solids (TDS) and sodium concentrations. A central assumption of CMB is that sampled spring water is locally derived and, after transport through the soil layer, does not descend to great depth, reside for long periods of time, nor react with geological units that may provide sources of chloride and thus invalidate assumptions. Results of the general chemistry analysis done on the first round of samples are shown in Table A-1, water types by geographic location are shown in Figure A.4.

The Guadalupe Mountains and the Mogollon Plateau (i.e., Gila N.F.), along with SR-0033 at Pecos Canyon had magnesium-dominated sample waters, with smaller charge-equivalent portions of calcium. The Mogollon Plateau had minor portions of the sodium cation. All other sites had sampled waters dominated by the calcium cation, with the exception of SR-0015, which was dominated by the sodium cation. All sampled waters were dominated by the bicarbonate anion, with several springs found to have a smaller sulfate anion component.

Overall dissolved solids concentrations in the sampled waters were low ($< 400 \text{ mg L}^{-1}$), with the highest concentrations found at low ($< 2200 \text{ m}$) elevation springs in the Guadalupe Mountains and at Alamosa Spring, in Pecos Canyon. Low TDS samples were found at the highest springs in areas with the greatest precipitation (i.e., San Mateo Mountains, Mogollon Plateau (Gila N.F.), Magdalena Ridge, and Mogote Ridge). Concentrations of sodium were generally less than 10 mg L^{-1} , with elevated concentrations found in the San Francisco

Mountains of Apache N.F (17.3, 18.3, and 91.9 mg L⁻¹). The sampled waters are calcium-dominated, which suggest relatively young water that has not reacted chemically with the rock to a great degree (Figure A.4). The one exception was SR-0015 (San Francisco Mountains, Apache N.F.), a sodium-rich spring.

Table A-1 Data from the 21 sampling sites for which general chemistry was analyzed.

Site ID	Region	SC (µS/cm)	Lab pH	TDS	Water Type	Ca	Na	Ca:Na Ratio	Mg	K	HCO3	SO4	Cl	Br	Cl:Br Ratio	Sample Date
SR-0003A	Gualadule Mtns	676	8.4	397	Mg-Ca-HCO3	65.6	4.10	16.0	55.4	0.790	431	37.0	5.46	0.1	52	3/15/2015
SR-0005A	Gualadule Mtns	587	8.2	326	Mg-Ca-HCO3	60.9	3.28	18.6	39.9	0.731	375	19.8	3.27	0.034	97	3/16/2015
SR-0006A	Gualadule Mtns	664	8.1	374	Mg-Ca-HCO3	51.6	3.34	15.4	57.9	0.485	431	31.1	4.35	0.03	131	3/16/2015
SR-0008A	San Mateo Mtns	130	7.9	120	Ca-Na-Mg-HCO3-SO4	14.2	10.2	1.4	1.89	1.27	51	14.8	4.21	0.02	234	3/28/2015
SR-0009A	San Mateo Mtns	85	7.8	77	Ca-Na-Mg-HCO3-SO4	7.61	6.81	1.1	1.47	0.939	34	10.9	2.18	0.03	70	4/4/2015
SR-0013A	Apache N.F.	243	8.5	169	Ca-Mg-Na-HCO3	24.0	17.3	1.4	5.92	0.753	138	11.3	4.04	0.09	45	5/2/2015
SR-0014A	Apache N.F.	435	7.5	290	Ca-Mg-Na-HCO3	63.3	18.3	3.5	10.8	0.864	281	6.99	2.90	0.11	26	5/2/2015
SR-0015A	Apache N.F.	404	7.2	313	Na-Ca-HCO3	4.86	91.9	0.1	2.24	0.818	249	10.6	3.10	0.05	61	5/2/2015
SR-0018A	Gila N.F.	186	7.2	147	Mg-Ca-Na-HCO3-SO4	17.7	6.39	2.8	7.85	2.75	73	23.1	5.90	0.01	454	5/9/2015
SR-0020A	Gila N.F.	83	6.6	67	Mg-Ca-Na-HCO3-SO4	9.33	3.53	2.6	2.14	0.511	39	6.66	1.94	0.04	53	5/15/2015
SR-0021A	Magdalena Ridge	158	7.8	102	Ca-Mg-HCO3	25.5	2.83	9.0	3.17	0.965	85	6.53	1.24	0.03	36	5/21/2015
SR-0022A	Magdalena Ridge	174	7.6	103	Ca-Mg-HCO3	22.6	2.81	8.0	5.84	0.884	99	6.64	1.18	0.03	37	5/21/2015
SR-0023A	Magdalena Ridge	99	7.4	62	Ca-HCO3-SO4	13.9	2.14	6.5	1.02	1.10	46	5.44	1.32	0.01	120	5/21/2015
SR-0025A	Magdalena Ridge	228	7.2	137	Ca-Mg-HCO3	36.7	4.11	8.9	4.52	0.827	133	7.56	1.64	0.04	42	5/21/2015
SR-0026A	Mogote Ridge	90	6.2	70	Ca-HCO3-SO4	11.8	2.57	4.6	1.47	0.923	41	6.86	1.33			5/22/2015
SR-0027A	Mogote Ridge	91	6.2	72	Ca-HCO3-SO4	11.4	2.28	5.0	2.06	1.19	39	8.47	1.30	0.07	20	5/22/2015
SR-0029A	San Pedro Ridge	262	7.0	181	Ca-HCO3	54.1	2.02	26.8	1.23	1.58	160	4.20	1.0	0.01	107	6/1/2015
SR-0030A	San Pedro Ridge	336	7.0	198	Ca-HCO3	55.0	4.27	12.9	7.25	2.19	208	5.63	1.47	0.02	98	6/1/2015
SR-0031A	Pecos Canyon	354	7.2	204	Ca-HCO3	70.4	1.32	53.3	2.27	0.310	206	16.0	1.10	0.01	152	6/2/2015
SR-0032A	Pecos Canyon	345	8.0	200	Ca-Mg-HCO3	68.0	1.26	54.0	2.20	0.305	203	15.6	1.13	0.02	54	6/2/2015
SR-0033A	Pecos Canyon	534	7.4	322	Mg-Ca-Na-HCO3	107	4.62	23.2	5.22	0.571	312	31.7	4.11	0.06	74	6/2/2015

Chloride concentrations in analyzed samples ranged from 1.0 to 6.2 mg L⁻¹ with a median value of 1.64 mg L⁻¹. Bromide concentrations ranged from 0.005 to 0.113 mg L⁻¹. Cl concentrations for many of the springs remained quite constant through the sampling period with a mean variance of 0.11 mg L⁻¹ Cl (Figure A.5).

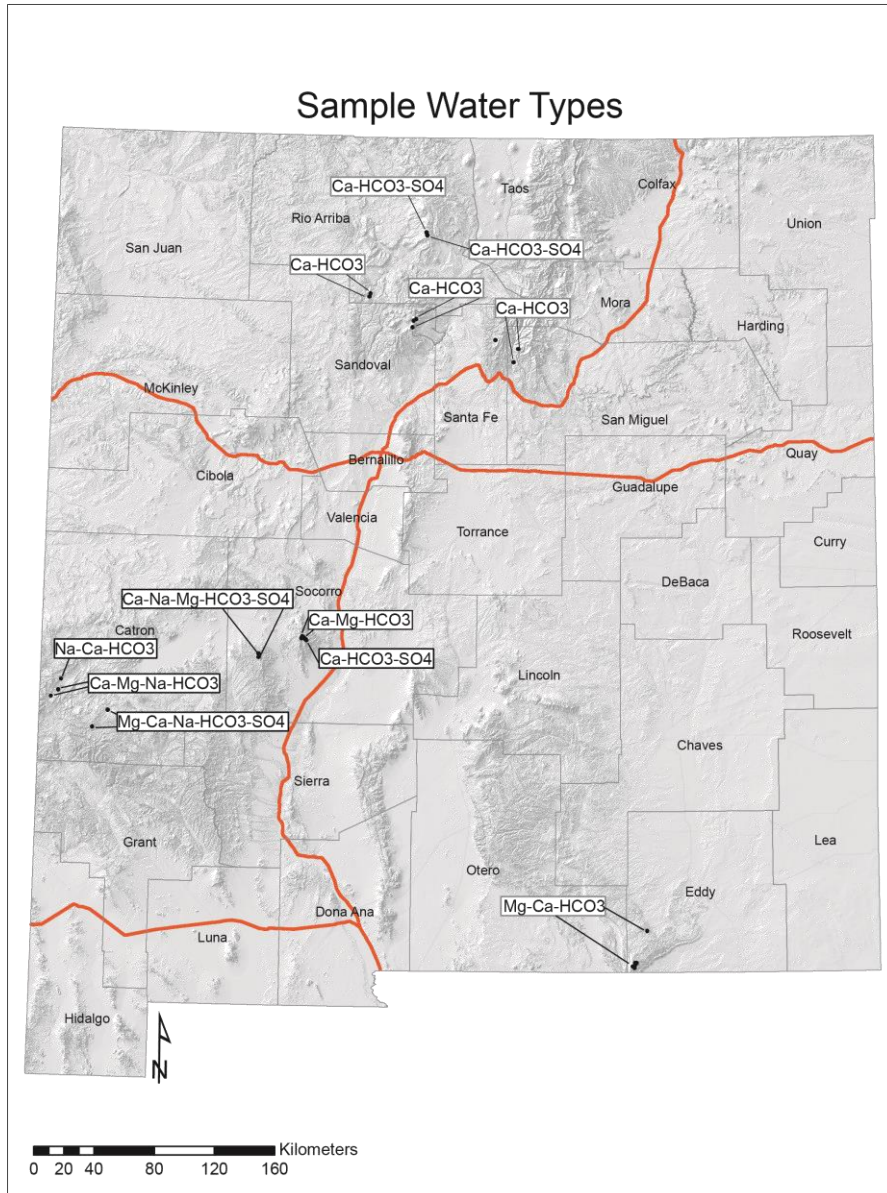


Figure A.4 The map of sample sites and corresponding water type from general chemistry analysis.

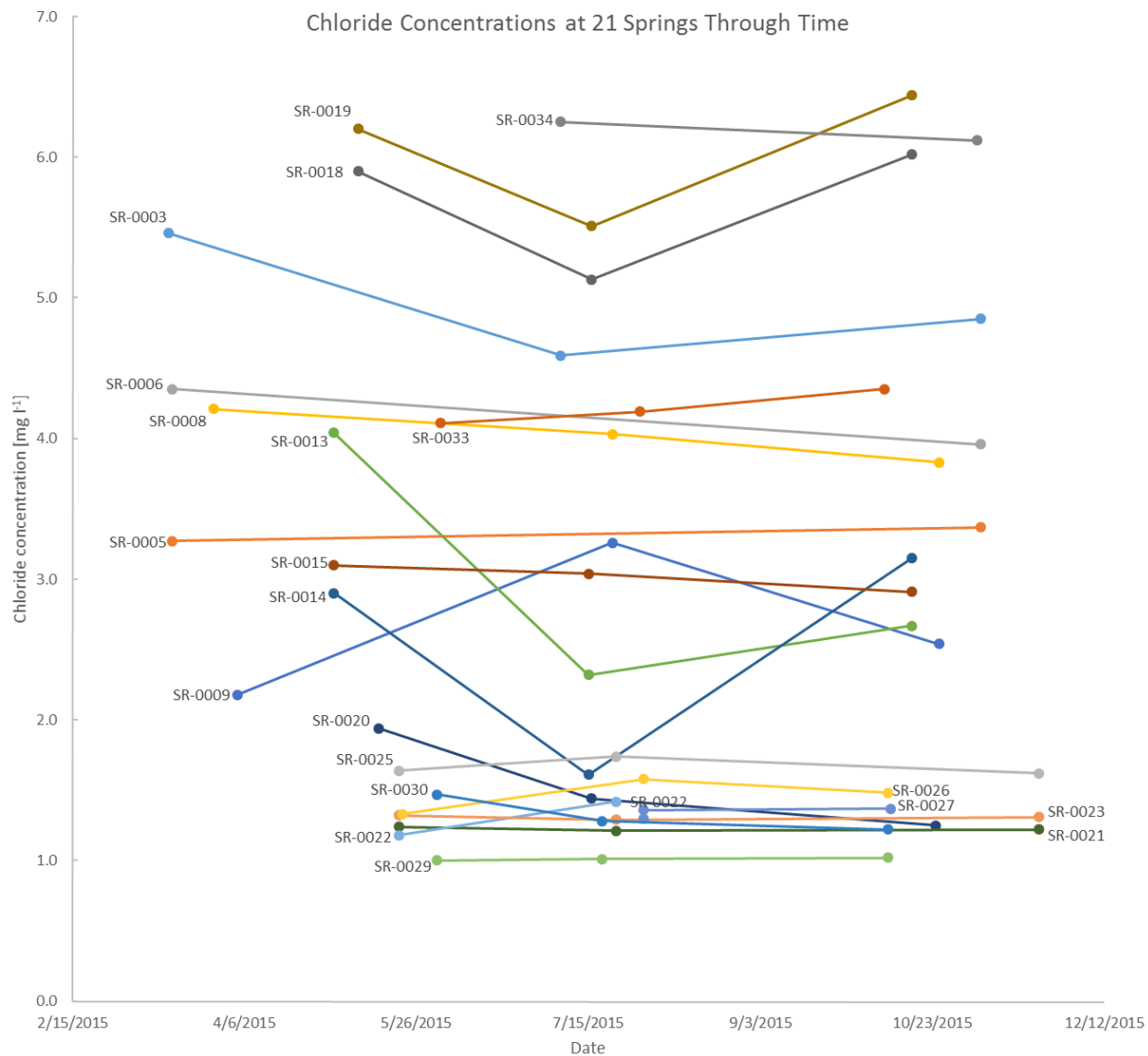


Figure A.5 Chloride concentration for each of the sample sites which were repeatedly sampled. Most sites had relatively constant chloride concentrations through time.

Chloride/bromide mass ratios were found using the the first sample from each site. Cl/Br ratios ranged from 20 to 454 with a median ratio of 97 (Table A-1) (Figure A.6). Generally, precipitation ranges from 50 to 150, shallow groundwater from 100 to 200, and waters affected by the dissolution of sodium chloride (halite) from 1000 to 10,000 (Davis et al., 1998). The low Cl/Br ratios suggest that most sampled waters were from shallow groundwater systems and had little or no contribution of Cl from geologic sources.

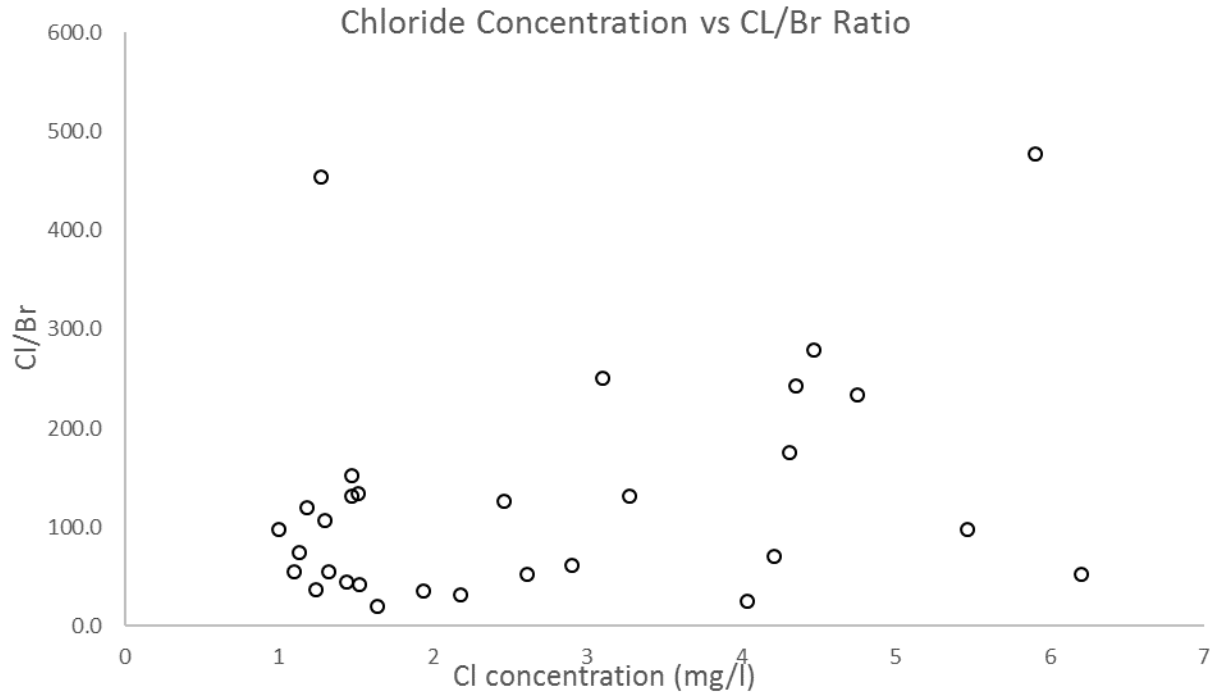


Figure A.6 Chloride concentrations and chloride/bromide ratios from 29 sites. Chloride

Samples with Cl/Br ratios approaching or exceeding the upper limit of Cl/Br ratios for shallow groundwater generally had relatively high Cl concentrations in this study, with the two highest recorded Cl concentrations having Cl/Br ratios over 450. These samples were possibly influenced by addition of geologic chloride.

The elevations of the sample sites in this study correlate positively with PRISM average annual precipitation totals, as is common worldwide due to the orographic effect of mountains on precipitation (Figure A.7). Sample Cl concentration, however did not correlate strongly with precipitation (Figures A.8), but rather had a weak negative correlation with elevation (Figure A.9).

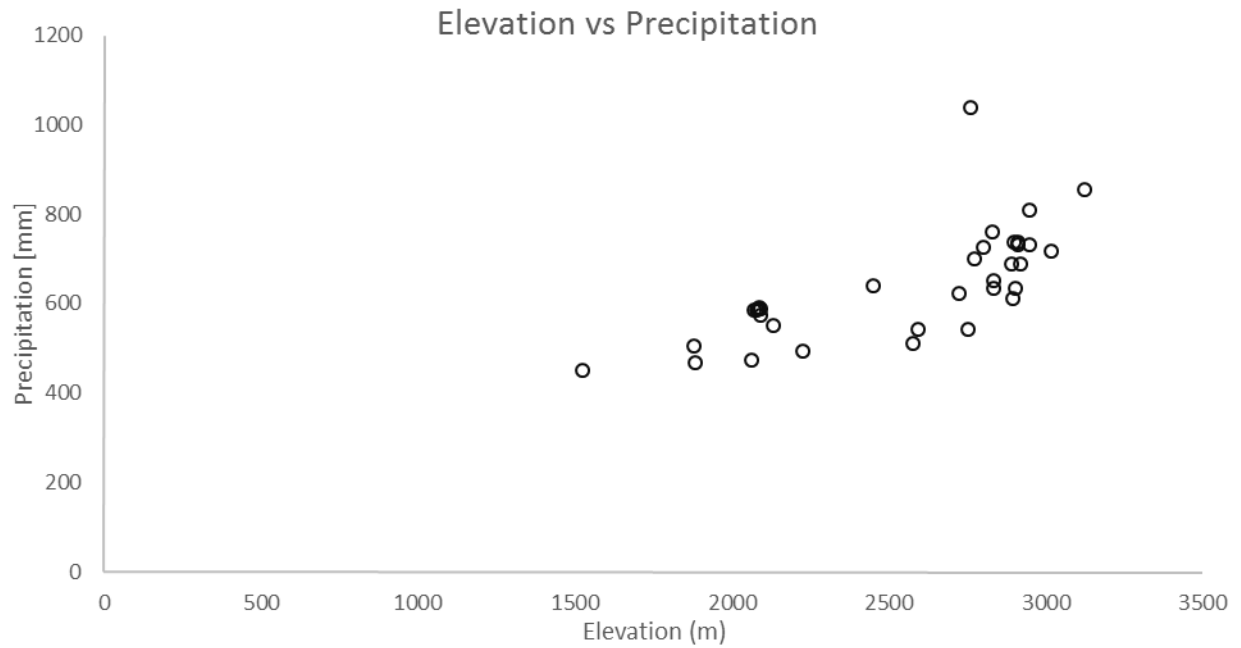


Figure A.7 Sample sites from the study showed the expected correlation between elevation and average precipitation from 1981-2010 PRISM normals.

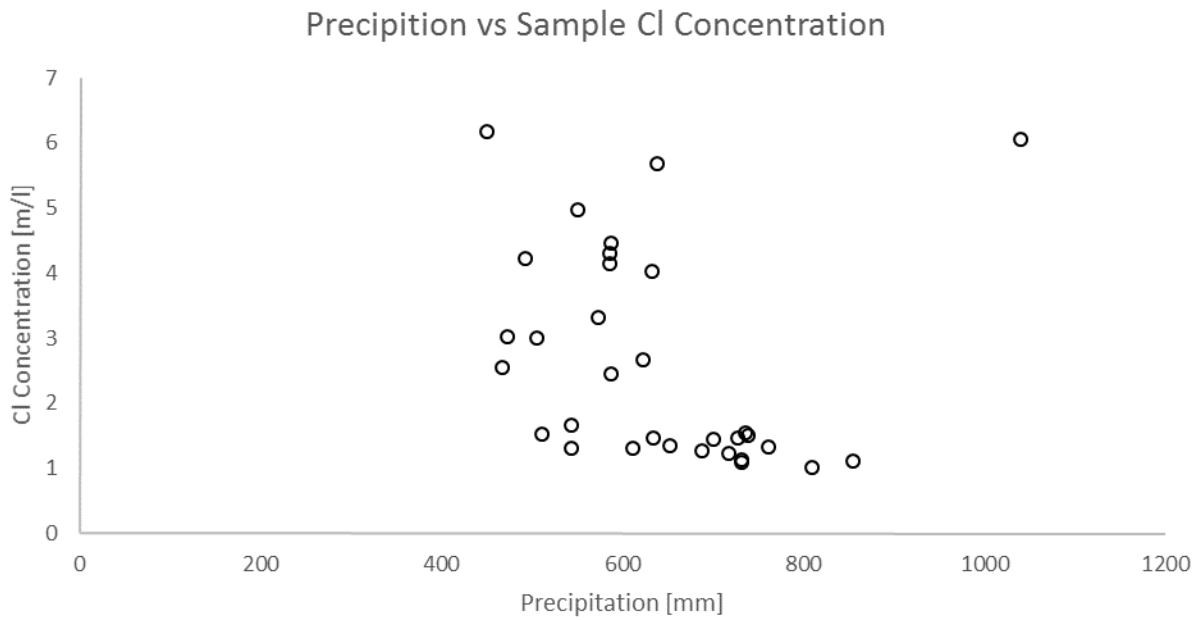


Figure A.8 Precipitation amounts had a weak or nonexistent relationship to chloride concentration at the study sites.

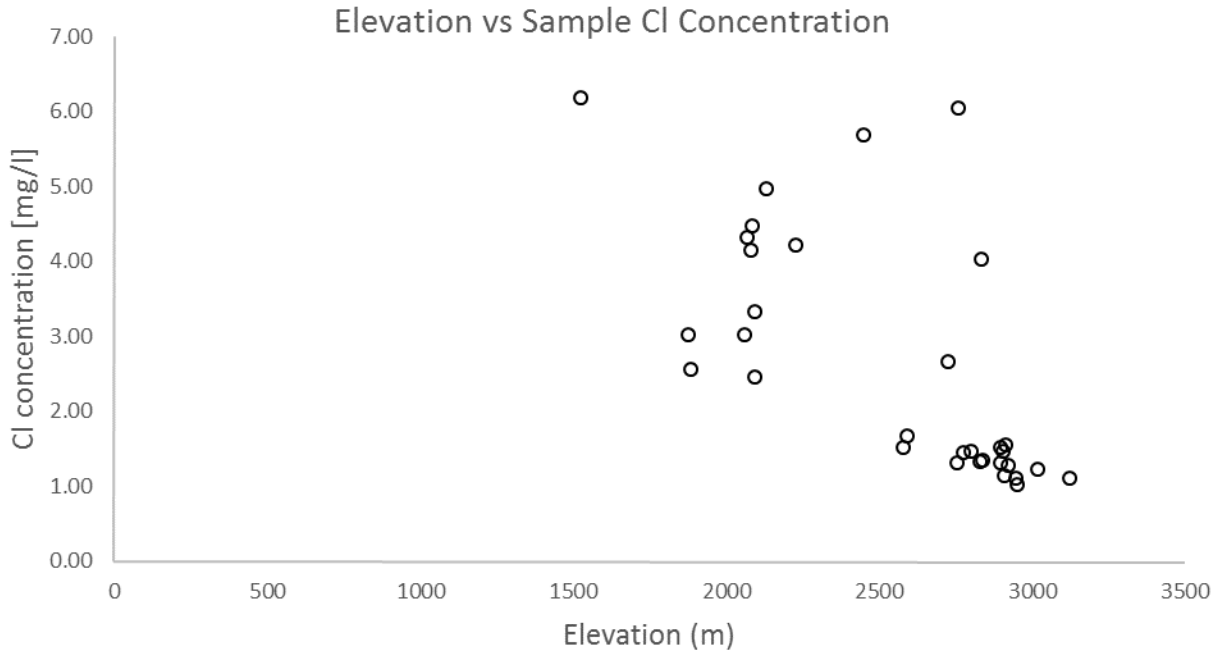


Figure A.9 Sample chloride concentration had a weak negative correlation with elevation.

Stable isotope compositions of sampled waters ranged from -14.2 to -5.4‰ $\delta^{18}\text{O}$ (i.e., $^{18}\text{O}/^{16}\text{O}$ sample vs. $^{18}\text{O}/^{16}\text{O}$ in Standard Mean Ocean Water, or SMOW) with a median value of -10.5‰ $\delta^{18}\text{O}$, and from -102 to -42‰ δD (i.e., $^2\text{H}/^1\text{H}$ vs. SMOW) with a median value of -69‰. Stable isotopic composition of spring samples fell into two categories: tightly grouped compositions and scattered compositions from repeated measurements (Figure A.10 and A.11). Stable isotopic composition of precipitation depends on the temperature when the precipitation occurred, the ultimate source of the precipitation, and the nature of the precipitation event, among other factors, thus composition of infiltrating waters would be expected to vary considerably through time. The variation in composition thus reflects the mixing of the groundwater; well-mixed groundwater would be expected to have relatively constant stable isotopic composition and represent a time-averaged water composition, while time-varying stable isotopic composition suggests the water arrives quickly and represents variations in seasonal precipitation or the source of the water. Fifteen of the 22 springs repeatedly sampled in the study discharged water of near-constant (i.e., variation of $\leq 0.5\text{‰}$ $\delta^{18}\text{O}$) stable isotopic composition; seven of the 22 sites repeatedly sampled had time-varying compositions (i.e., variation of $\geq 0.5\text{‰}$ $\delta^{18}\text{O}$).

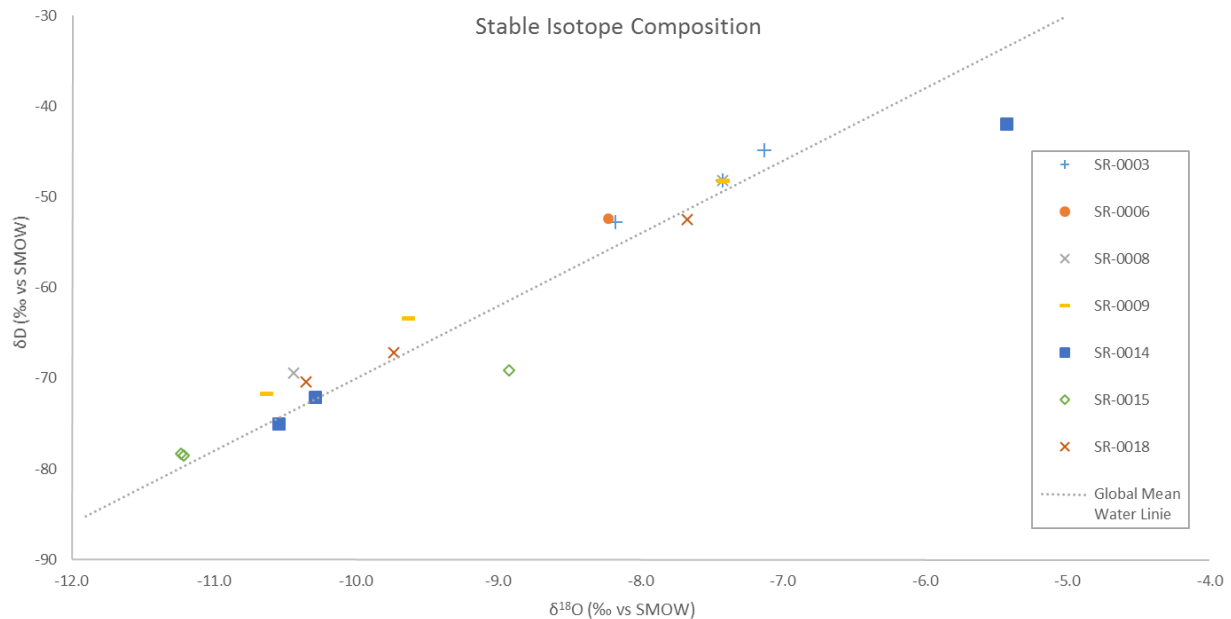


Figure A.10 Scatter plot shows sample sites at which individual sampling events yielded scattered stable isotopic compositions. Seven of 21 sample sites with repeated sampling events showed time-varying (≥ 0.5 ‰ $\delta^{18}\text{O}$ variation) stable isotopic composition.

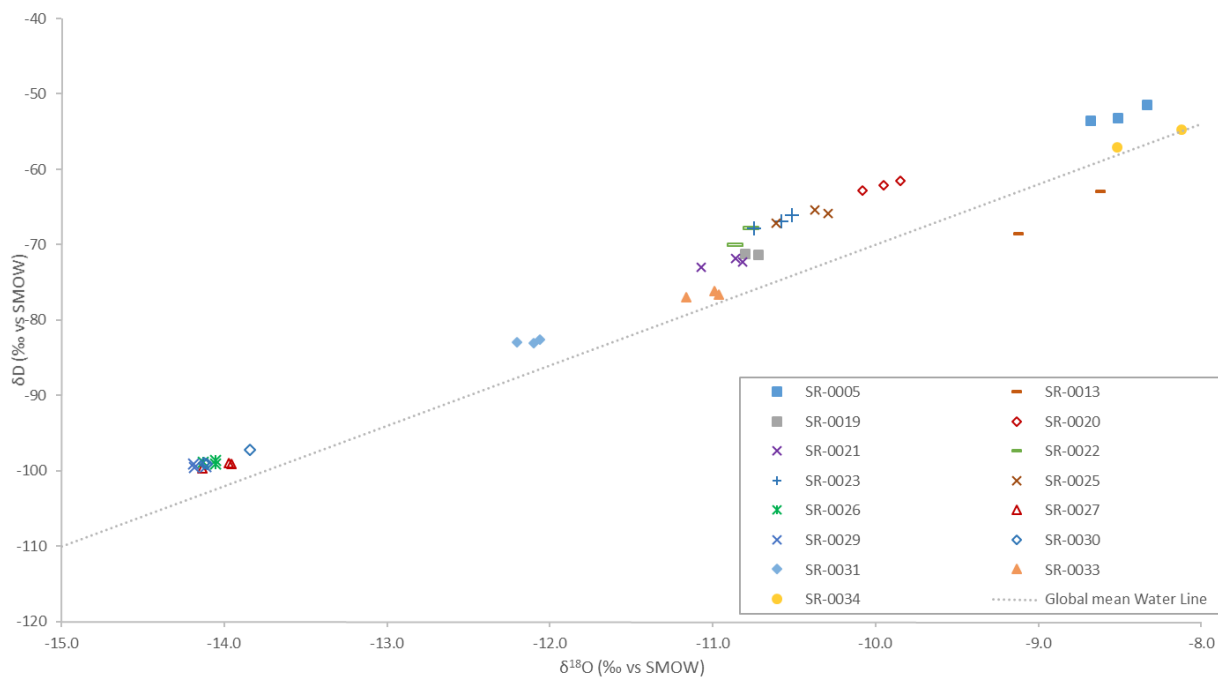


Figure A.11 Scatter plot shows tightly grouped stable isotopic composition of waters sampled repeatedly. Fifteen of 22 sample sites with repeated sampling events showed near-constant (≤ 0.5 ‰ $\delta^{18}\text{O}$ variation) stable isotopic composition.

The parameters used to estimate recharge using CMB are summarized in Table A-2. Interpretation of NADP and data from Sterling (2000) show that effective Cl concentration in infiltrating waters to range from 0.08 to 0.20 mg I⁻¹ with a median value of 0.16 mg I⁻¹. Precipitation from the 1984-2013 PRISM data set shows a range of precipitation amounts from 450 mm at SR-0034 at 1524 m elevation in the Guadalupe Mountains to 1039 mm at SR-0019 at 2759 m elevation on the Mogollon Plateau.

Table A-2. Summary of average annual precipitation, estimated average annual wet Cl deposition, dry deposition as percentage of wet deposition, and effective Cl concentration in infiltrating water was used to estimate annual average recharge at sample points of springs sampled at least o

Point ID	PRISM 30 Year Mean Precipitation [mm]	Average NADP Chloride Concentration in Precipitation [mg/l]	Dry Deposition as Percentage of Total (Wet + Dry)	Estimated Effective Chloride Concentration in Infiltrating Water [mg/l]	Estimated Average Annual Recharge [mm]	Recharge as Percentage of Precipitation
SR-0001	587	0.11	45%	0.20	27	4.6%
SR-0002	587	0.11	45%	0.20	49	8.3%
SR-0003	550	0.11	45%	0.20	23	4.1%
SR-0004	592	0.11	45%	0.20		
SR-0005	573	0.11	45%	0.20	35	6.1%
SR-0006	586	0.11	45%	0.20	29	0.5%
SR-0007	586	0.11	45%	0.20	28	4.7%
SR-0008	633	0.10	35%	0.17	24	3.9%
SR-0009	623	0.10	35%	0.17	36	5.8%
SR-0010	738	0.06	25%	0.15	41	5.6%
SR-0011	727	0.06	25%	0.15	42	5.7%
SR-0012	700	0.06	25%	0.15	41	5.9%
SR-0013	506	0.12	30%	0.16	30	5.9%
SR-0014	468	0.12	30%	0.16	32	6.9%
SR-0015	473	0.12	30%	0.16	28	5.8%
SR-0016	687	0.09	40%	0.18	84	12.3%
SR-0017	687	0.09	40%	0.18		
SR-0018	639	0.11	30%	0.16	18	2.9%
SR-0019	1039	0.12	30%	0.16	28	2.7%
SR-0020	736	0.12	30%	0.16	79	10.8%
SR-0021	717	0.09	40%	0.18	92	12.8%
SR-0022	611	0.09	40%	0.18	73	12.0%
SR-0023	543	0.09	40%	0.18	65	11.9%
SR-0024	511	0.09	40%	0.18	52	10.2%
SR-0025	543	0.09	40%	0.18	51	9.3%
SR-0026	633	0.06	20%	0.14	35	5.5%
SR-0027	652	0.06	20%	0.14	39	5.9%
SR-0028	855	0.07	30%	0.16	72	8.4%
SR-0029	810	0.06	20%	0.14	65	8.0%
SR-0030	760	0.06	20%	0.14	46	6.1%
SR-0031	731	0.07	25%	0.15	59	8.1%
SR-0032	731	0.07	25%	0.15	57	7.9%
SR-0033	493	0.07	25%	0.15	10	2.1%
SR-0034	450	0.11	45%	0.20	15	3.3%

Generally, recharge rates were greater at higher elevations with correlation coefficients of $r = 0.49$ and $r = 0.67$ between elevation and average annual recharge [mm] and average annual recharge as a percentage of average precipitation, respectively (Table A-3; Figure A.12). There was also a positive correlation ($r = 0.39$) between average recharge and precipitation (data not

shown). The correlation was weak ($r = 0.08$) between average recharge as a percentage of precipitation and average annual precipitation (Figure A.13). Table A-3 show correlation coefficients for all regression analyses that were conducted.

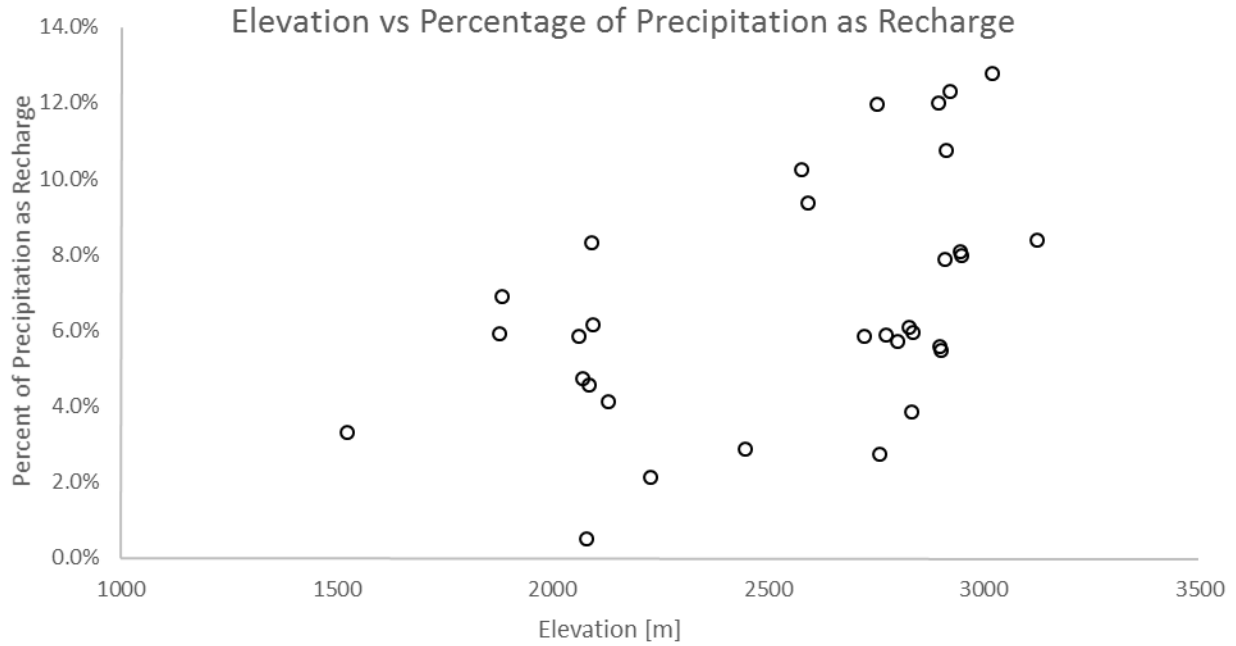


Figure A.12 Elevation and percentage of precipitation as recharge were positively correlated ($r=0.67$).

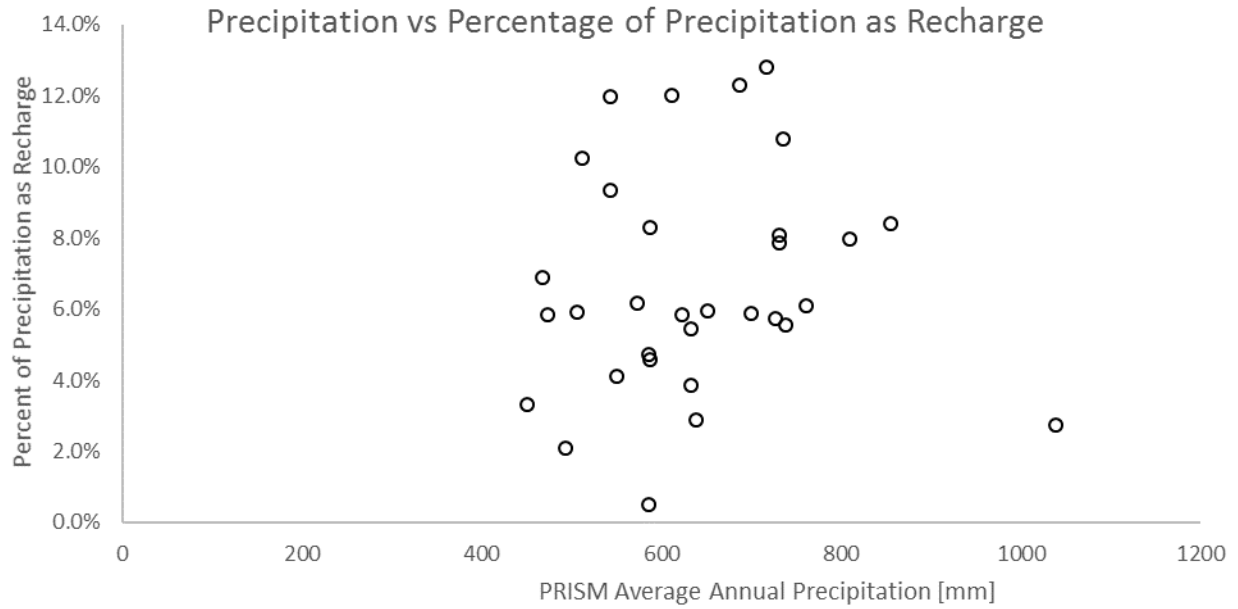


Figure A.13 There was a weak correlation ($r = 0.08$) between precipitation and estimated recharge as percent of precipitation.

Table A-3 Summary of correlation coefficient between selected variables from the chloride mass balance study.

	Average Annual Recharge as Percent of Precipitation	Average Annual Recharge [mm]	Elevation	Average Annual Precipitation	Effective Chloride Concentration in Infiltrating Waters [mg/l]	Average Cl Concentration [mg/l]
Correlation Coefficients (r)						
Average Annual Recharge as Percent of Precipitation	1.00	0.90	0.49	0.08	0.06	-0.73
Average Annual Recharge [mm]		1.00	0.67	0.39	-0.05	-0.76
Elevation			1.00	0.71	-0.52	-0.67
Average Annual Precipitation				1.00	-0.44	-0.22
Effective Chloride Concentration in Infiltrating Waters [mg/l]					1.00	0.41
Average Cl Concentration [mg/l]						1.00

A.5 Discussion

Generally, the geochemical composition of the sample springs, and their variation through time support using this data to make estimates of recharge. With the exception of one sample, Na was a minor anion in all sampled waters, indicating little geochemical evolution of groundwaters discharged at the study sites. Low TDS concentrations and the dominance of the calcium cation also suggest the sampled waters were young and had reacted little with the

subsurface geology. Chloride concentrations over repeated sampling events were quite constant from spring through fall, with several exceptions. This suggests the waters were well mixed and samples taken any other time would likely have a similar composition. Springs sampled repeatedly showed a maximum variation of 1.72 mg l^{-1} at SR-0013. All but two water samples showed Cl/Br ratios below 200, an upper limit for shallow groundwater according to Davis et al (1998). The two samples exceeding this threshold had Cl/Br ratios of 234 (SR-0008) and 454 (Sr-0018), and contained Na as a secondary and tertiary cation, respectively. The presence of Na and the relatively high Cl/Br ratio indicate possible mixing of shallow groundwater with deeper water that may have been impacted by geologic sources of Cl. The majority of stable isotope data also suggest these sites discharge well-mixed water, though 7 of the 22 repeated samples had scattered stable isotopic compositions. Removing the sites of repeated sampling that had a range of Cl concentration greater than 1.0 mg l^{-1} , and which had a range of $\delta^{18}\text{O}$ greater than 0.5‰ leaves 14 sites of consistent water chemistry, all of which had Cl/Br ratios of 152 or less. These sites show the most potential to be used in calibration and corroboration of the ETRM.

Sample sites with only one sample were intended to find the shallow groundwater Cl concentration during the spring snow melt pulse. While this is a temporally limited glimpse into the composition of infiltrating snowmelt, the spring snowmelt was shown by the ETRM to be important; this data was therefore used cautiously in comparisons to modeled recharge.

APPENDIX B: ETRM SNOW MODEL

B.1 Background

Regions with a positive water balance (i.e., stream production and likely groundwater recharge) in New Mexico generally occur in the mountains and highlands, where annual snow fall stored in snowpack forms a significant percentage of the total annual precipitation. This makes having a reasonable estimate of water stored in snow cover necessary for predicting recharge. In particular, by storing water in the snowpack through the winter, spring snow melt releases concentrates the infiltration of water into an extended, low-intensity event that during a time of year with low incoming energy fluxes and low plant transpiration rates. In other words, snow melt can release stored water to infiltrate while ET rates are low. The accurate modeling of the winter snowpack in the mountains of New Mexico is necessary to mimic both the storage of precipitation as snow in the winter snowpack and the release in the spring of the snow as meltwater. A simple analysis was performed on PRSIM data from 2000-2014, under the assumption that all precipitation falling on a day when the mean of the PRISM maximum and minimum air temperature was below 0°C fell as snow (Figure B.1). This analysis indicates that over 23% of the area of New Mexico receives 10% or more of its total precipitation in the form of snow, and about 5% of the state receives over 20% of its total precipitation as snow. This flux of water from snowmelt represents a large fraction of the annual incoming water to the soil layer in many places after snowy winters. The combination of months of stored precipitation being released over a short period and low available energy can create conditions in the soil conducive to high recharge rates.

There are a range of snow models designed to predict the behavior of snow over the winter and during periods of melt. Snow models are constrained in complexity by the availability of observational data that can be used to verify model parameters and optimize model performance through calibration. Models thus generally fall in two categories: those that attempt to solve the snowpack energy balance and depend on intensive data collection (usually over small areas) and model computation; and those aimed at achieving adequate simulation of snow accumulation and melt for operational purposes over large areas that lack extensive instrumentation. Perhaps the simplest method for modeling snow is the degree day factor (DDF) or temperature-indexing approach, which relies on observed temperature to calculate melt (Rango and Martinec, 1995). These models typically ignore the movement of snow by wind and ablation, the vaporization of snow, and effects of snow metamorphism. The simplicity of areal air temperature estimates and their widespread use has resulted in the frequent application of DDF models in the Western US. (Flint and Flint, 2008; Hevesi, 2003).

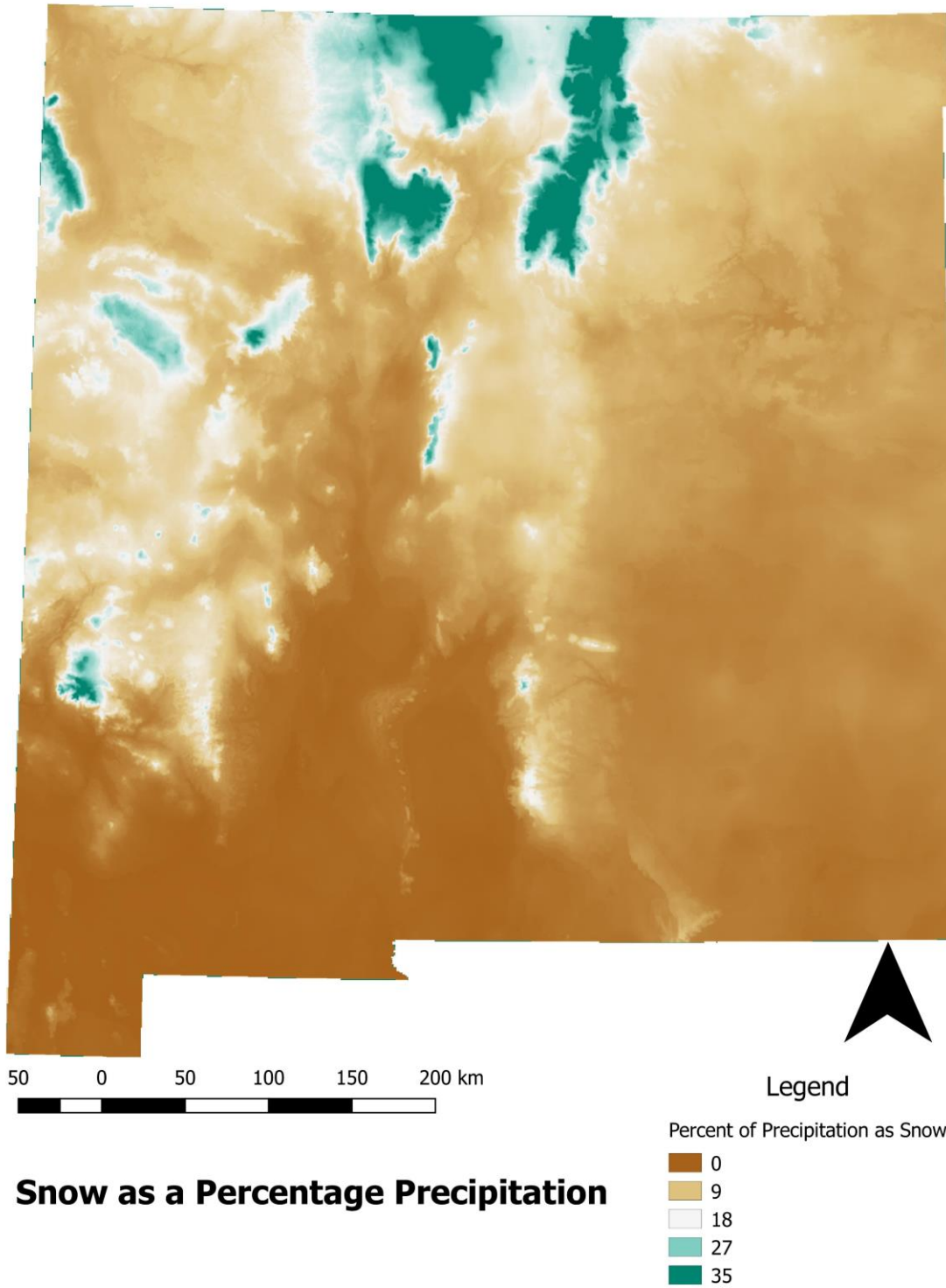


Figure B.1 Snowfall as a percent of 2000-2013 precipitation totals.

Remotely sensed measurements of snow cover has been incorporated into this approach in order to improve runoff estimates during melt events (Martinec, 1975; Rango and Martinec, 1994; Siedel and Martinec, 2004) The success of air temperature as the only physical input to snow melt models may be its high correlation with other energy fluxes (Hock, 2003), especially the longwave radiation and sensible heat components, which, together, may account for over 70% of available energy for melt (Ohmura, 2001). Temperature-index snow modeling assumes, however, that the components of the heat energy balance maintain constant relative contributions, an assumption weakened by seasonally varying shortwave radiation due to changes in sun angle, day length, and by spatial variations in sheltering by terrain features. To account for the temporally and spatially varying energy balance components, more rigorous, physically-based snow modeling approaches have been taken (Anderson, 1976; USACE, 1998; Koivusalo and Kokkonen, 2002). At a minimum, the energy- or process-based models account for sensible and latent heat transfer, conduction of heat through the snow pack, long- and short-wave radiation flux, heat flux in rain, ground heat flux, and storage of heat energy in the snowpack. Additional model parameters may be added to account for the blowing snow, and the interception and sublimation of snow in vegetation, among other parameters. While physically-based models may more accurately depict the myriad of processes that occur in snowpack from formation to melt, both their computational requirements, and the need for detailed and complete physical observations renders them unsuitable for operational use in large scale distributed hydrologic models at the present time.

Efforts have been made to strike a balance between the easy deployment of large scale temperature-index or DDF snow models and the ability of physical models to account for melt under varying surface and atmospheric conditions. These have led to the combination of temperature indices with radiation-based parameters tailored to the site-specific characteristics of study areas in an attempt to account for parameters (e.g., shortwave radiation) that influence melt rates independently of air temperature. Brubaker and others (1996) described the possible improvements to snowmelt-runoff models using this combination approach. Cazorzi and Dall Fontana (1996) combined the DDF method with 5 energy index maps per winter to calculate melt. Each map was created using a simple algorithm to compute potential energy using apparent sun motion and elevation, topographic aspect, shading, and slope from a digital terrain model. Diffuse radiation, reduced by a sky-view factor was added and an energy index of local variability of potential energy. Hock (1999) developed this method further at a small alpine glacier by reducing the time step of the melt calculation from daily to hourly and creating an hourly energy index based on a 30-m DEM. They found that by increasing the spatial and temporal resolution, the model was better able to reflect the diurnal spatial variation in melt rates. Both of these temperature/energy-index snow models rely on an empirical radiation factor that was used to calibrate the snow model to match observations. Both of these models exceeded the performance of DDF methods by simulating the spatial variability of melt due to topographic effects on available energy.

B.2 Methods

The ETRM snow model takes a simple approach to modeling the snow cycle. PRISM temperature and precipitation are used to account for snowfall. The mean of the maximum and minimum daily temperature is found; any precipitation falling during a day when this mean temperature is less than 0°C is assumed to be stored as snow. While other snow-modeling

techniques assume that a transition zone exists over which the percent of precipitation falling as snow varies over a range of elevation or temperature, the ETRM assumes all precipitation on any given day falls either entirely as snow or as rain. The storage mechanism in the ETRM simply stores the snow as a snow water equivalent (SWE). No attempt is made to model the temporal and spatially-varying density and texture of snow during its duration in the snow pack, nor to model the effect the snow has on the underlying soil layers. In the ETRM, ablation of snow by sublimation and the movement of snow by wind is ignored.

In computing the melting rate of snowpack in above-freezing conditions, a balance has been sought between the use of available physical parameters in a simple and computationally efficient model and the representation of important physical parameters. The ETRM uses incident shortwave radiation (R_{sw}), a modeled albedo with a temperature-dependent rate of decay, and air temperature (T_{air}) to find snow melt. Flint and Flint (2008) used Landsat images to calibrate their soil water balance model, and found that a melting temperature of 0°C had to be adjusted to 1.5°C to accurately represent the time-varying snowpack in the Southwest United States; we have implemented this adjustment in the ETRM.

(42)

$$melt = (1 - a_i) * R_{sw} * \alpha + (T_{air} - 1.5) * \beta$$

where $melt$ is snow melt (SWE), a_i is albedo [-], R_{sw} is incoming shortwave radiation [$W\ m^{-2}$], α is the radiation-term calibration coefficient [-], T is temperature [$^{\circ}C$], and β is the temperature correlation coefficient [-]

Albedo is computed daily, is reset following any new snowfall exceeding 3 mm SWE to 0.90, and decays according to an equation after Rohrer (1991):

$$a_i = a_{min} + (a_{i-1} - a_{min}) * f(T_{air}) \quad (43)$$

$$f(T_{air}) = e^{-0.05t}, T_{air} < 0 \quad (44)$$

$$f(T_{air}) = e^{-0.12t}, T_{air} > 0 \quad (45)$$

where a_i and a_{i-1} are albedo on the current and previous day, respectively, a_{min} is the minimum albedo of 0.45 (Wiscombe and Warren; 1980), a_{prev} is the previous day's albedo, and k is the decay constant. The decay constant varies depending on temperature, after Rohrer (1991).

The ETRM snow model depends on two disparate available parameters (i.e., T_{air} and rg) to compute melt daily that must be calibrated using observed snowpack and meteorological data. In our current application this calibration data is provided by the National Resources Conservation Service's Snowpack Telemetry (SNOTEL) network (NRCS). These sites are equipped with instrumentation to measure the SWE of snow on the ground, air temperature, and

precipitation. SNOTEL operates 27 sites in New Mexico (Figure B-2). Of these sites, 23 had sufficiently complete data for use in calibration. Most sites are located in two distinct geographic areas. The majority of SNOTEL sites (16 of 23) are located in the southern Rocky Mountains. These sites tend to be located on steep mountains that rise abruptly from the surrounding Colorado Plateau. The remaining SNOTEL stations are scattered around southwestern and south-central New Mexico. These sites (with the exception of Sierra Blanca) are sited on mountains with less topographic prominence than the northern sites. Additionally, these sites generally receive a greater part of their annual precipitation as rain rather than snow.

For the calibration process, all ETRM input parameters were extracted for the period of 1 January 2000 through 31 December 2013 at the geographic location of each of the 23 SNOTEL sites. SNOTEL data was gathered for the same period where possible. These data include observed SWE on the ground, air temperature, and precipitation, among others. The ETRM was then used in dozens of simulations using the SNOTEL temperature and precipitation in place the PRISM data set. The use of data taken from the SNOTEL site itself was intended to reduce the error introduced by the 800 m PRISM product that could mask the efficacy of the snow model. We then ran the ETRM using a range of calibration parameter value pairs previously determined to be physically reasonable. We used the difference in modeled and observed SWE and duration of snow cover over a season as our objective function. The calibration coefficients leading to the lowest mean error for all sites for up to 14 years were chosen and applied to the ETRM over the entire state. Over 1000 calibration coefficient pairs were tested.

B.3 Calibration Results

It was found that the smallest error in the calculated snow melt was achieved by applying $\alpha = 0.07$ and $\beta = 1.0$, resulting in a mean error in winter maximum snowpack in SWE of 31.3%, and a mean error in snowpack duration in days of 20.8%. The minimum error of 3.5% in snow cover duration was found at the Taos Powderhorn SNOTEL site (Figure B.3), the maximum error was 40.3% at Tres Ritos (Figure B.4). The minimum error of 11.0% in maximum winter snow cover in SWE was found at Tolby (Figure B.5), the maximum error of 72.9% was found at Frisco Divide SNOTEL site (Figure B.6).

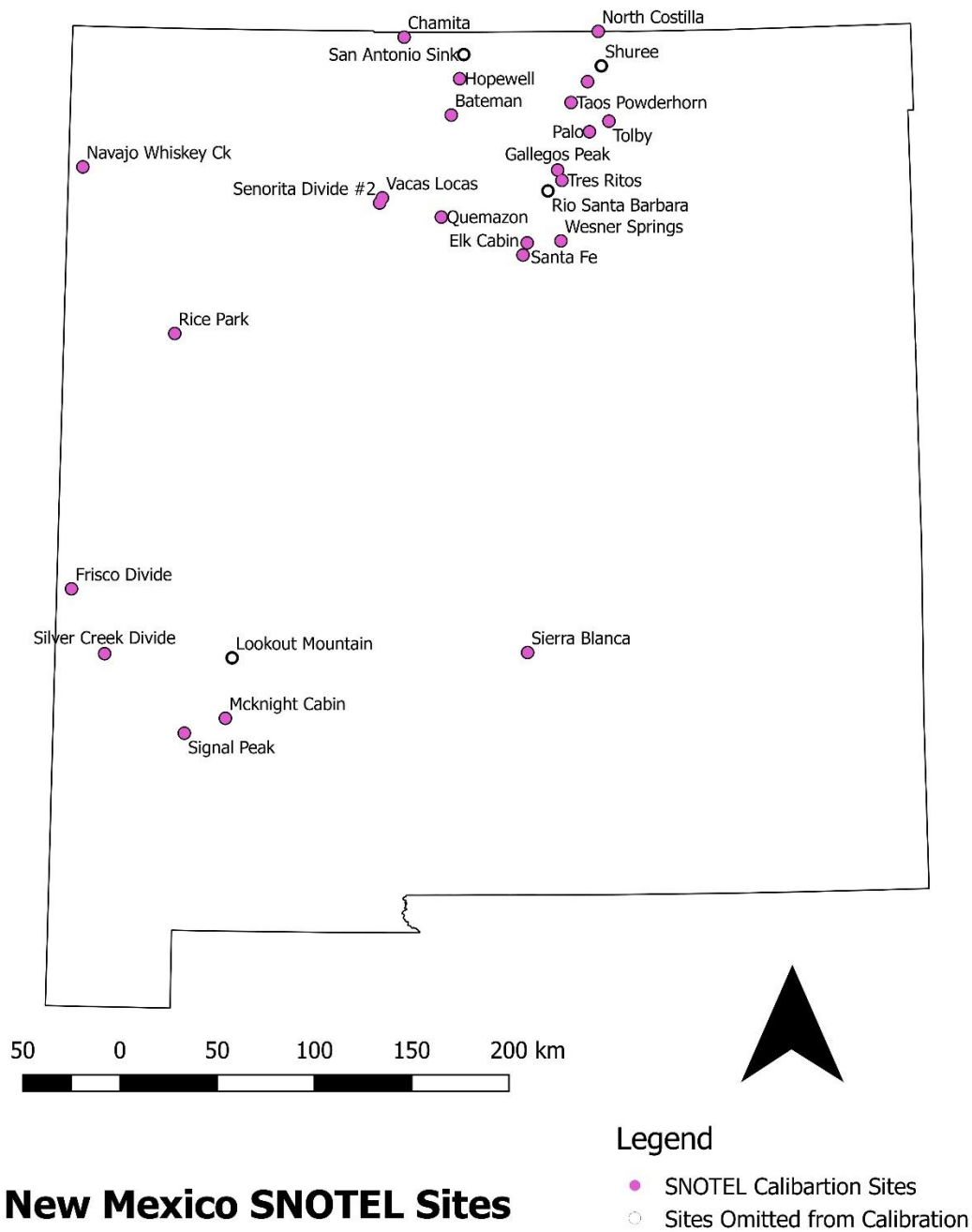


Figure B.2 Map of 24 Natural Resources Conservation Service Snowpack Telemetry sites chosen for ETRM snow model calibration in New Mexico. Four sites had incomplete data and were excluded.

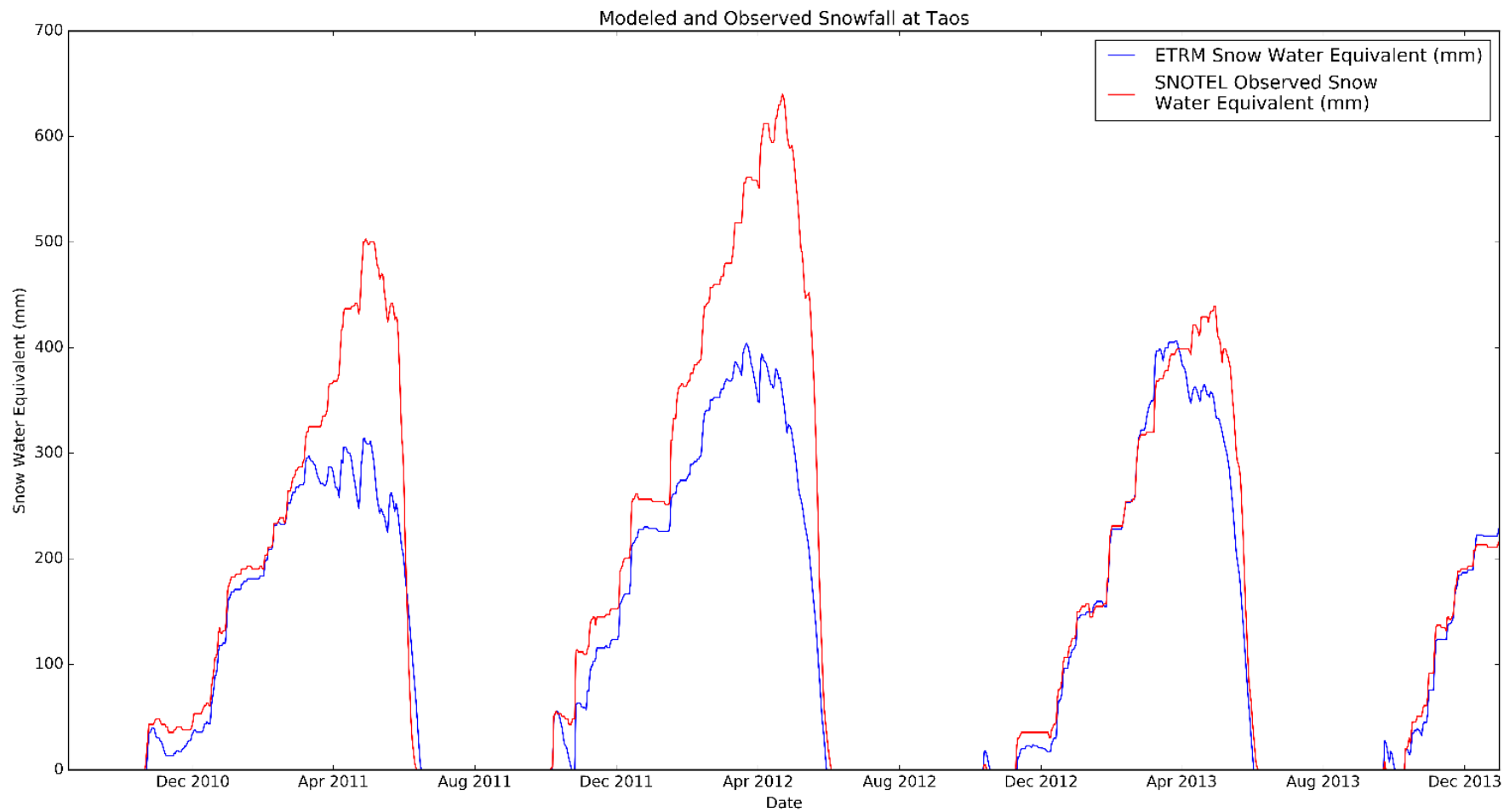


Figure B.3 The ETRM snow model compared with observed SNOTEL data at the Taos Powderhorn SNOTEL station. The ETRM modeled snow cover duration in days differed by a mean of 3.5% over the 14 model winters at the site. The duration of snowpack at this site is well simulated, while the maximum SWE has considerable error in the winters of 2010/2011 and 2011/2012.

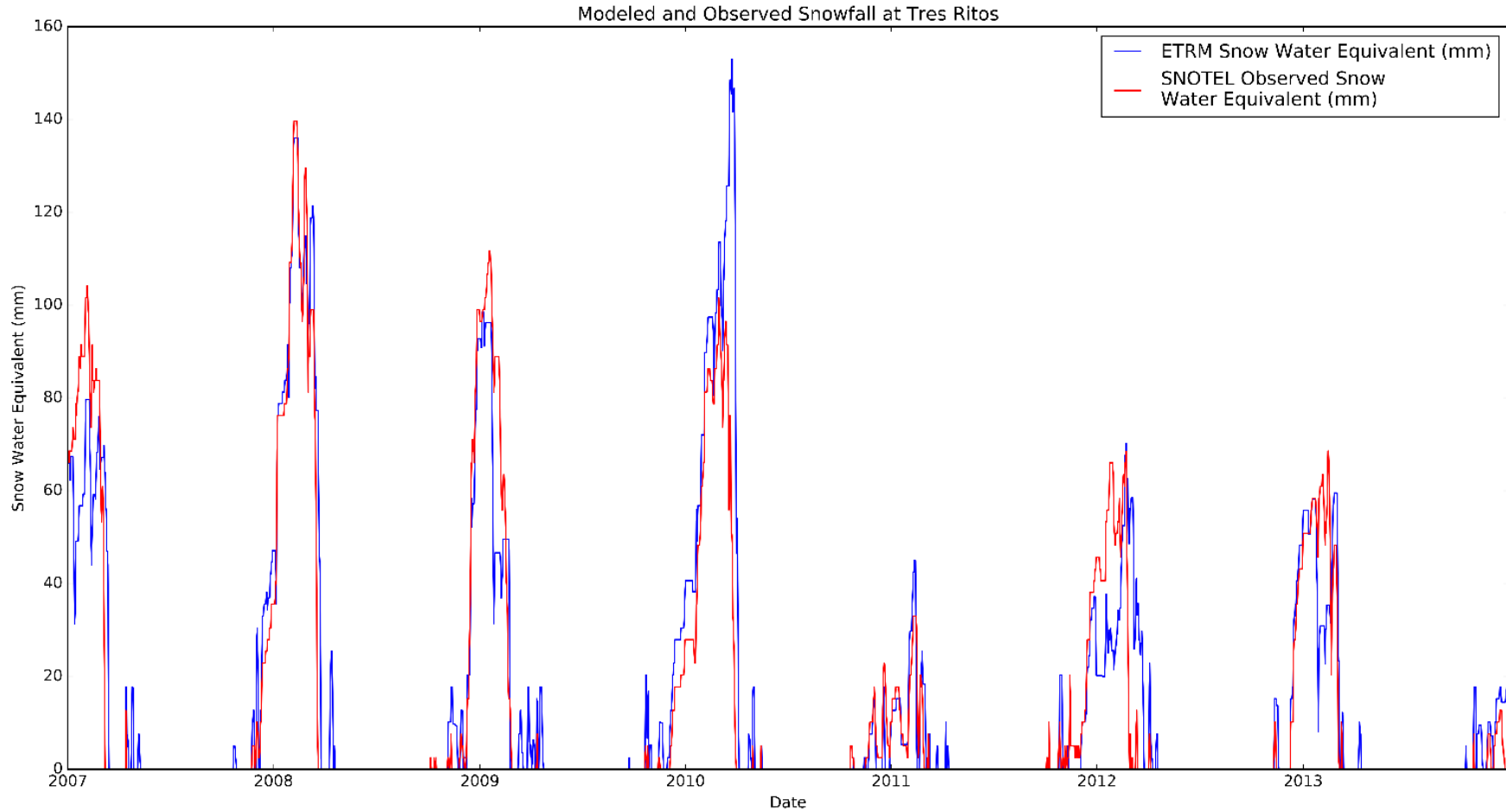


Figure B.4 The ETRM snow model compared with observed SNOTEL data at the Tres Ritos SNOTEL station. The ETRM modeled snow cover duration in days differed by a mean of 40.3% over the 14 model winters at the site. The ETRM produces mid-winter melt events on many cases that did not occur at the station.

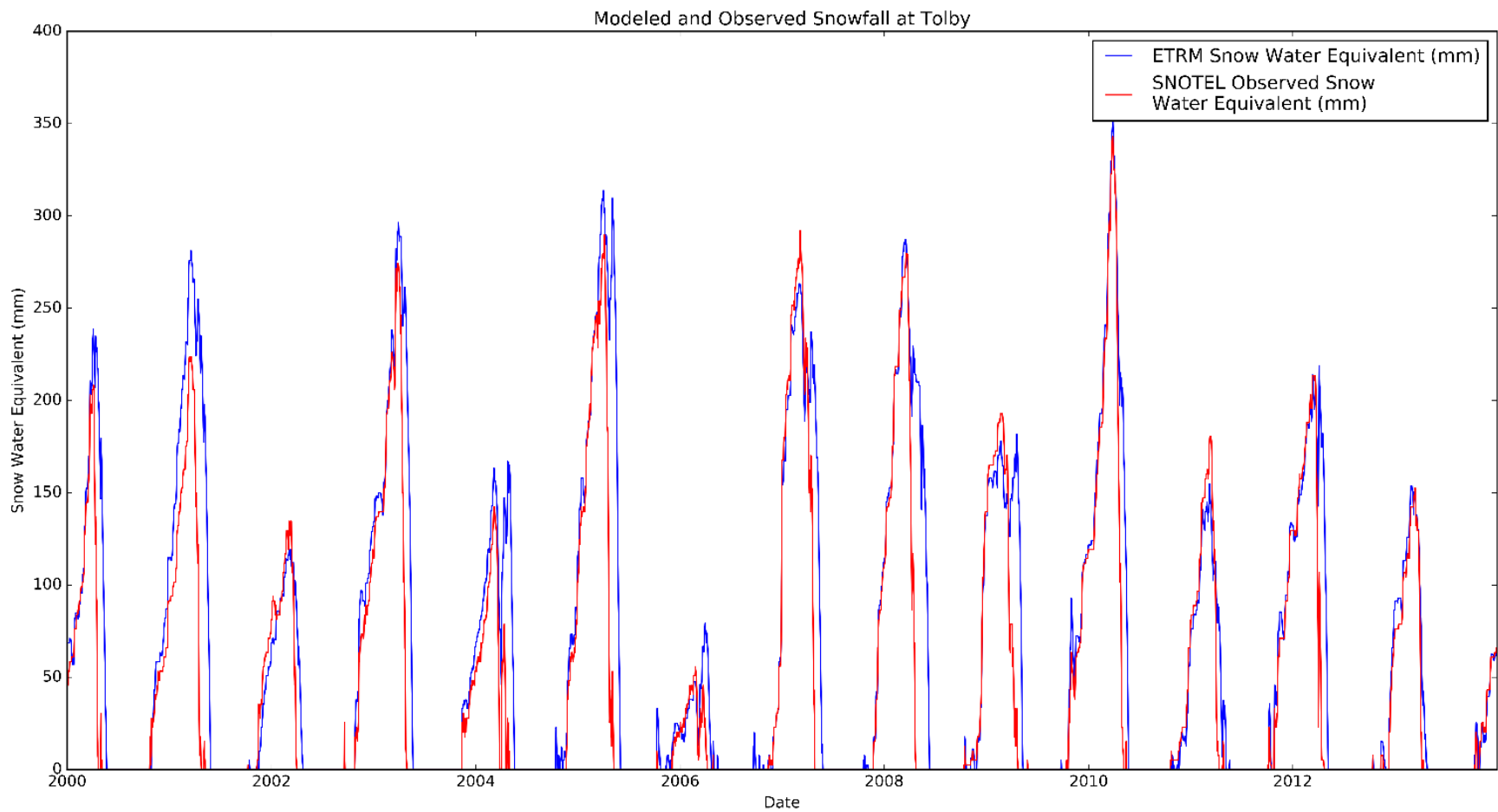


Figure B.5 The ETRM snow model compared with observed SNOTEL data at the Tolby SNOTEL station. The ETRM modeled snow cover duration in days differed by a mean of 11.0% over the 14 model winters at the site.

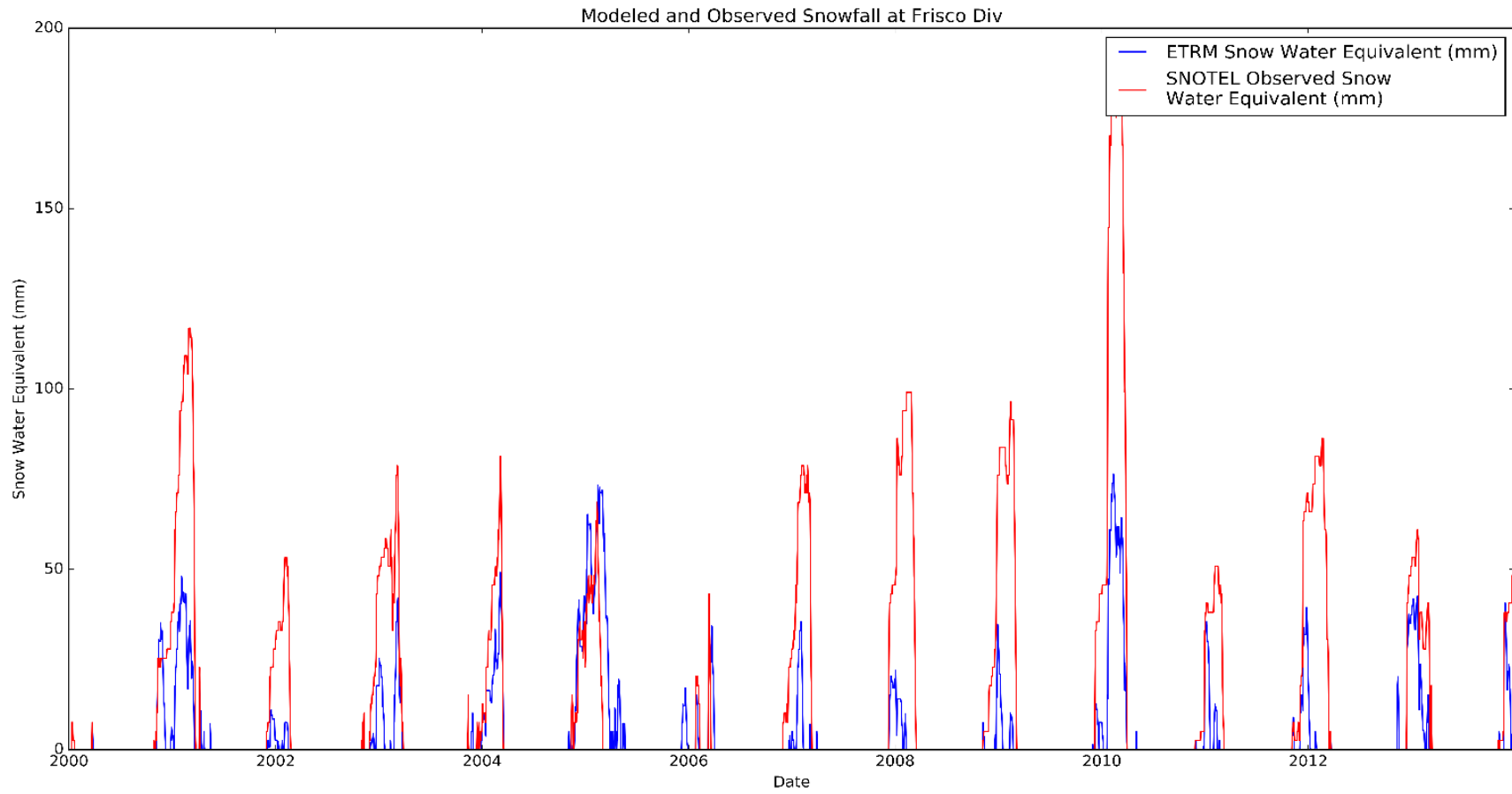


Figure B.6 The ETRM snow model compared with observed SNOTEL data at the Frisco Divide SNOTEL station. The ETRM modeled snow cover duration in days differed by a mean of 72.9% over the 14 model winters at the site.

B.4 Discussion

Under the current calibration, the ETRM accomplishes the simulation of snow cover duration more effectively than maximum snow cover as measured in SWE. This is likely due to the relatively abrupt change from daily below-freezing temperatures to mean daily temperatures above freezing. This appears to prevent the persistence of snow pack at warmer air temperatures. The available radiation at each site is likely the cause of large differences in the performance of the ETRM snow model between sites. Using a radiation term based on a 250m grid cell cannot account for the very local scales (10s of m) variations in vegetation that most certainly control the rate of melting and the opportunity for winter melting events at the site scale. Most sites are in forested and mixed forest and parkland environments where, while temperatures may be representative of the larger area, small scale differences in forest canopy, turbulent air flow, and topographic aspect likely cause patchy melting in the spring, with great variations over small distances in snowpack SWE.

The ETRM snow model performs best at northern stations. Southern stations are few and likely have a distinct winter climate from the densely clustered and very numerous stations in the San Juan and Sangre de Cristo Mountains. As the calibration is focused on minimizing total error over all stations, and equal weight is given to each SNOTEL site, calibration favoring northern sites' performance is an expected bias of the snow model. This is justified as the northern part of the states receives the vast majority of snowfall in terms of volume. Future work may consider an examination of the fundamental climatic differences between southern and northern sites and a separate calibration for each.

The most serious weakness of the ETRM snow model is that the SNOTEL sites against which its performance is calibrated and measured fall in a narrow elevation range from 2380 m.a.s.l. to 3290 m.a.s.l. This narrow envelope of terrain represents only the snowiest accessible sites in the state. A model based on snow behavior at this range of elevations probably performs poorly at lower elevations where snows are less frequent and snowpack less persistent because calibration efforts have focused on higher and snowier sites. While snowfall may represent a smaller portion of the total water balance at these sites, its contribution to springtime soil moisture may have a considerable impact on early summer ET rates and thus water availability for recharge.

The use of remote sensing offers an opportunity to improve the ETRM snow model through its use in further calibration. Identification of SWE to within a few tens of millimeters is possible with passive microwave satellite data using several novel approaches (Tait, 1998; Singh and Gan, 2000; Pulliainen, 2006). Recent developments in the use of MODIS and Landsat data to estimate snow coverage and SWE provide an opportunity to calibrate the ETRM snow model to areal snow coverage and SWE at high frequency (Liang, 2008; Gao et al., 2010 [a, b]; Ying, 2015). In addition to the calibration parameters described above, the ETRM snow model would

likely benefit from a calibration based on the rate of melting in terms of SWE and areal coverage using methods developed by the workers noted above.

APPENDIX C: DERIVATION OF ETRM INPUTS

C.1 Choice of GIS

While a plethora of open-source geographic information systems exist, the utility of ESRI© ArcMap™ cannot be overstated. The graphical user interface (GUI) is intuitive, the “toolbox”, especially with a student or institutional (free) license is diverse, and online documentation of even seemingly obscure GIS methods and solved problems is abundant. Perhaps most importantly, a Python package is installed automatically with ArcMap that allows the automation of geoprocessing tasks that would otherwise need to be repeated “by hand”. In this study, GIS was an integral part of the work flow; data was inspected and simple modifications performed on a regular basis using the ArcMap GUI. Data with incorrect projection, transformation, or extent could easily go unnoticed without this useful tool for visual inspection. The ease of cartography using Arc GIS products is also difficult to overstate. Maps displaying important project-related data are easily composed over a base-map one can make with free GIS products (e.g., digital elevation models (DEM), feature labels, political boundaries) available online.

ESRI© product licenses for private use may be prohibitively expensive. Additionally, while the ETRM code is heavily dependent on functions provided in the ArcPy Python package, many of the simple raster processing tools are available from other, free python packages, as well as in other programming languages such as R. This project could be duplicated using only open-source software; one would be advised to investigate the feasibility of using python packages such as GDAL, OSGR, PCRaster and others. Open-source GIS GUIs worth investigating include GRASS GIS, QGIS, and POSTGIS. All of these GIS tools can be found by web search.

The following explanation of methods used to derive or acquire inputs required by the current version of the ETRM assume the user has access to a licensed copy of ArcMap 10.2.2 or later.

C.2 Model Geographic Extent, Coordinate System, and Projection

The model geographic extent is simply the boundary of the State of New Mexico. This, and many other useful GIS products can be found as the United States Department of Agriculture National Resources Conservation Service (USDA NRCS) “Geospatial Data Gateway” website (<https://gdg.sc.egov.usda.gov/>; Order by State > Select State > New Mexico > Government Units). Under the NM WRI SWA, a project-specific polygon was created that includes all state territory as well as the headwaters of any stream flowing into the state. Contact NM WRI to obtain this product.

All map spatial products in this study, as in the WRI SWA overall, have been projected to the North American Datum of 1983 (NAD83), Universal Transverse Mercator Zone 13 North. NAD83 is a reference surface that approximates the imperfectly ellipsoidal surface of the earth in North America. Note that the global positioning system uses “GCS_WGS_1984”; NAD83 was

based on WGS84 at the time of definition (1986) and in 2016 differences in point locations of the same coordinate should be less than 1 m. As the WGS84 is based on a world system of continuously operating reference stations while NAD83 uses reference stations on the North American plate, the two datums will continue to diverge by 1-2 cm per year as the surface shifts relative to the rest of the globe. Use of any of the products associated with these efforts will be spatially inaccurate unless the proper projection is ensured before analysis.

C.3 Reference ET

This study used two types of input data that drove the energy balance, first a reference ET product derived from the National Land Data Assimilation System (NLDAS; Cosgrove et al., 2003; Abatzoglou, 2011), and later a custom Penman-Monteith (PM) product produced in 2016 at New Mexico Tech under the NM WRRRI Statewide Water Assessment (ReVelle et al., in press). The NLDAS, available free online, has high temporal resolution of daily and even hourly raster images, but low spatial resolution of $1/8^\circ$ (approximately 12 km). The PM reference ET product was derived specifically for this and related studies and has up to an hourly temporal, and 250 m spatial resolution.

NLDAS-Based Reference ET

During the development of the ETRM to identify potential recharge areas in New Mexico, NLDAS was used to drive energy in the ETRM. The NLDAS project was created to produce forcing parameters to improve land surface modeling results in the conterminous U.S. in real time and retrospectively. The NLDAS provides nine primary and six secondary (used for validation) forcing parameters. Climate forcings include precipitation, temperature, various radiation measures, directional wind parameters, derived from both model-based or observation-based estimates. In the case of precipitation, daily observed values are disaggregated using precipitation intensity data derived from radar observations.

To find reference ET, Abatzoglou (2013) used a combination of NLDAS and PRISM data to solve the simplified Penman-Monteith equation from Allen (1998) by scaling bias-adjusted parameters from the high-frequency NLDAS to lower-frequency (monthly) 800 m PRISM data. Assuming fixed wind resistance and albedo, ET_0 can be calculated. This method was repeated over the state of New Mexico to drive the energy component of the ETRM during initial model development.

High-Resolution Penman-Monteith Reference ET

In mountainous topography, large variations in slope, aspect, and topographic shading over short distances cause corresponding variations in net solar radiation (Aguilar, 2010). Thus, it is critical that the energy component of the ETRM reflects this spatial variability by taking topography into account in the calculation of reference ET. This was achieved by a partner study under the WRRRI SWA, which developed the Gridded Atmospheric Data Downscaling Evapotranspiration Tools (GADGET) for High-Resolution Distributed Reference ET in Complex

Terrain using three operational gridded products: NLDAS, METDATA (see below), and a 30 m resolution DEM resampled to 250 m.

To find reference ET, first NLDAS data providing 1/8° resolution incoming solar radiation is resampled to the DEM resolution. The radiation flux is then corrected for elevation adjusting for the optical path length (after Krieder & Kreith, 1975) difference in elevation between each high resolution 250 m pixel contained within each 1/8° NLDAS DEM grid cell. This intermediate product is then portioned into diffuse and beam radiation components using a clearness index (after Ruiz-Arias, 2010). The QGIS-SAGA and GRASS r.sun GIS tools are then used to adjust horizontal diffuse and direct beam components using pre-calculated raster maps of hourly solar incidence angles to account for the slope, azimuth, and terrain shadowing to produce an hourly topography-adjusted global solar radiation map in raster format. These hourly global solar radiation maps are then summed to produce daily global solar radiation that is used to determine net radiation (R_n) in the PM reference ET calculation. GADGET then corrects METDATA, 1/24° resolution meteorological data, downscaled to 250 m. Corrections (after ASCE, 2005) include adjusting 10 m wind speeds to 2 m height, the air pressure and temperature to the DEM elevation, having a constant relative humidity with elevation, and checking daily dew point and minimum temperature differences and applying an aridity correction if necessary. These data are then applied to the following daily Penman-Monteith reference ET equation:

$$ET_{r,PM24} = \left(\frac{0.408\Delta(R_n - G) + K_{time}\rho_a c_p \left(\frac{e_s - e_a}{r_a} \right)}{\Delta + \gamma \left(1 + \frac{r_s}{r_a} \right)} \right) / \lambda \quad (46)$$

where $ET_{r,24PM}$ is the daily tall crop reference ET, Δ is the slope of the saturation vapor pressure curve, γ is the psychrometric constant, R_n is corrected incoming solar radiation, G is ground heat flux (assumed to be zero at the daily time step, as in the ETRM), r_a and r_s are aerodynamic and surface resistance of the tall reference crop, $e_s - e_a$ is the difference between saturated and actual vapor pressure (or the vapor pressure deficient), and ρ_a and c_p are the mean density of air and the specific heat of water at constant pressure, respectively.

The results from the ETRs calculations are calculated at a daily time step, and resampled from a 250 m equivalent WGS 1984 grid and reprojected to the 250 m standard grid used in ETRM.

Vegetation Index

The vegetative cover on the surface of the earth provides an important pathway for the flux of water from the soil layer to the atmosphere. The energy used in this process is provided by sunlight. The leaves through which this flux occurs have evolved to absorb visible light at an energy level useful for photosynthesis, while effectively scattering near-infrared light which

could cause thermal damage to the plant’s tissue (Gates, 1980). Remote sensing techniques have been designed to take advantage of this selective absorption of light by plants. Sensors including Landsat, SPOT, MODIS, AVHRR, and IKONOS among others, have been deployed on earth-orbiting satellites to detect the intensity of spectra known to be scattered by vegetative cover (Xie et al., 2008). One measure of the relative difference between absorbed, photosynthetically active radiation and scattered, near-infrared radiation, around 0.4 to 0.7 μm and 0.7 to 1.1 μm (McCree, 1972), respectively, is the NDVI (after Rouse et al., 1974):

$$NDVI = \frac{(X_{NIR} - X_{VIS})}{(X_{NIR} + X_{VIS})} \quad (47)$$

where NIR and VIS are the proportion of light in the near-infrared and visible (red), respectively. In this study, the MOD-13 (Huete et al., 1999) NDVI product was used, where X can be computed from raw digital counts, fractional reflectance, at-instrument radiance, normalized radiances, or apparent reflectance. This data is the product of images collected by the moderate-resolution imaging spectroradiometer (MODIS), mounted on the NASA satellites *Aqua* and *Terra*. In the current algorithm, MOD-13 NDVI uses atmospherically corrected surface reflectance [-] for X. This study makes use of the highest spatial resolution MOD-13 NDVI product (250 m) at the only temporal resolution available (16-day).

The problem of long intervals between NDVI images was overcome by a linear interpolation to add data to the missing values between MODIS images. This was completed using a raster linear interpolation model in Erdas© Imagine™.

C.4 Precipitation and Temperature

Spatially distributed precipitation (mm) and temperature (minimum and maximum, °C) parameters for this study were derived from the Parameter-elevation Regressions on Independent Slopes Model (PRISM; Daly, 1997; Daly, 2008). PRISM is an 800 m gridded data set derived from interpolation of weather station data covering the conterminous United States. PRISM has been applied to precipitation, minimum and maximum temperature, dew point, and minimum and maximum vapor pressure deficit over the conterminous U.S. Mean temperature and vapor pressure have been derived to a lesser extent. The PRISM model has been applied to varying spatial and temporal resolutions ranging from 30-year means, to annual, monthly, and daily values at 4 km and 800 m spatial scale. The PRISM dataset used in this study was the gridded 800 m, daily precipitation and minimum and maximum temperature raster data sets. While 1984–2013 are available, modeling used only 2000-2013, the period for which the NDVI product was also available.

The sophisticated method of interpolation used to derive PRISM involves using topographic and geographic parameters such as the elevation, the spatial scale of orographic effects (“effective terrain height”), slope orientation/aspect (“topographic facet”), coastal

proximity, vertical atmospheric layer (accounts for inversions), and cold air drainage. Rather than creating a regression function with many independent variables, PRISM uses a local linear regression for each grid cell in the DEM in which the climate element (precipitation or temperature, in this case) depends on elevation. The local regression slope depends on elevation, resulting in high spatial variability of climatic parameters in mountainous terrain. Each of 13,000 weather stations in the U.S. is assigned a weighting factor based on the physical parameters listed above; an interpolated value is assigned to each grid cell between stations according to neighboring station weights. The station weights are designed to increase with increasing physiographic similarity to nearby target cells. This method thus avoids applying excess weight to a weather station that may be nearby, but could be at a very different elevation or physical situation (e.g., on the other side of a rain shadow).

C.5 Soil Parameters

This project has made use of two important soil databases compiled and released by the NRCS, the Digital General Soil Map of the United States (STATSGO2) and the Soil Survey Geographic Database (SSURGO; NRCS, 2016). The STATSGO2 product is an extensive and generalized soils inventory mapped at the 1:250,000 scale, with near continuous coverage over the conterminous United States. STATSGO2 was designed to be used in regional and national-scale planning, management, and geographic analysis. SSURGO is a detailed soils data product consisting of surveys by county or hydrologic unit at a scale of 1:12,000 to 1:63,000. This larger scale provides detailed information for use by landowners, towns, and counties. Many of these surveys were conducted on foot by soil scientists, and some data include data from laboratory analysis. This product is updated frequently and represents data collected over more than 100 years of soil observations. Neither of these products covers the entire state.

Both of these products can be downloaded from the Geospatial Data Gateway in a format clipped to a state, county, or a user-specified latitude and longitude-bounded rectangle. The digital download includes a Microsoft© Access™ template database, an instructional text file, and folders for spatial and tabular data. The database is designed to shield users from the complexities of the data format, and is related to the spatial data via unique map unit keys. The spatial data simply consists of a polygon map layer (in New Mexico STATSGO2 has around 2,000 polygons, SSURGO over 198,500), with each polygon represented by a unique “map unit” identifier. In order to extract useful information about the soils from the database, the user must load the spatial data onto ArcMap and open Soil Data Viewer (SDV), a free ArcMap add-on available at the NRCS website. Using the SDV allows the user to simply choose from a menu of dozens of soil-derived parameters to be mapped. This tool is sufficient to map soil parameters statewide with STATSGO or over a single county using SSURGO data; a STATSGO download for New Mexico or a SSURGO download for a single county contains only one file and necessitates the use of only one Access database. Downloading multiple SSURGO files to merge into one, SDV-compatible map layer is more complicated, see instructions below.

The map units of which the STATSGO2 and SSURGO databases consist are linked to databases that describe the area of each map unit as a combination of a set of components (e.g.,

clay). Each component represents a percentage of the total attribute class (e.g., particle size) within each soil horizon. Mapping derived soil parameters (e.g., field capacity) using the SDV necessitates quantifying these physical properties in each horizon and representing the aggregate with a single numerical value for each map unit. Many aggregation options are available; in this study the “dominant component” was chosen to represent component aggregation. A sub-process of component aggregation is aggregation of components which are properties of soil horizons themselves. In this study, the horizon thickness is used to weight each horizon property over all layers in the soil column.

Creating a Statewide SSURGO Soils Map

In order to generate a statewide soil parameter map using the more detailed SSURGO soil data, one must use the Soil Data Development Toolbox, available on the NRCS website (www.nrcs.usda.gov > Soil Survey > Soil Geography > Description of Gridded Soil Survey Geographic (gSSURGO) Database). The SSURGO data for the entire state includes small portions of surveys labeled under the state abbreviation of Colorado and Arizona, thus it is advantageous to use the “By State” option on the Geospatial Data Gateway and choosing the SSURGO download option, as the choice of New Mexico will include these extra downloads, while use of the toolbox SSURGO data download script will only select surveys with the “NM” label. The necessary template database can be found at the Web Soil Survey site (websoilsurvey.sc.egov.usda.gov > Start Web Soil Survey > Download Soils Data > Download SSURGO Template Databases > US). Once all the SSURGO files (.zip) have downloaded, select “Process WSS Downloads” in the Soil Data Development Toolbox. This will unzip and rename the files. Use the “Merge Template Databases” tool to create a database containing all SSURGO data from the unzipped files, then the “Merge Soil Shapefiles by DB” tool to create a single polygon for the entire state. Open SDV while this merged shapefile is in the Table of Contents on a blank ArcMap document. If the “Synchronization” indicator on the lower right of the SDV window is red, click the database folder icon and browse to the merged template database. This will allow maps of any of the desired soil parameters to be mapped.

The SSURGO dataset does not provide soils data for the entire state; it is necessary to perform a union operation in GIS to unite the STATSGO data with the SSURGO data. This will create a multilayer feature class for each soil property being processed. Selecting the empty SSURGO polygons and using a field calculator to replace “no data” and “0” values with values from STATSGO will result in greater data coverage.

Total Available Water, Field Capacity, Wilting Point, Rooting Depth

In the Dual Crop Coefficient Method, the parameter TAW (total available water, [mm]) is defined as the total water available to plant roots for transpiration (eqn. 82, Allen, 1998):

$$TAW = 1000(FC - 0.5 WP) * z_r \quad (48)$$

where FC is the soil field capacity, the volumetric water content above which the soil will drain [-], WP is wilting point, the volumetric water content below which most plants are unable to extract water for transpiration [-], and z_r is plant rooting depth [m]. Field capacity is defined within the SDV as the saturation of a soil experiencing a matric potential (negative water pressure) of 1/3 bar (33.3 kPa), wilting point is defined as 15 bar (1500 kPa). Soil data viewer offers this property in Advanced > Soil Physical Properties section, under the name Available Water Storage (AWS). It was found in this study that the AWS of SSURGO data was unrealistically low in places. Areas with these issues are described in the discussion of Chapter 4. These low SSURGO AWS areas can be replaced with STATSGO AWS data using the field calculator.

The rooting depth parameter, z_r , was generated using the National Landcover Dataset (NLCD; Homer et al., 2011). General land cover types in the data set were reclassified according to estimated rooting depth estimates given in Zhou et al (2006).

Total Evaporable Water, Readily Evaporable Water

In the dual-crop coefficient method, the parameter total evaporable water (TEW) is the water near the surface that is subject to vaporization via diffusion through the soil surface layer. Allen (2011) suggested that this distance from the surface (evaporation depth, z_e) is typically about 100 mm. The TEW, like TAW, uses the field capacity and wilting point to then compute the water [mm] available to evaporation via diffusion through the soil, also known as stage-two evaporation. Allen (2011) further suggested adding an additional soil layer subject to the maximum rate of evaporation, limited only by water and energy availability, called ‘readily available water’ (REW). This soil layer may range to as much as 12 mm in depth, and is user defined.

C.6 Plant Height and Rooting Depth

The Multi-Resolution Characteristics Consortium (MRLC) periodically releases the National Land Cover Database (NLCD; Homer et al., 2011). This 30 m gridded product classifies the United States in 16 land cover data types, including various human-impacted and natural vegetation type land cover types. For use in the ETRM each land cover type was classified with a rooting depth and a plant height after Zhou and others (2006).

APPENDIX D: References Cited

- Abatzoglou, J.T. 2013. Development of gridded surface meteorological data for ecological applications and modelling. *International Journal of Climatology*, 33(1), pp.121-131.
- Aguilar, C., J. Herrero and M.J. Polo. 2010. Topographic effects on solar radiation distribution in mountainous watersheds and their influence on reference evapotranspiration estimates at watershed scale. *Hydrology and Earth System Sciences*, 14(12), pp.2479-2494.
- Aishlin, P. and J.P. McNamera. 2011. Bedrock infiltration and mountain block recharge accounting using chloride mass balance. *Hydrological Processes* 25: 1934-1948.
- Albuquerque Journal. When the well runs dry... <http://www.abqjournal.com/216274/news/when-the-well-runs-dry.html> (accessed January 7, 2016)
- Allison, G.B., G.W. Gee, and S.W. Taylor. 1994. Vadose-zone techniques for estimating groundwater recharge in arid and semiarid regions. *Soil Science Society of America Journal*, 58(1): 6-14.
- Allen, R.G., 1996. Assessing integrity of weather data for reference evapotranspiration estimation. *Journal of Irrigation and Drainage Engineering*, 122(2), pp.97-106.
- Allen, R. G., L. S. Pereira, D. Raes and M. Smith. 1998. FAO Irrigation and drainage paper No. 56. Rome: Food and Agriculture Organization of the United Nations, 26-40.
- Allen, R.G., L.S. Pereira, M. Smith, D. Raes and J.L. Wright. 2005. FAO-56 dual crop coefficient method for estimating evaporation from soil and application extensions. *Journal of Irrigation and Drainage Engineering*, 131(1), pp.2-13.
- Allen, R.G. 2011. Skin layer evaporation to account for small precipitation events—An enhancement to the FAO-56 evaporation model. *Agricultural Water Management*, 99(1), pp.8-18.
- American Society of Civil Engineers. 2005. The ASCE standardized reference evapotranspiration equation. In *Proceedings of the National Irrigation Symposium, 2000*. Ed., R.G. Allen, I.A. Walter, R. Elliott, T. Howell, D. Itenfisu, and M. Jensen. Environment and water resources institute of the ASCE.
- Anderson, E.A. 1976. A point energy and mass balance model of a snow cover: Silver Spring, Maryland: National Oceanographic and Atmospheric Administration Technical Report NWS 19, 150 p.
- Anderholm, S.K. 1994. Mountain-front recharge along the eastern side of the Middle Rio Grande Basin, Central New Mexico. Middle Rio Grande Basin Study: U.S. Geological Survey Water-Resources Investigations Report no. 94-4078. p. 46.
- Anderholm, SK. 2001. Mountain-front recharge along the eastern side of the Middle Rio Grande Basin, Central New Mexico (Revised 2001). U.S. Geological Survey Water Resources Investigations Report, no. 00-4010. p. 34.
- Avon, L. and T. J. Durbin. 1994. Evaluation of the Maxey-Eakin method for estimating groundwater recharge in Nevada. *Journal of the American Water Resources Association*. 30: 99-111.
- Bartolino, J.R. and W.L. Cunningham. 2003. Ground-water depletion across the nation. U.S. Geological Survey Fact Sheet (No. 103-03). 4 p.
- Bartos, T.T. and K.M. Ogle. 2002. Water quality and environmental isotopic analyses of ground-

water samples collected from the Wasatch and Fort Union formations in areas of coalbed methane development: implications to recharge and ground-water flow, eastern Powder River Basin, Wyoming. U.S. Geological Survey Water-Resources Investigation Report No. 2002-4045.

- Basu, N.B., P.S.C. Rao, H.E. Winzeler, S. Kumar, P. Owens and V. Merwade. 2010. Parsimonious modeling of hydrologic responses in engineered watersheds: Structural heterogeneity versus functional homogeneity. *Water Resources Research*, 46(4). DOI: 10.1029/2009WR007803.
- Bedinger, M.S., W.H. Langer and J.E. Reed 1989. Ground-water hydrology. in Bedinger, M.S., K.A. Sargent and W.H. Langer, eds., *Studies of geology and hydrology in the Basin and Range Province, South-western United States, for isolations of high-level radioactive waste—Characterization of the Death Valley region, Nevada and California*. U.S. Geological Survey Professional Paper 1370-F, p. 28-35.
- Bentley, H.W., F.M. Phillips, and S.N. Davis. 1986. Chlorine-36 in the terrestrial environment. In *Handbook of Environmental Isotope Geochemistry*, Vol. 2, Eds. P. Fritz and J.C. Fontes, pp. 427-480. Elsevier.
- Bexfield, L.M. and S.K. Anderholm. 2002. Estimated water-level declines in the Santa Fe Group aquifer system in the Albuquerque area, central New Mexico, predevelopment to 2002. U.S Department of the Interior, US Geological Survey. 1 p.
- Burman, R. D., J. L. Wright, and M. E. Jensen. 1975. Changes in Climate and Potential Evapotranspiration Across a Large Irrigated Area in Idaho. *Transaction of the ASAE*, 18(6), 1089-1093.
- Campbell, G.S. 1985. Soil physics with BASIC: Transport models for soil plant systems: Amsterdam, Elsevier, *Developments in Soil Science*, no. 14, 150 p.
- Carpenter, J.H. and Rimmer, D.F., 1978. Microwave spectrum of three isotopic species of carbonyl chloride. *Journal of the Chemical Society, Faraday Transactions 2: Molecular and Chemical Physics*, 74, pp.466-479.
- Cazorzi, F. and G. Dalla Fontana. 1996. Snowmelt modelling by combining air temperature and a distributed radiation index. *Journal of Hydrology*, 181(1), pp.169-187.
- Cosgrove, B.A., D. Lohmann, K.E. Mitchell, P.R. Houser, E.F. Wood, J.C. Schaake, A. Robock, C. Marshall, J. Sheffield, Q. Duan and L. Luo. 2003. Real-time and retrospective forcing in the North American Land Data Assimilation System (NLDAS) project. *Journal of Geophysical Research: Atmospheres*, 108(D22). DOI: 10.1029/2002JD003118.
- Daly, C., G.H. Taylor, and W.P. Gibson, 1997. The PRISM approach to mapping precipitation and temperature. In *Proc., 10th AMS Conf. on Applied Climatology*. pp. 20-23.
- Daly, C., M. Halbleib, J. I. Smith, W. P. Gibson, M. K. Doggett, G. H. Taylor and P. P. Pasteris. 2008. Physiographically sensitive mapping of climatological temperature and precipitation across the conterminous United States. *International Journal of Climatology*, 28(15), 2031-2064.
- Daniel B. Stephens & Associates, Inc. 2010. Draft - Manual for the Distributed Parameter Watershed Model (DPWM). Report, Daniel B. Stephens & Associates, Inc., Albuquerque, New Mexico. 83 pp.
- Davis, S.N. and R.J.M. DeWiest. 1966. Hydrogeology: New York, John Wiley, 463 p.

- Davis, S. N., D.O. Whittemore, and J. Fabryka-Martin. 1998. Uses of chloride/bromide ratios in studies of potable water. *Groundwater* 36(2): 338-350.
- Dettinger, M.D., D.R. Cayan, G.J. McCabe, and J.A. Marengo. 2000, Multiscale streamflow variability associated with El Niño/Southern Oscillation, in Diaz, H.F. and Markgraf, V., eds., *El Niño and the Southern Oscillation, multiscale variability and global and regional impacts*: Cambridge, Cambridge University Press, p. 113–147.
- Eriksson, E., 1960. The Yearly Circulation of Chloride and Sulfur in Nature; Meteorological, Geochemical and Pedological Implications. Part III. *Tellus*, 12(1), pp.63-109.
- Essery, R., S. Morin, Y. Lejeune and C.B. Ménard. 2013. A comparison of 1701 snow models using observations from an alpine site. *Advances in Water Resources*, 55, pp.131-148.
- Fabryka-Martin, J. T., A.V. Wolfsberg, P.R. Dixon, S. Levy, J. Musgrave and H.J. Turin. 1996. Summary report of chlorine-36 studies: sampling, analysis and simulation of chlorine-36 in the Exploratory Studies Facility. *Los Alamos National Laboratory Milestone Report M*, 3783.
- Feth, J.H. 1981. Chloride in natural continental water – a review. U.S. Geological Survey Water-supply Paper no. 2176. 36 p.
- Flint, A.L., S.W. and Childs. 1987, Calculation of solar radiation in mountainous terrain. *Journal of Agricultural and Forest Meteorology*, v. 40, p. 233–249
- Flint, A.L., L.E. Flint, E.M. Kwicklis, J.T. Fabryka-Martin and G.S. Bodvarsson. 2002. Estimating recharge at Yucca Mountain, Nevada, USA: comparison of methods. *Hydrogeology Journal*, 10(1), pp.180-204.
- Flint, A.L., L.E. Flint, J.A. Hevesi and J.B Blainey. 2004. Fundamental concepts of recharge in the Desert Southwest: a regional modeling perspective. In *Groundwater Recharge in a Desert Environment: The Southwestern United States*, pp.159-184. American Geophysical Union.
- Flint, A. L., and L.E. Flint. 2007a. Application of the basin characterization model to estimate in-place recharge and runoff potential in the Basin and Range carbonate-rock aquifer system, White Pine County, Nevada, and adjacent areas in Nevada and Utah. U.S. Geological Survey Scientific Investigations Report, no. 2007-5099. 30 p.
- Flint, L. E. and A.L. Flint. 2007b. Regional analysis of ground-water recharge. In *Ground-water recharge in the arid and semiarid southwestern United States*. pp. 29-59. U.S. Geological Survey Professional Paper no. 1703.
- Flint, A. L., L. E. Flint and M.D. Masbruch. 2011. Appendix 3: Input, calibration, uncertainty, and limitations of the basin characterization model. Conceptual Model of the Great Basin Carbonate and Alluvial Aquifer System, U.S. Geological Survey Scientific Investigations Report no 2010-5193. 149-163.
- Freeze, R.A., and J.A. Cherry. 1979. *Groundwater*: Englewood Cliffs, New Jersey, Prentice-Hall, 604 p.
- Gates, D. M. 1980. *Biophysical Ecology*, Springer-Verlag, New York, 611 p.
- Glancy, P.A. 1986. Geohydrology of the basalt and unconsolidated sedimentary aquifers in the Fallon area, Churchill County, Nevada: U.S. Geological Survey Water Supply Paper 2263, 62 p.
- Gonzalez-Dugo, M.P., C.M.U Neale, L. Mateos, W.P. Kustas, J.H. Prueger, M.C. Anderson and F. Li. 2009. A comparison of operational remote sensing-based models for estimating

- crop evapotranspiration. *Agricultural and Forest Meteorology*, 149(11), pp.1843-1853.
- González-Dugo, M.P., S. Escuin, F. Cano, V. Cifuentes, F.L.M. Padilla, J.L. Tirado, N. Oyonarte, P. Fernández and L. Mateos. 2013. Monitoring evapotranspiration of irrigated crops using crop coefficients derived from time series of satellite images. II. Application on basin scale. *Agricultural Water Management*, 125, pp. 92-104.
- Guentner, A., S. Uhlenbrook, C. Leibundgut and J. Sieber. 1999. Estimation of saturation excess overland flow areas: comparison of topographic index calculations with field mapping. *International Association of Hydrological Sciences*. 254: 203-210.
- Hainsworth, L.J., 1994. Spatial and temporal variations in chlorine-36 deposition in the northern United States. PhD Dissertation. Univ. of Maryland College Park.
- Hassan-Esfahani, L., A. Torres-Rua and M. McKee. 2015. Assessment of optimal irrigation water allocation for pressurized irrigation system using water balance approach, learning machines, and remotely sensed data. *Agricultural Water Management*, 153, pp.42-50.
- Havens, J.S., 1966. Recharge studies on the High Plains in northern Lea County, New Mexico. U.S. Geological Survey Water-Supply Paper no. 1819-F. 64 p.
- Healy, R.W. 2006. Estimating rates of water drainage through the unsaturated zone at the East Poplar oil field on the basis of concentration profiles of chloride and nitrate, 2006. In Thamke, J. N., & B.D. Smith. 2014. *Delineation of brine contamination in and near the East Poplar oil field, Fort Peck Indian Reservation, northeastern Montana*, 2004–09. U.S. Geological Survey Scientific Investigations Report, 5024(40), 21 p.
- Hemakumara, H.M., L. Chandrapala and A.F. Moene. 2003. Evapotranspiration fluxes over mixed vegetation areas measured from large aperture scintillometer. *Agricultural Water Management*, 58(2), pp.109-122.
- Hendrickx, J.M., R.G. Allen, A. Brower, A.R. Byrd, S.H. Hong, F.L. Ogden, N.R. Pradhan, C.W. Robison, D. Toll, R. Trezza, and T.G. Umstot. 2016. Benchmarking Optical/Thermal Satellite Imagery for Estimating Evapotranspiration and Soil Moisture in Decision Support Tools. *JAWRA Journal of the American Water Resources Association*, 52(1), pp.89-119.
- Hevesi, J. A., A. L. Flint and L.E. Flint. 2003. Simulation of net infiltration and potential recharge using a distributed-parameter watershed model of the Death Valley region, Nevada and California. U.S. Geological Survey Water-Resources Investigations Report 03-4090. 171 p.
- Hintze, L.F., G.C. Willis, D. Laes, D.A. Sprinkel and K.D. Brown, 2000. Digital geologic map of Utah: Utah Geological Survey Map 179DM, scale 1: 500,000.
- Hock, R. 2003. Temperature index melt modelling in mountain areas. *Journal of Hydrology*, 282(1), pp.104-115
- Homer, C.G., J.A. Dewitz, L. Yang, S. Jin, P. Danielson, G. Xian, J. Coulston, N.D. Herold, J.D. Wickham, and K. Megown. 2015, Completion of the 2011 National Land Cover Database for the conterminous United States-Representing a decade of land cover change information. *Photogrammetric Engineering and Remote Sensing*, v. 81, no. 5, p. 345-354.
- Hoogendoorn, C.J., 1977. Solar heating and cooling: Jan F. Kreider and Frank Kreith, *Scripta*, Washington DC (1975) 342 pp.
- Iqbal, M., 1983. An introduction to solar radiation: Academic Press, 309 p.
- Jennings, C.W. 1977. Geologic map of California: California Division of Mines and Geology

- Geologic Data Map no. 2, 1 sheet, scale 1: 750,000.
- Jennings, M. D. 2000. Gap analysis: concepts, methods, and recent results. *Landscape Ecology*, 15(1), 5-20.
- Jensen, M. E., R. D. Burman and R.G. Allen. 1990. Evapotranspiration and irrigation water requirements. ASCE Manual of Practice No. 70. American Society of Civil Engineers, New York, NY.
- Jabloun, M. D. and A. Sahli. 2008. Evaluation of FAO-56 methodology for estimating reference evapotranspiration using limited climatic data: Application to Tunisia. *Agricultural Water Management*, 95(6), 707-715.
- Johnson, B.R. and G.L. Raines. 1996. Digital representation of the Idaho state geologic map, a contribution to the Interior Columbia Basin Ecosystem Management Project: U.S. Geological Survey Open-File Report 95-690, 24 p.
- Johnson, G.L., C. Daly, G.H. Taylor and C.L. Hanson. 2000. Spatial variability and interpolation of stochastic weather simulation model parameters. *Journal of Applied Meteorology*, 39(6), pp.778-796.
- Koivusalo, H. and T. Kokkonen. 2002. Snow processes in a forest clearing and in a coniferous forest. *Journal of Hydrology*, 262(1), pp.145-164.
- Körner, C. 1995. Leaf diffusive conductances in the major vegetation types of the globe. In *Ecophysiology of Photosynthesis*. pp. 463-490.
- Lundquist, J.D. and A.L. Flint. 2006. 2004 onset of snowmelt and streamflow: How shading and the solar equinox may affect spring runoff timing in a warmer world: *Journal of Hydrometeorology*, v. 7, p. 1,199-1,217.
- Leake, S.A., A.D. Konieczki and J.A. Rees. 2000. Desert basins of the Southwest. US Geological Survey Fact Sheet No. 086-00. 4 p.
- Lewis, W.M. Jr., M.C. Grant and J.F. Saunders, III. 1984. Chemical patterns of bulk atmospheric deposition in the state of Colorado. *Water Resources Research*. 20(11), pp. 1691-1704.
- Li, Y. 1992. Seasalt and pollution inputs over the continental United States. *Water, Air, and Soil Pollution* 64, pp. 561-573.
- Lyapustin, A.I., Y. Wang, I. Laszlo, T. Hilker, F.G. Hall, P.J. Sellers, C.J. Tucker and S.V. Korkin. 2012. Multi-angle implementation of atmospheric correction for MODIS (MAIAC): 3. Atmospheric correction. *Remote Sensing of Environment*, 127, pp.385-393.
- Mateos, L., M.P. González-Dugo, L. Testi and F.J. Villalobos. 2013. Monitoring evapotranspiration of irrigated crops using crop coefficients derived from time series of satellite images. I. Method validation. *Agricultural Water Management*, 125, pp.81-91.
- Martinez, J. 1975. Snowmelt-runoff model for stream flow forecasts. *Hydrology Research*, 6(3), pp.145-154.
- Mattick, J.L. 1986. *Quantification of Ground-Water Recharge Rates in New Mexico Using Bomb-36Cl and Bomb-3H as Soil-Water Tracers*. New Mexico Water Resources Research Institute, Technical Completion Report Nos. 1423638 and 1423654. 193 p.
- Maxey, G.B. and T. E. Eakin. 1949. Ground water in White River Valley, White Pine, Nye, and Lincoln Counties, Nevada. Nevada State Engineer.
- Mazor, E. and Mero, F., 1969. The origin of the Tiberias-Noit mineral water association in the Tiberias-Dead Sea rift valley, Israel. *Journal of Hydrology*, 7(3), pp.318-333.

- McAda, D.P., and M. Wasiolek. 1988. Simulation of the Regional Geohydrology of the Tesuque Aquifer System near Santa Fe, New Mexico. U.S. Geological Survey Water-Resources Investigations Report 87-4056. 87 p.
- McCoy, K.J. and P.J. Blanchard. 2008. Precipitation, Ground-water Hydrology, and Recharge Along the Eastern Slopes of the Sandia Mountains, Bernalillo County, New Mexico. U.S. Geological Survey Scientific Investigations Report 2008-5179. 33p.
- McCree, K.J. 1972. Test of current definitions of photosynthetically active radiation against leaf photosynthesis data. *Agricultural Meteorology*, 10, pp.443-453.
- Mednick, A.C., 2008. Comparing the use of STATSGO and SSURGO soils data in water quality modeling: A literature review. Bureau of Science Services, Wisconsin Department of Natural Resources.
- Mitchell, T.D., T.R. Carter, P.D. Jones, M. Hulme and M. New. 2004. A comprehensive set of high-resolution grids of monthly climate for Europe and the globe: the observed record (1901–2000) and 16 scenarios (2001–2100). Tyndall Centre for Climate Change Research. Working Paper no. 55(0), p.25.
- Miura, T., H. Yoshioka, K. Fujiwara and H. Yamamoto. 2008. Inter-comparison of ASTER and MODIS surface reflectance and vegetation index products for synergistic applications to natural resource monitoring. *Sensors*, 8(4), pp.2480-2499.
- Moriassi, D.N. and P.J. Starks. 2010. Effects of the resolution of soil dataset and precipitation dataset on SWAT2005 streamflow calibration parameters and simulation accuracy. *Journal of Soil and Water Conservation*, 65(2), pp.63-78.
- Moysey, S., S.N. Davis, M. Zreda and L.D. Cecil. 2003. The distribution of meteoric $^{36}\text{Cl}/\text{Cl}$ in the United States: a comparison of models. *Hydrogeology Journal*, 11(6), pp.615-627.
- National Atmospheric Deposition Program (NRSP-3). 2007. NADP Program Office, Illinois State Water Survey, 2204 Griffith Dr., Champaign, IL 61820.
- National Oceanic and Atmospheric Administration, National Weather Service, Albuquerque, NM Office. NWS Albuquerque Climate Feature. http://www.srh.noaa.gov/abq/?n=clifeature_1941precip (accessed July 10, 2016).
- Naus, C.A., D.P. McAda, and N.C. Meyers. 2006. Questa baseline and pre-mining ground-water quality investigation. 21. Hydrology and water balance of the Red River Basin, New Mexico 1930-2004. U.S. Geological Survey Scientific Investigations Report 2006-5040. 43p.
- New Mexico Bureau of Geology and Mineral Resources. 2003. Geologic Map of New Mexico, scale 1: 500,000:
- Newton, B.T., G.C. Rawling, S.S. Timmons, L. Land, P.S. Johnson, T.J. Kludt, and J.M. Timmons. 2012. Sacramento Mountains Hydrogeology Study. Prepared for Otero Soil and Water Conservation District. New Mexico Bureau of Geology and Mineral Resources, Open-file Report no. 543. 84 p.
- Nuclear Waste Technical Review Board. 2007. Technical Evaluation of US Department of Energy Yucca Mountain Infiltration Estimates. Report to US Congress and the Secretary

of Energy. 92 p.

- Ohmura, A. 2001. Physical basis for the temperature-based melt-index method. *Journal of Applied Meteorology*, 40(4), pp.753-761.
- Pan, T., S. Wu, E. Dai and Y. Liu. 2013. Estimating the daily global solar radiation spatial distribution from diurnal temperature ranges over the Tibetan Plateau in China. *Applied Energy*, 107, pp.384-393.
- Peck, A.J., C.D. Johnston, and D.R. Williamson. 1981. Analyses of solute distributions in deeply weathered soils. *Agricultural Water Management* 4, no. 1-3: 83-102.
- Penman, H. L. 1948. Natural evaporation from open water, bare soil and grass. In *Proceedings of the Royal Society of London A: Mathematical, Physical and Engineering Sciences* (Vol. 193, No. 1032, pp. 120-145). The Royal Society.
- Phillips, F.M. 1994. Environmental tracers for water movement in desert soils of the American Midwest. *Soil Science Society of America Journal* 58, no.1: 15-24.
- Plummer, L.N., W.E. Sanford, L.M. Bexfield, S.K. Anderholm, and E. Busenberg. 2004. Using geochemical data and aquifer simulation to characterize recharge and groundwater flow in the Middle Rio Grande Basin, New Mexico. In *Groundwater Recharge in a Desert Environment: The Southwestern United States, Water Science and Application* 9: 185-216.
- Ponce-Campos, G.E., M.S. Moran, A. Huete, Y. Zhang, C. Bresloff, T.E. Huxman, D. Eamus, D.D. Bosch, A.R. Buda, S.A. Gunter and T.H. Scalley. 2013. Ecosystem resilience despite large-scale altered hydroclimatic conditions. *Nature*, 494(7437), pp.349-352.
- Priestley, C.H.B., and R.J. Taylor. 1972. On the assessment of surface heat flux and evaporation using large-scale parameters: *Monthly Weather Review*, v. 100, p. 81–92. Priestley, C.H.B., and Taylor, R.J., 1972, On the assessment of surface heat flux and evaporation using large-scale parameters: *Monthly Weather Review*, v. 100, p. 81–92.
- Rango, A. and Martinec, J., 1994. Areal extent of seasonal snow cover in a changed climate. *Hydrology Research*, 25(4), pp.233-246.
- Rawling, G.C. and B.T. Newton. 2016. Quantity and location of groundwater recharge in the Sacramento Mountains, south-central New Mexico (USA), and their relation to the adjacent Roswell Artesian Basin. *Hydrogeology Journal*, pp.1-30.
- Rice, S.E. and D.M. Crilley. 2014. Estimates of Groundwater Recharge Rates and Sources in the East Mountain Area, Eastern Bernalillo County, New Mexico, 2005-12. U.S. Geological Survey Scientific Investigations Report 2014-5181. 24 p.
- Ritchie, J. T. 1983. Efficient water use in crop production: discussion on the generality of relations between biomass production and evapotranspiration. In *Limitations to efficient water use in crop production*, pp. 29-44. American Society of Agronomy.
- Rittenhouse, G. 1967. Bromine in oil-field waters and its use in determining possibilities of origin of these waters. *AAPG Bulletin*, 51(12), 2430-2440.

- Rohrer, M.B. 1991. *Die Schneedecke im schweizerischen Alpenraum und ihre Modellierung*. Doctoral dissertation, ETH Zurich.
- Ruiz-Arias, J.A., H. Alsamamra, J. Tovar-Pescador and D. Pozo-Vázquez. 2010. Proposal of a regressive model for the hourly diffuse solar radiation under all sky conditions. *Energy Conversion and Management*, 51(5), pp.881-893.
- Sandia National Laboratories. 2007. Simulation of net infiltration for present-day and potential future climates. Technical Report MDL-NBS-HS-000023 REV 01, Dep. of Energy, Las Vegas, Nev. 456 p.
- Sandvig, R. M. and F. M. Phillips. 2006. Ecohydrological controls on soil moisture fluxes in arid to semiarid vadose zones. *Water Resources Research*, 42(8).
- Schwarz, G. E., and R. B. Alexander. 1995. State Soil Geographic (STATSGO) data base for the conterminous United States. National Resources Conservation Service. No. 95, 449 p.
- Scanlon, B.R. 1991. Evaluation of moisture flux from chloride data in desert soils. *Journal of Hydrology* 128: 137-156.
- Scanlon, B.R. and R.S. Goldsmith. 1997. Field study of spatial variability in unsaturated flow beneath and adjacent to playas. *Water Resources Research*, 33-10. pp 2239-2252.
- Scanlon, B.R., Reedy, R.C., and J.A. Tachovsky. 2007. Semiarid unsaturated zone chloride profiles: Archives of past land use change impacts on water resources in the southern High Plains, United States. *Water Resources Research*, 43, pp. 1-13.
- Sesnie, S.E., B.G. Dickson, S.S. Rosenstock and J.M. Rundall. 2012. A comparison of Landsat TM and MODIS vegetation indices for estimating forage phenology in desert bighorn sheep (*Ovis canadensis nelsoni*) habitat in the Sonoran Desert, USA. *International Journal of Remote Sensing*, 33(1), pp. 276-286.
- Sharma, M.L. and M.W. Hughes. 1985. Groundwater recharge estimation using chloride, deuterium and oxygen-18 profile in the deep coastal sands of Western Australia. *Journal of Hydrology* 81(1), 93-109.
- Shuttleworth, W.J. 1993, Evaporation, chap. 4 of Maidment, D.R. ed., *Handbook of hydrology*: New York, McGraw-Hill, p. 4.1–4.53.
- Soil Conservation Service. 1991. State soil geographic data base (STATSGO), data users guide: Washington, D.C., Soil Conservation Service, Miscellaneous Publication 1492, 88 p.
- Spiegel, Z., and B. Baldwin. 1963. Geology and water resources of the Santa Fe area, New Mexico. U.S. Geological Survey Water-Supply Paper no. 1525. 274 p.
- Sterling, J.M. 2000. Spatial distribution of chloride and chloride-36 deposition in the conterminous United States. Unpublished independent study. New Mexico Institute of Mining and Technology.
- Stewart, J.H., J.E. Carlson, G.L. Raines, K.A. Connors, L.A. Moyer, and R.J., Miller. 2003. Spatial digital database for the geologic map of Nevada: U.S. Geological Survey Open-File Report 03–66, version 3.0, 32 p.

- Stone, W.J., and B.E. McGurk. 1985. Ground-water recharge on the Southern High Plains, East-Central New Mexico. *New Mexico Geological Society Guidebook, 36th Field Conference, Santa Rosa NM*: pp. 331-35.
- Stone, W.J. 1984. Recharge in the Salt Lake Coal Field based on chloride in the unsaturated zone. New Mexico Bureau of Mines & Mineral Resources Open-File Report no. 214. 67 p.
- Swinbank, W. C. 1963. Long-wave radiation from clear skies. *Quarterly Journal of the Royal Meteorological Society*, 89(381), 339-348.
- Topp, G. C., and P.A. Ferre. 2002. *Methods of Soil Analysis*, Part 4: Physical Methods. Methods for measurement of soil water content: Thermogravimetric using convective oven drying, pp. 422-424.
- US Army Corps of Engineers. 1998. Runoff from snowmelt. Manuals, U.S. Army Corps of Engineers, Engineering Manual 1110-2-1406. 142 p.
- USDA. 1994. Natural Resources Conservation Services (NRCS). State Soil Geographic (STATSGO) Data Base: Data Use Information Lincoln, NE: National Soil Survey Center.
- USDA. 1995. Natural Resources Conservation Services (NRCS). Soil Survey Geographic (SSURGO) Data Base: Data Use information. Lincoln, NE: National Soil Survey Center.
- US Nuclear Waste Technical Review Board. 2007. Technical Evaluation of US Department of Energy Yucca Mountain Infiltration Estimates. Report to the US Congress and the Secretary of Energy. 32 pp.
- Waltemeyer, S.D., 1994. Methods for estimating streamflow at mountain fronts in southern New Mexico. US Department of the Interior, US Geological Survey Water-Resources Investigation Report no. 93-4213. 21 p.
- Waltemeyer, S.D. 2001. Estimates of mountain-front streamflow available for potential recharge to the Tularosa Basin, New Mexico. U.S. Geological Survey Water-Resources Investigations Report no. 2001-4013.
- Walvoord, M.A. and F.M. Phillips. 2004. Identifying areas of basin-floor recharge in the Trans-Pecos region and the link to vegetation. *Journal of Hydrology* 292: 59-74.
- Whitehead, H.C. and J.H. Feth. 1964. Chemical composition of rain, dry fallout, and bulk precipitation at Menlo Park, California, 1957–1959. *Journal of Geophysical Research*, 69(16), pp.3319-3333.
- Wiscombe, W.J. and S.G. Warren. 1980. A model for the spectral albedo of snow. I: Pure snow. *Journal of the Atmospheric Sciences*, 37(12), pp.2712-2733.
- Williams, D. G., W. Cable, K. Hultine, J. C. B. Hoedjes, E. A. Yopez, V. Simonneaux and F. Timouk. 2004. Evapotranspiration components determined by stable isotope, sap flow and eddy covariance techniques. *Agricultural and Forest Meteorology*, 125(3), 241-258.
- Wilson, K.B., P.J. Hanson, P.J. Mulholland, D.D. Baldocchi, and S.D. Wullschleger. 2001. A comparison of methods for determining forest evapotranspiration and its components: sap-flow, soil water budget, eddy covariance and catchment water balance. *Agricultural and Forest Meteorology*, 106(2), 153-168.
- Winograd, I.J. and W. Thordarson. 1975. Hydrogeologic and hydrochemical framework, south-central Great Basin, Nevada-California, with special reference to the Nevada Test Site. U.S. Geological Survey Professional Paper 712-C, 126 p.

- World Meteorological Organization, 1996. WMO guide to meteorological instruments and methods of observation. p. 677.
- Wood, W.W. and W.E. Sanford. 1994. Chemical and isotopic methods for quantifying groundwater recharge in a regional, semiarid environment. *Groundwater* 33, no. 3: 458–468.
- Wood, W.W. 1999. Use and misuse of the chloride-mass balance method in estimating groundwater recharge. *Groundwater* 37(1), pp. 2-3.
- Xie, Y., Z. Sha and M Yu. 2008. Remote sensing imagery in vegetation mapping: a review. *Journal of plant ecology*, 1(1), pp.9-23.
- Zhou, M.C., H. Ishidaira, H.P. Hapuarachchi, J. Magome, A.S. Kiem and K. Takeuchi. 2006. Estimating potential evapotranspiration using Shuttleworth–Wallace model and NOAA-AVHRR NDVI data to feed a distributed hydrological model over the Mekong River basin. *Journal of Hydrology*, 327(1), pp.151-173.